

ABSTRACT

Title of Document: Flux Maps Obtained from Core Geometry Approximations: Monte Carlo Simulations and Benchmark Measurements for a 250 kW TRIGA Reactor

Ali Bellou Mohamed, Doctor of Philosophy, 2009

Directed By: Professor, Mohamad Al-Sheikhly and Professor Emeritus Joseph Silverman, Graduate Program in Nuclear Engineering, Materials Science and Engineering Department

Two MCNP models (detailed and approximated) of the University of Maryland Training Reactor were created. The detailed model attempted to simulate the reactor according to engineering specifications while the simplified model eliminated all structural materials above and below the core. Neutron flux spectrum calculations for both models within the core showed that the results obtained from both models agreed within less than 0.5%. It was concluded that reactors equipped with standard TRIGA fuels enriched to 20 percent in uranium-235 can be modeled with all structures above and below the core eliminated entirely from the model without increasing the error due to geometry modeling simplifications of the core. In TRIGA reactors supplied with standard TRIGA fuels enriched to 20 percent in U-235, the graphite reflectors above and below the fuel act as “neutron energy regulators.”

Neutrons reflected back into the core through the graphite reflectors quickly become thermalized even if their energies were altered due to the change in materials properties above and below the core. Both MCNP models results agree well with measured data. It was also found that simplification in the target geometry leads to substantial uncertainty in the calculated results. The neutron energy spectrum, thermal flux, and total flux were calculated at the thermal column access plug face; in the pneumatic transfer system rabbit, and on top and bottom sections of the most center fuel element. The thermal flux and the total flux at the thermal column access plug face both agreed with measured data within a 5% uncertainty. The thermal flux, fast flux, and the total flux in the rabbit differ by 18.8%, 35%, and 5.7% respectively, from the measured data. The relatively high uncertainty (in the neutron energy distribution but not the total neutron flux) was attributed to the use of air as the target irradiated inside the rabbit. For such a thin target (15 mg/cm^2), a precise neutron balance between reflection and absorption events is difficult to obtain; that will alter the thermal or fast flux values.

The contribution of this work to the reactor users is that a virtual reactor model that compared well with experiment is created. Experiments utilizing the reactor experimental facilities (thermal column, through tube, pneumatic transfer system rabbit, and beam ports) can now be optimized before they are executed.

The contribution of this work to the research reactor community is that research reactors equipped with standard TRIGA fuels enriched to 20 percent in U-235 can be modeled with core geometry approximations, such as these adopted in this work, without affecting the precision and accuracy of the Monte Carlo calculations.

FLUX MAPS OBTAINED FROM CORE GEOMETRY APPROXIMATIONS:
MONTE CARLO SIMULATIONS AND BENCHMARK MEASUREMENTS FOR
A 250 KW TRIGA REACTOR

By

Ali Bellou Mohamed

Dissertation submitted to the Faculty of the Graduate School of the
University of Maryland, College Park, in partial fulfillment
of the requirements for the degree of
Doctor of Philosophy
2009

Advisory Committee:
Professor Mohamad Al-Sheikhly, Chair
Professor Emeritus Joseph Silverman
Professor Mohammad Modarres
Professor Gary Pertmer
Professor Shapour Azarm

© Copyright by
Ali Bellou Mohamed
2009

Dedication

To My Mother Amna

Acknowledgements

First, I would like offer my sincere gratitude to my advisor Mohamad Al-Sheikhly, Professor and Director of the Radiation Facilities and Nuclear Reactor, for his continued support and guidance for my Ph.D. research, and patience with me throughout the course of this work.

Words simply are shy to express my utmost sincere gratitude to my co-advisor Joseph Silverman, Professor Emeritus, for his unconditional support for my research, and in personal matters. Professor Silverman stimulating ideas are always around the corner. Professor Silverman, thank you for every thing.

I would like to thank my dissertation committee: Professor Gary Pertmer, Associate Dean, Professor Mohammad Modarres, and Professor Shapour Azarm, for their encouragement, insightful comments, and useful and thoughtful suggestions.

I would like to offer my deepest thank and appreciation and give full credit to Eric Burgett, fellow doctoral candidate at Georgia Institute of Technology, and Ian Gifford, fellow doctoral candidate here at the University of Maryland, for performing the difficult neutron spectrum unfolding at the thermal column and providing me with the unfolded data.

I would like specially thank my fellow doctoral candidate Colonel Donald Hall for his insight and without his suggestions, some issues, especially burnup, could not have been resolved in time.

I would like specially to thank Vincent Adams for always being thoughtful and for answering my difficult questions about the Maryland reactor, and providing

me with the necessary experimental data; without his help, this work wouldn't be complete.

Table of Contents

| | |
|--|------|
| Dedication..... | ii |
| Acknowledgements..... | iii |
| Table of Contents..... | v |
| List of Tables..... | vii |
| List of Figures..... | viii |
| Chapter 1 : Introduction..... | 1 |
| 1.1 Objective and Research Needs..... | 1 |
| 1.2 Literature Review..... | 2 |
| Chapter 2 : Nuclear Reactor Theory..... | 5 |
| 2.1 Neutron Transport and Reactor Theory..... | 5 |
| 2.2 The Neutron Transport Equation..... | 5 |
| 2.3 Approximation to the Neutron Transport Equation..... | 7 |
| 2.4 The P_N Approximation and Diffusion Theory..... | 8 |
| 2.5 The Discrete Ordinate Method..... | 9 |
| 2.6 The Monte Carlo Method..... | 11 |
| 2.7 The Physics of TRIGA Reactors..... | 17 |
| Chapter 3 : Reactor Model Development..... | 21 |
| 3.1 Description of MUTR..... | 21 |
| 3.2 The MCNP/MCNPX Code..... | 22 |
| 3.3 Description of the MCNP/MCNPX Model..... | 23 |
| 3.3.1 Outline of MCNP Model description..... | 23 |
| 3.3.2 Standard TRIGA Fuel Element Description..... | 25 |
| 3.3.3 Four-Rod Fuel Cluster Description..... | 29 |
| 3.3.4 MCNP Model of the Four-Rod Fuel Cluster..... | 30 |
| 3.3.5 Control Rods..... | 33 |
| 3.3.6 Control Rod Fuel Cluster..... | 33 |
| 3.3.7 MCNP Model of Control Rod Fuel Cluster..... | 33 |
| 3.3.8 The Pneumatic Transfer System—the Rabbit..... | 35 |
| 3.3.9 Neutron Moderator and Reflector..... | 36 |
| 3.3.10 The Thermal Column..... | 37 |
| 3.4 MCNP Geometry Model of MUTR..... | 38 |
| 3.5 Materials Used in the MCNP Model..... | 41 |
| 3.6 MCNP Criticality Calculation Setup..... | 43 |
| 3.6.1 Structure of the MCNP Input File..... | 43 |
| 3.6.2 Setup of the MCNP Criticality Calculations..... | 45 |
| 3.7 Precision of the Monte Carlo Calculations..... | 46 |
| 3.8 Variance Reduction..... | 46 |
| 3.9 Analog and Non Analog Monte Carlo Sampling..... | 47 |
| 3.10 Validity of the Monte Carlo Precision..... | 49 |
| Chapter 4 : Results and Discussion..... | 50 |

| | | |
|---|--|-----|
| 4.1 | Summary of the Results | 50 |
| 4.2 | Reactor Core Criticality Calculations | 52 |
| 4.3 | Calculation of the Neutron Flux Spectrum at the Thermal Column | 54 |
| 4.4 | Weight Windows | 55 |
| 4.5 | The Thermal Column Flux Calculation Optimization | 57 |
| 4.6 | Results of the thermal Column Calculations | 59 |
| 4.7 | Neutron Spectrum Unfolding Measurements | 63 |
| 4.8 | Results and Analysis of Core Geometry Approximations | 66 |
| 4.8.1 | Survey of TRIGA Fuels | 70 |
| 4.8.2 | Graphite Reflectors Neutronic Effects | 71 |
| 4.9 | Results of Uncertainty Calculations | 74 |
| 4.10 | Fuel Burnup Effect | 75 |
| 4.11 | Short Term Reactivity Effects—Fission Products Poisoning | 75 |
| 4.12 | Long Term Reactivity Effects | 76 |
| 4.13 | MCNPX Burnup Process | 78 |
| 4.14 | Results of Flux Calculations in The Rabbit System | 79 |
| 4.15 | Study of Fuel Burnup Using Cell Calculations | 81 |
| Chapter 5 : Conclusions and Recommendations | | 83 |
| Appendix A | | 85 |
| A.1 | MCNP Model of the Detailed MUTR Core | 85 |
| A.2 | MCNP Model of the Simplified Core of MUTR | 104 |
| A.3 | MCNP Model of MUTR Pin Cell (Unit Cell) | 119 |
| Bibliography | | 122 |

List of Tables

| | |
|--|----|
| Table 3.1: Materials Composition used in MCNP Model of MUTR | 41 |
| Table 4.1: Comparison of Experimental and MCNP Calculated Flux Data..... | 51 |
| Table 4.2: Neutron Flux-to-Dose Rate Conversion Factors [6]..... | 62 |
| Table 4.3. Thermal Neutron Activation Reactions. | 66 |
| Table 4.4: Scattering and Absorption Cross Sections For Water and Aluminum [...] | 68 |
| Table 4.5 :Multiplication factor benchmarks during initial reactor startup | 68 |
| Table 4.6: Standard TRIGA Fuel Element Dimensions | 71 |
| Table 4.7: Change of keff with Graphite Reflector Thickness | 72 |
| Table 4.8: Flux for Graphite Reflectors with at Different Lengths | 73 |
| Table 4.9: Three-parameter Uncertainty Matrix..... | 74 |
| Table 4.10: Thermal Cross Sections Data (0.0253 eV) for Fissile and Fertile Nuclides [,]..... | 78 |

List of Figures

| | |
|--|----|
| Figure 2.1: Conservation of Neutrons in a Small Volume Element | 6 |
| Figure 2.2: Typical Particle Trajectories Through a Material | 12 |
| Figure 2.3: Calculation of Distance to the Next Collision..... | 13 |
| Figure 2.4: Flow Diagram for a Monte Carlo Calculation..... | 16 |
| Figure 3.1: TRIGA Fuel-Moderator Element [31] | 26 |
| Figure 3.2: MCNP Model of the UMTR TRIGA Fuel Element..... | 27 |
| Figure 3.3: TRIGA Fuel Element Dimensions | 28 |
| Figure 3.4: Four-Rod Fuel-Moderator Cluster..... | 29 |
| Figure 3.5: MCNP Model of the U-ZrH Fuel-Moderator Element Lattice Cell..... | 32 |
| Figure 3.6: MCNP Model the Four-Rod Cluster Lattice | 32 |
| Figure 3.7 :MCNP Model of Control Rod Fuel Cluster | 34 |
| Figure 3.8: Pneumatic Transfer System Terminus: Rabbit..... | 35 |
| Figure 3.9: MCNP model of the Graphite Reflector Block | 36 |
| Figure 3.10: Thermal Column [27]..... | 38 |
| Figure 3.11: Current MUTR Core Layout | 39 |
| Figure 3.12: MCNP Model of MUTR | 39 |
| Figure 3.13: Core Lattice Filled with Universes During Initial Startup | 40 |
| Figure 3.14: Combinatorial Geometry Logic..... | 43 |
| Figure 3.15: MCNP Input File Structure | 44 |
| Figure 3.16: A Simple MCNP Input File..... | 44 |
| Figure 4.1: MCNP Model of UMD Reactor Core, Grid Plates, Beam Tubes, Thermal Column..... | 54 |
| Figure 4.2: A Close-up view of the UMD Reactor Detailed Core Model | 55 |
| Figure 4.3: Geometry Splitting and Russian Roulette | 56 |
| Figure 4.4: Top View of UMTR Core and Experimental Facilities | 58 |
| Figure 4.5: Particle Tracks for Analog and Non Analog Transport | 59 |
| Figure 4.6: Weight Window Mesh for Thermal Column | 60 |
| Figure 4.7: Neutron Spectrum Computed at the Thermal Column Access Plug..... | 63 |
| Figure 4.8: Side View of Simplified and Detailed Cores | 67 |
| Figure 4.9: Neutron Spectrum at Top of Most Center Fuel..... | 69 |
| Figure 4.10: Neutron Energy Spectrum at the Top and Bottom of Fuel..... | 69 |
| Figure 4.11: Pin Cell Neutron Energy Spectrum | 73 |
| Figure 4.12: Fission Cross Section for Fissile Materials | 77 |
| Figure 4.13: Rabbit in the Core..... | 79 |
| Figure 4.14: Neutron Flux at The Pneumatic Tube Transfer System Rabbit | 80 |
| Figure 4.15: MCNP Model of A Unit Cell | 82 |
| Figure 4.16: Neutron spectrum inside a Unit Cell After 40 MWD Irradiation..... | 82 |

Chapter 1: Introduction

1.1 Objective and Research Needs

The objective of this research is to characterize the neutron and gamma fluxes of the Maryland University Training reactor (MUTR), and to determine the uncertainty in the neutron and gamma fluxes arising from geometry approximations when modeling the reactor by the Monte Carlo method. Fluxes are determined in all the reactor experimental facilities: the thermal column, beam ports, through tube, and the pneumatic tube system or the rabbit. The MUTR is utilized for important research in radiobiology, especially, Boron Neutron Capture Therapy (BNCT), where thermal neutron fluxes with minimum uncertainty are needed. The MUTR configuration is unique and no existing studies to assess the uncertainty obtained by approximations of the core geometry for this MUTR were found. If the results from this research conclude that the uncertainty obtained by modeling approximations is of quite significance, then the near-exact modeling of geometrical configurations of the reactor core and its auxiliaries will be a requirement for similar research reactors involved in sensitive research areas such as BNCT and microdosimetry. In this instance this research will have major positive contribution to the quality of research in areas such as radiobiology, microdosimetry and nuclear medicine. If we were to conclude that geometry approximation bears little on the magnitude of the uncertainty in fluxes obtained in desired locations in the reactor, then results from this research would have major positive contributions to research reactors with similar designs

because tremendous savings in modeling efforts could be claimed by modeling reactor core geometry with tolerated approximations.

1.2 Literature Review

Characterization of neutron beam experimental facilities using Monte Carlo methods and experiment is performed worldwide. However no where in the literature, where Monte Carlo modeling of TRIGA (Training, Research, Isotopes production, General Atomics) reactors is undertaken [1, 2, 3, 4], an assessment of uncertainty in neutron and gamma fluxes maps (in different parts of the reactor experimental facilities) arising from geometry approximations, were found. A detailed characterization of a 1 MW TRIGA Mark II reactor [3] at the University of Texas (UT) was undertaken but geometry effects on flux uncertainty were not studied. Also, UT reactor configuration is fundamentally different from the MUTR TRIGA reactor. The only similarity between the two reactors is that they have similar, but not identical, TRIGA fuels. It was reported that [5] agreement between MCNP (Monte Carlo N-Particle) [6] Monte Carlo calculation of neutron spectrum of the Sandia Pulsed Reactor III [5] and experiments were fairly good, but the discrepancy between calculations and experiment were found in the thermal spectrum region. It was concluded that the thermal spectrum were sensitive to modeling details, or geometry approximations, of items located near and above the reactor core. Better agreement between MCNP calculations were achieved when auxiliary equipments were included in the Monte Carlo model. However it is believed that for irradiation of relatively high neutron and gamma ray dose rates—in the kGy/h range—approximation to core geometry is acceptable because the uncertainty arising is small compared to the dose

applied. However, for relatively low dose rates—sub-Gy/min—near-exact modeling of reactor core geometry may be essential.

The TRIGA Mark II research reactor of Jozef Stefan Institute, Ljubljana, Solvenia, is an example of a well characterized and studied research reactor. Numerous studies [7, 8] and benchmarks had been carried out using MCNP and other deterministic codes. Sensitivity analysis on materials and geometry were conducted in order to analyze their effect on criticality. Results Monte Carol calculations were found to agree well with experiment—however, because TRIGA Mark II is quite different from our TRIGA conversion reactor, conclusions could not be drawn as applicable to our reactor.

Characterization of neutron and gamma fluxes with minimum uncertainty is of utmost importance to basic radiation research in nuclear medicine and radiobiology, in particular boron neutron capture therapy (BNCT) as well as microdosimetry. This type of research involves the application of relatively low neutron and gamma doses for a wide range of neutron energies that span the energy spectrum from fast to thermal neutrons and at those levels of low doses, the uncertainty of neutron fluxes might exceed the dose applied. Relatively low doses (2.5-25 cGy/min) are usually encountered in cell survival studies [9], to assess the radiobiological effectiveness (RBE) of epithermal neutrons in BNCT. Response of healthy tissue to damage by epithermal neutrons irradiation during BNCT is simulated by imbedding cells in water-filled phantoms and determining the RBE as a function of depth. Uncertainty arises in measurement of fast neutron dose rates with the use of ionization chambers, especially tissue equivalent ionization chambers [10]. This because the neutron

sensitivity of tissue-equivalent ionization chambers is averaged over a wide neutron energy range and neutron energy spectra will be present which results in a linear energy transfer (LET) that is energy dependent. Currently, there is a need to evaluate the thermal neutron flux with minimum uncertainty in the beam ports of the MUTR to perform prompt gamma neutron activation (PGNA) on concrete samples in order to find the depth profile of chlorine in reinforced concrete. The chloride ion is an important promoter of the corrosion of iron reinforcements in concrete.

It is then essential when modeling the reactor, accurate assessment of neutron and flux maps be considered.

Chapter 2: Nuclear Reactor Theory

2.1 Neutron Transport and Reactor Theory

The behavior of a nuclear reactor is governed by the distribution in space, energy and time of neutrons in the system. The main objective of reactor theory is to predict this distribution. This could be accomplished by solving the neutron transport equation analytically or numerically or by using Monte Carlo methods. As a result of the solution of the neutron transport equation, the neutron flux and other important quantities fundamental to design of nuclear reactors can be determined.

2.2 The Neutron Transport Equation

As neutrons move within a medium, which may be gaseous, liquid, or solid, they collide with nuclei of the atoms in the medium. In the collision, a neutron may be absorbed by the nucleus or may be scattered elastically or inelastically. Absorption may lead to fission, radiative capture, or other neutron or charged particle producing reactions. The neutron transport equation [11, 12, 13] expresses the net rate of change of the neutron density in a unit volume of a medium. In other words, the neutron transport equation is a statement of conservation of neutrons in space, energy, and time. The equation is derived by considering the rates at which neutrons of different energies moving in different directions enter and leave a small volume element (Figure 2.1).

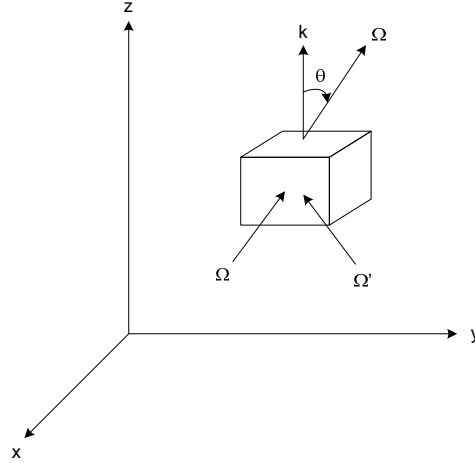


Figure 2.1: Conservation of Neutrons in a Small Volume Element in a small volume element moving in the direction, Ω , Ω' , where Ω , and Ω' are unit vectors in the directions shown.

The steady-state transport equation is can be written as:

$$\begin{array}{cccc}
 -\Omega \cdot \nabla \Phi & -\Sigma \Phi & + \iint \Sigma' f \Phi' d\Omega' dE' & + S = 0 \\
 \text{I} & \text{II} & \text{III} & \text{IV}
 \end{array} \tag{2.1}$$

where the symbol ∇ represent the gradient; the other quantities are as follows:

- $\Phi \equiv \Phi(r, \Omega, E)$ Angular flux of neutrons at position r with energy E moving in direction Ω
- $\Phi' \equiv \Phi'(r, \Omega', E')$ Angular flux of neutrons at position r with energy E' moving in direction Ω'
- $\Sigma \equiv \Sigma(r, E)$ Total macrsopic cross section for all interactions of neutrons of energy E at r
- $\Sigma' \equiv \Sigma(r, E')$ Total macrsopic cross section for all interactions of neutrons of energy E' at r
- $f' \equiv f(r; \Omega', E' \rightarrow \Omega, E)$ Probability that a neutron at r with E' and direction Ω' will have energy E and direction Ω after an interaction
- $S \equiv S(r, \Omega, E)$ Source (or sources) of neutrons at r of energy E and direction Ω

The physical meaning of the four terms in the transport equations is as follows:

| | |
|----------|---|
| Term I | Rate of loss of (Ω, E) neutrons from the specified volume element as a result of leakage |
| Term II | Rate of loss of (Ω, E) neutrons as a result of neutrons interactions of all types |
| Term III | Rate of gain (Ω, E) neutrons as a result of neutrons interactions of all types |
| Term IV | Gain of (Ω, E) neutrons from a source (or sources) |

2.3 Approximation to the Neutron Transport Equation

The transport equation is solved exactly in only a few simple cases. In reactor design calculations, it is necessary to use approximations to the neutron transport equation; and when closed form solutions are available, they can be used to validate these approximations. Two important approximation methods to the transport equation, also known as deterministic methods, namely the P_N [14, 15, 16] and its derivative, the P_1 , or diffusion approximation and discrete ordinate, are widely used in reactor design. However deterministic methods suffer because they cannot accurately represent the geometry of the system. Thus deterministic methods provide an exact solution to an approximation of the problem geometry. In contrast, Monte Carlo methods have proven to be superior to deterministic methods for the following reasons: Monte Carlo methods represent the geometry and nuclear data more accurately than do deterministic techniques; Monte Carlo methods use continuous energy cross section data while deterministic methods use multigroup approximations. The P_N approximation and the discrete ordinates method are discussed briefly in this work. In-depth discussions and elaborate derivations can be found in the literature [14, 15, 16, 17].

2.4 The P_N Approximation and Diffusion Theory

The one speed transport equation in one dimension can be written as [14]:

$$\mu \cdot \frac{d\Phi}{dz}(z, \mu) + \Sigma\Phi(z, \mu) = S(z, \mu) + \int_{-1}^1 \Phi(z, \mu') N_s \sum_{l=0}^{\infty} \frac{2l+1}{2} \sigma_{sl} P_l(\mu) P_l(\mu') d\mu' \quad (2.2)$$

where μ is the cosine of the scattering angle, Σ is the total macroscopic cross section, S is the angular source (sources) of neutrons, and N_s the scattering atom density.

The one speed angular flux is written as:

$$\Phi(z, \mu) = \sum_{i=0}^{\infty} \frac{2i+1}{2} \Phi_i(z) P_i(\mu) \quad (2.3)$$

where $\Phi_i(z) = \int_{-1}^1 \Phi(z, \mu) P_i(\mu) d\mu$ and $P_i(\mu)$ are Legendre Polynomials [14]

which satisfy the orthogonality condition

$$\int_{-1}^1 P_l(\mu) P_i(\mu) d\mu = 0 \quad \text{if } l \neq i$$

$$= \frac{2}{2l+1} \quad \text{if } l = i.$$

If Equation 2.2 is multiplied first by $P_0(\mu)$ and integrated over all values of μ (the cosine of the scattering angle) then multiplied again by $P_1(\mu)$ and then integration over all μ is also performed, two equations in $\Phi_0(z)$ and $\Phi_1(z)$ would result. If

$\Phi_1(z)$ is eliminated, the resulting single equation is

$$\frac{1}{3(\Sigma_t - N_s \sigma_{s1})} \frac{d^2 \Phi_0(z)}{dz^2} - \Sigma_a \Phi_0(z) + S_0(z) = 0 \quad (2.4)$$

If an average cosine of scattering angle is defined as $\bar{\mu}_0$, then

$$\sigma_{s1} = \int_{-1}^1 \sigma_s(\mu_0) P_1(\mu_0) d\mu_0 = \bar{\mu}_0 \int_{-1}^1 \sigma_s(\mu_0) d\mu_0 = \bar{\mu}_0 \sigma_{s0}.$$

Equation 2.4 becomes:

$$\frac{1}{3(\Sigma_a + \Sigma_s - \bar{\mu}_0 N_s \sigma_{s0})} \frac{d^2 \Phi_0(z)}{dz^2} - \Sigma_a \Phi_0(z) + S_0(z) = 0$$

which looks like the familiar diffusion equation [14]

$$D \nabla^2 \Phi - \Sigma_a \Phi + S = 0,$$

with D , the diffusion coefficient, written as:

$$D = \frac{1}{3(\Sigma_a + \Sigma_s(1 - \bar{\mu}_0))} = \frac{1}{3(\Sigma_a + \Sigma_{tr})},$$

where Σ_{tr} is the macroscopic transport cross section.

2.5 The Discrete Ordinate Method

The discrete ordinates [15, 16, 18] or discrete S_n approximation method is similar to P_N method (Equation 2.2) but requires that the transport equation holds only for a number of discrete angles μ_n , hence the name “discrete ordinates”; and then applying quadrature approximation to the integral term. In discrete ordinates, Equation 2.2 can be written as:

$$\mu_n \cdot \frac{d\Phi_n}{dz}(z, \mu_n) + \Sigma \Phi_n(z, \mu_n) = s(z, \mu_n) + \sum_{l=0}^L (2l+1) P_l(\mu_n) N_s \sigma_l(x) \Phi_l(z)$$

where

$$\begin{aligned}\phi(z) &= \frac{1}{2} \sum_{n=1}^N w_n \Phi_n(z, \mu_n) \\ \phi_l(z) &= \frac{1}{2} \sum_{n=1}^N w_n P_l(\mu_n) \Phi_n(z, \mu_n) \\ \sigma_l(z) &= \frac{1}{2} \sum_{n=1}^N w_n P_l(\mu_n) \sigma_n(z, \mu_n) \\ \sum_n w_n &= 2\end{aligned}$$

with $-1 \leq \mu \leq +1$ divided into N ordinates with corresponding weights, w_n , the discrete ordinates approximation of order N results. The discrete ordinates method is the preferred method in nuclear reactor cell calculations to produce “group constants”, or flux weighted quantities, $D_g, \Sigma_g^t, \Sigma_{g'-g}^s, F_g$, the group diffusion coefficient, the group macroscopic total cross section, the group removal cross section, and the group reaction rate, respectively. In principle, a group constant when combined with the group flux, must give the same reaction rate as would be obtained by the summing (or integrating) all the energy dependent reaction rates over all neutron energies in the group. This is expressed as

$$\begin{aligned}\Sigma_g^i \phi_g &= \int_g \Sigma^i(E) \phi(E) dE \\ \Sigma_g^i &= \frac{1}{\phi_g} \int_g \Sigma^i(E) \phi(E) dE \\ \phi_g &= \int_g \phi(E) dE\end{aligned}$$

where $\Sigma^i(E)$, $\phi(E)$ are the energy dependent macroscopic cross section and energy dependent flux, respectively. $\Sigma^i(E)$ is known from evaluated cross section data, $\phi(E)$ can be calculated by solving a couple of discrete ordinate equations similar to the P_N method, and therefore, the group reaction rate can be calculated. In reactor cell

calculations usually 69-120 groups are used to evaluate group constants. Further, the groups are collapsed into few groups: fast (0.05 to 10 MeV), slowing-down region (50 to 0.5 keV), resonance (0.5 to 0.625 eV), and thermal region (< 0.625 eV); and group constants are evaluated. These constants are used to compute the spatial distribution of the neutron flux in the reactor core and perform criticality calculations.

2.6 The Monte Carlo Method

When a neutron traverses a material, it interacts with atoms of that material. It may get scattered, or absorbed (Figure 2.2). Scattering may be elastic or inelastic; absorption might lead to capture or fission. These processes occur statistically in nature with the probability of occurrence determined by a cross section. Using random numbers, the computer can generate a statistical history of the life of each neutron. That is a neutron may experience many scattering interactions before finally being absorbed or leaking out of the system. Random numbers are sampled uniformly between in the interval [0-1] are used in each interaction to determine the resulting direction of the particle, how much energy is lost, what is the new direction of the neutron, or how many neutrons are created in a fission event. The life of a neutron begins at birth, either from external neutrons sources or from a fission event, and ends with an absorption or scattering event that leads a neutron to vanish from the system. A large number of neutrons, or histories, are sampled and an average or expectation number of each event is evaluated to accurately describe what occurs. This is the Monte Carlo method applied to neutron transport.

In the application of the Monte Carlo method [19, 20, 28] in criticality calculations, the effective multiplication factor of an assembly is of primary interest.

In these calculations a group of neutron histories, referred to as a k_{eff} cycle (or neutron generation), with a multiplication factor of the assembly given by the ratio of the number of neutrons generated at the end of the k_{eff} cycle (those created in fission events in this cycle) to the number of neutrons whose histories are evaluated in this cycle (the number at the start of the generation).

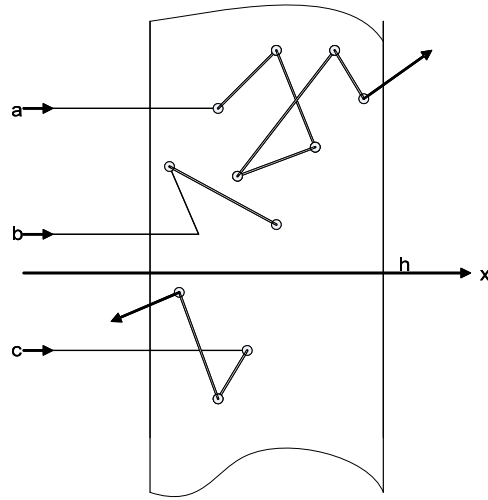


Figure 2.2: Typical Particle Trajectories Through a Material
Neutron a is transmitted, b is absorbed, and c is reflected.

As an example [20, 21, 22], Monte Carlo transport of neutron transmission through a plate is presented. Let us assume—for simplicity—only scattering and absorption collisions do occur, and neutrons during collision do not lose energy. Let a flux of monoenergetic neutrons be incident perpendicularly (angle of incidence = 90°) on a homogeneous infinite slab of thickness h ($0 \leq x \leq h$). Upon collision with atoms of the plate material, neutrons may be either elastically scattered or captured (Figure 2.2). It is required to calculate the probability of neutron transmission through the plate, p^+ ; the probability of neutron reflection by the plate, p^- ; and the probability of

neutron capture inside the plate, p^0 . Interaction of neutrons with matter is characterized—in this case by two constants: Σ_c and Σ_s , the capture and scattering cross sections, respectively. The sum of these two cross sections—strictly is the total cross section $\Sigma_t = \Sigma_c + \Sigma_s$. The probability of neutron capture upon collision with an atom is equal to Σ_c / Σ_t , and the probability of scattering is equal to Σ_s / Σ_t .

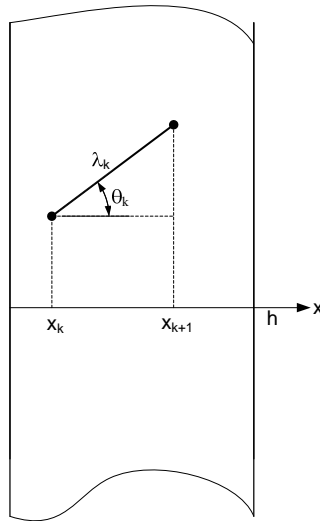


Figure 2.3: Calculation of Distance to the Next Collision

The mean free path, λ , of a neutron (the path from one collision to another) is a random variable.

If a single infinite region where particles are being tracked and the total interaction cross section for the region is $\Sigma_t(E)$, then the number of particles of energy E reaching to depth L out of a total of N_0 initial particles is:

$$N(L) = N_0 e^{-\Sigma_t(E)L}$$

And the probability to reach depth L is

$$P(L) = \frac{\text{number reaching depth } L}{\text{initial number}} = e^{-\Sigma_t(E)L}.$$

The probability of interaction at a path length $\leq L$ is thus given by

$$1 - P(L) = 1 - e^{-\Sigma_t(E)L}$$

If the path lengths are to be sampled at random, the random number, γ , is set equal to $P(L)$, or

$$\gamma = 1 - e^{-\Sigma_t(E)L}$$

which leads to

$$L = \frac{1}{\Sigma_t(E)} \ln(1 - \gamma) = \frac{1}{\Sigma_t(E)} \ln \gamma.$$

The above result is because $1-\gamma$ is distributed the same way as γ ; and the formula for drawing the λ random values is

$$\lambda = \frac{1}{\Sigma} \ln \gamma.$$

We now have to find out how to select a random direction of a neutron after scattering. As the problem is symmetrical about the x-axis, the direction is completely defined by an angle θ between the neutron velocity and the x-axis. If we assume the scattering is isotropic, then the cosine of the angle θ is uniformly distributed over the interval $[-1,1]$. The formula for drawing or playing for m values is

$$\mu = 2\gamma - 1.$$

To compute the probabilities, the real trajectories of interactions of the neutron can be simulated as follows.

Let us assume the neutron has undergone the k -th scattering inside the plate at a point with the abscissa x_k and started moving after it in the direction μ_k after it collided (Figure 2.3).

We now play for the free path length by drawing a random number γ and compute λ :

$$\lambda_k = -(1/\Sigma)\ln\gamma$$

and calculate the abscissa of the next collision (figure)

$$x_{k+1} = x_k - \lambda_k \mu_k .$$

Next, we check for the condition for neutron transmission through the plate:

$$x_{k+1} > h .$$

If this condition is satisfied, the computation of the trajectory is terminated and unity is added to the counter of the transmitted particles. If this condition is not satisfied, i.e., $0 \leq x_{k+1} \leq h$, it means that the neutron has undergone the $(k+1)$ -th collision inside the plate and its fate has to be drawn in this collision. To do this, we chose the next random number, γ , and check the capture condition

$$\gamma < \Sigma_c / \Sigma .$$

If this last inequality is satisfied, the trajectory is terminated and we add unity to the counter of captured particles. Otherwise, we assume that the neutron has undergone scattering at the point with abscissa x_{k+1} . In this case, a new random number must be drawn so to play for the direction of neutron after scattering

$$\mu_{k+1} = 2\gamma - 1$$

and the cycle is repeated. It must be pointed that whenever we draw a random number γ , it is always unique— γ should never be used more than once. In this case three

values of γ are necessary to complete one lap of the trajectory. The initial values of each trajectory (history) are:

$$x_0 = 0, \mu_0 = 1$$

and λ_0 is computed from the first drawn random number as $\lambda_0 = -1/\Sigma \ln \gamma$.

After N histories or trajectories are sampled, we obtain that N^+ neutrons were transmitted through the plate, N^- neutrons were reflected and N^0 neutrons were captured within the plate. The probabilities can be computed as the ratios:

$$p^+ \approx N^+/N, \quad p^- \approx N^-/N, \quad p^0 \approx N^0/N.$$

A block diagram or flowchart for the flow of the calculation of this problem is shown in Figure 2.4.

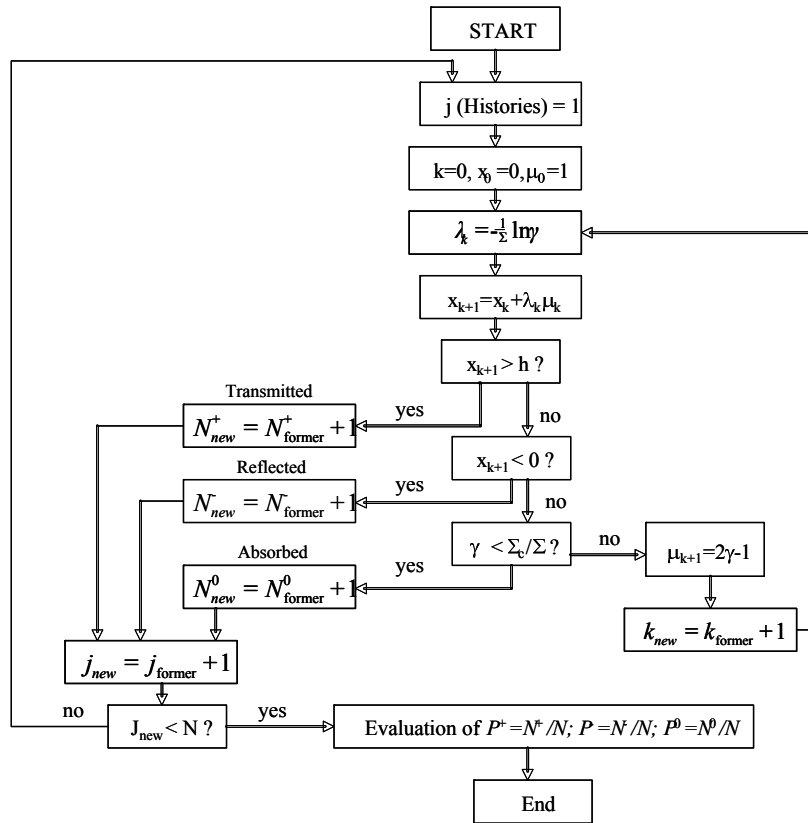


Figure 2.4: Flow Diagram for a Monte Carlo Calculation

2.7 The Physics of TRIGA Reactors

The original TRIGA patent [23, 24] “Reactor with Prompt Negative Temperature Coefficient and Fuel Element Thereof,” outlined the concept of an “inherently” safe reactor, or inherent safety guaranteed by the laws of physics; in contrast to “engineered safety,” or the prevention of accidents by designing a reactor control and safety system. In an inherently safe reactor—TRIGA—if a reactor were to start from a startup condition (low-power critical) and suddenly all control rods were removed (large positive reactivity insertion) at once, the reactor would settle to steady level of operation without melting any of its fuel or releasing fission products—hence a reactor with “large” negative prompt temperature coefficient is inherently safe. This special feature is because TRIGA uses the uranium zirconium hydride (U-ZrH) fuel [25]. In TRIGA fuels, the solid internal moderator (ZrH)—which is to be distinguished from the external moderator (H₂O)—and the fissionable material (U-235) are homogeneously mixed (U-ZrH), hence their temperature is the same and an increase in the fuel temperature will lead to an instantaneous increase in the internal moderator temperature. An increase in fuel and the internal moderator material temperature will lead to “hardening” or shift to higher energies, of the neutron flux spectrum in the fuel. The negative fuel-temperature coefficient results from the following effects [26]: “fuel element expansion effect,” the “warm neutron effect,” the “leakage effect,” and the “neutron Doppler effect.” A further contribution to the prompt negative temperature coefficient can be obtained by adding burnable “poisons” in the reactor fuel material.

The warm neutron effects and leakage effects operate as follows: following sudden positive large reactivity insertion, the intimately mixed fuel and internal moderator become hotter and neutrons within the fuel element “warm up.” Because of the rise of the average neutron energy, the fission cross section in the fuel is decreased resulting in a decreased absorption of neutrons in the fuel. A larger proportion of the neutrons escape from the fuel element into the external moderator and smaller proportion are available for fission. Those neutrons that arrived in the external moderator are rapidly cooled and absorbed with a fixed probability independent of the fuel temperature. This differential absorption of neutrons is what is known as the “warm neutron effect.”

In the “leakage effect,” neutrons leak from the core and the reflector; and higher proportions are captured in the external moderator or pass out of the system—the overall reactivity of the system is lowered.

The “Doppler effect” increases the prompt negative temperature coefficient by the following mechanism: by including in the homogeneous mixture of the fuel (U-ZrH), a suitable material, such as U-238, having a large number of strong narrow resonance bands at energies above thermal, a further significant contribution to prompt negative temperature of reactivity can be achieved. Because the width of the resonance bands increases with temperature and the resonance absorption cross sections are very large, all of neutrons having energies which fall within the individual resonance bands in the resonance region are captured. This widening of the resonance bands or “broadening,” results in decrease of the resonance escape probability. This is the famous “nuclear Doppler effect.”

The “fuel element expansion effect,” the “warm neutron effect,” the “leakage effect,” and the “neutron Doppler effect” have—each—an average prompt negative temperature coefficient of about $-2 \times 10^{-5} \Delta k/k/^{\circ}\text{C}$, with a combined total effect of more than $7 \times 10^{-5} \Delta k/k/^{\circ}\text{C}$, where k is the effective multiplication factor.

The transient behavior of TRIGA reactors was successfully explained by applying—with some approximation—the Fuchs-Hansen model [15, 26], which neglects the effect of delayed neutrons and of heat transfer. Because of these assumptions, the Fuchs-Hansen model is limited to beyond prompt critical reactivity insertions—positive reactivity insertions of more than 1.00 “dollar.” A dollar is equal to the delayed neutron fraction β , for U-235, $\beta = 0.0065$. The Fuchs-Hansen model can be written as:

$$\frac{1}{P} \frac{dP}{dt} = \frac{1}{\tau_0} - b \int_0^t P(t) dt$$

where P (watts) is the reactor power, τ_0 (seconds) is the asymptotic period, and b is the energy shutdown coefficient in reactivity per joule-second; and for TRIGA reactors, an average b is found to be $2 \times 10^{-5} \text{ watts}^{-1} \text{ sec}^{-2}$ for transient data beyond prompt critical.

If the power excursion goes through a maximum, then $dP/dt = 0$ at P_{max} .

The energy at maximum power, E_{max} is found as:

$$E_{\text{max}} = 1/b \tau_0$$

and the maximum power can be found as:

$$P_{\max} = \frac{1}{(\tau_0)E} - (b/2)E_{\max}^2 + P_0 \quad (2.5)$$

where P_0 is an arbitrarily small starting power level, usually in milliwatts. Using Equation (2.5) for a 10 millisecond initial period, the maximum power is found $P_{\max} = 250$ megawatts, the total energy generated during the excursion is 10 megajoules, and the prompt burst fuel temperature rise can be found as [26]:

$$T_p(^{\circ}\text{C}) = 2/\tau_0$$

and for this initial period the temperature rise T_p is 200 $^{\circ}\text{C}$.

Chapter 3: Reactor Model Development

3.1 Description of MUTR

The MUTR [27] is an open pool-type reactor with a maximum licensed, steady state, thermal power of 250 kW. There is no pulsing capability. The reactor is fueled with 24 modified TRIGA fuel clusters. The reactor core consists of 93 fuel rods; 20 fuel clusters each contain four fuel rods, one fuel cluster contains three fuel rods and an instrumented fuel rod, and the remaining three assemblies each contain three fuel rods and a control rod guide tube. The fuel-moderator rods are enriched to <20 w/o U-235 and each of the fuel rods contains a top and bottom slug of graphite which acts as reflectors. Additionally, two graphite reflector elements are positioned in the assembled core, adjacent to two of the outer fuel assemblies.

The MUTR is light water cooled and moderated, and the water also serves as a neutron reflector and as part of the biological shielding. The reactor is cooled by natural convection. The Reactor Coolant and Purification System (RCPS) circulate the reactor coolant through a filter and demineralizer to maintain required water chemistry. The RCPS also provides a flow path through a heat exchanger, which is cooled by city water, if forced convection cooling is desired.

The reactor contains five experimental facilities. The graphite filled thermal column provides an ex-core beam of thermal neutrons for experiments. Large samples, up to approximately 13.3 cm (5.25”) in diameter, can be placed adjacent to

the core in either the beam tubes (two) or the through tube. The beam and through tubes can also provide ex-core gamma and neutron beams. Finally, in-core irradiations of small samples (maximum size of approximately 2.5 cm (1”) diameter by 5 cm (2”) in length) can be done using the pneumatic transfer system.

3.2 The MCNP/MCNPX Code

MCNP [28] is a general-purpose Monte Carlo N-Particle code that can be used for neutron, photon, electron, or coupled neutron/photon/electron transport, including the capability to calculate eigenvalues (k or α) for critical systems. MCNP treats an arbitrary three-dimensional configuration of materials in geometric cells bounded by first- and second-degree surfaces and fourth-degree elliptical tori. The “repeated structures” [28, 29] geometry capability of MCNP is one of the most powerful and useful feature that makes it stand out among all transport codes. The primary goal of the repeated-structures capability is to make it possible for one description of the cell and surfaces of one structure to be applied to the description of the geometry model. Without this capability, the work presented here, or any other large scale repeated structures, such the nuclear reactors with thousands of identical objects, would be a near impossible task to model accurately.

Pointwise cross-section data are used. For neutrons, all reactions given in a particular cross-section evaluation (such as ENDF/B-VI, VII) are accounted for. Thermal neutrons are described by both the free gas and $S(\alpha,\beta)$ models to account for molecular binding effects below 4 eV. For photons, the code accounts for incoherent and coherent scattering, the possibility of fluorescent emission after photoelectric absorption, absorption in pair production with local emission of annihilation

radiation, and bremsstrahlung. A continuous-slowing-down model is used for electron transport that includes positrons, k x-rays, and bremsstrahlung, but does not include external or self-induced fields. Important standard features that make MCNP/MCNPX very versatile and easy to use include a powerful general source, criticality source, and surface source; both geometry and output tally plotters; and a rich collection of variance reduction techniques. Further description of the MCNP code can be found in the literature [28].

3.3 Description of the MCNP/MCNPX Model

The MCNP model of the MUTR comprises several units. These units are the fuel and lattice elements, four-rod fuel cluster, four-rod fuel and control cluster, cluster top handle, bottom fittings, core lattice, core grid plate, graphite reflectors, the thermal column, beam tubes (ports), through tube, plutonium beryllium source holder, and an in-core irradiator—the pneumatic transfer system. In the next sections, an outline of how the MCNP model is built, together with details of each unit or component are presented.

3.3.1 Outline of MCNP Model description

1. The heart of the MCNP model is the reactor core. The lattice cell is fundamental object of the reactor core. Once a lattice is created, it can be replicated or translated. In MCNP terminology, this is known as a “universe” concept. The fuel and control elements are two distinct universes; a four-rod fuel cluster and a four-rod fuel and control cluster are also distinct universes.

The four rod cluster's top handle and bottom fitting are modeled as separate universes. Although a universe can be very complicated to build, it has an advantage; in that its geometry can be developed accurately and rapidly. Changes are made to one lattice without affecting other parts of the core geometry. Control rods are inserted, removed or modified in any desired location in the core by inserting the appropriate universe number in the core lattice.

2. From the fuel and control element lattices, a four-rod fuel and a four-rod fuel and control cluster are constructed. The four-rod cluster, the top handle and bottom fittings are combined into a single universe—the four-rod fuel or four-rod fuel and control assemblies. From the four-rod cluster assemblies, the core lattice is built to reflect the startup or initial fresh core loading.
3. All objects internal to the core but are not fuel or control elements, are modeled as part of the core lattice elements. For example, the pneumatic transfer system—the rabbit system, the graphite reflectors, and the plutonium beryllium (PuBe) graphite source holder, were modeled separately but are inserted as lattice elements within the core lattice.
4. The reactor core is housed in a virtual window so it can easily be modified, or removed without affecting the whole reactor geometry model.

5. Features and objects external to the reactor core—such as: thermal column, beam tubes, through tube, and auxiliaries around the core periphery, were not part of any universe and are modeled separately so that they can easily be removed and worked on without affecting the geometry of the reactor model.

Modeling details based on the above outline are presented for each component in the following sections.

3.3.2 Standard TRIGA Fuel Element Description

The MUTR utilizes TRIGA fuel-moderator elements, which are identical to the standard TRIGA [30] fuel element with the same fuel-moderator specifications, except that the diameter is made slightly smaller, 3.58 cm (1.41 in), to maintain proper metal-to-water ratio in the core. The top and bottom end fittings have been modified to fit into a cluster that is fixed into the existing MUTR grid plate.

The zirconium hydride moderator is homogeneously combined with partially enriched uranium fuel. The fueled section of these fuel-moderator elements, which measures 38.1 cm (15 in) in length and 3.48 cm (1.37 in) in diameter, contains approximately 8.5% of the net weight in uranium enriched at 19.75 w/o in U-235. The hydrogen-to-zirconium atom ratio of the fuel-moderator material is about 1.65-1.7 to 1. To facilitate hydriding, a 4.57 mm (0.18 in) diameter hole is drilled through along the axis of the active section. A zirconium rod is inserted in this hole after hydriding is complete. As shown in Figure 3.1, graphite slugs, 8.76 cm (3.45 in) in length and 3.48 cm (1.37 in) in diameter, act as top and bottom reflectors. The active

fuel section and the top and bottom graphite slugs are contained in a stainless-steel can that has a wall thickness of 0.51 mm (0.020 in) and 1.55 cm (0.61 in) thick at the top and bottom. The overall length of the steel can is 58.74 cm (23.13 in). The stainless-steel can is welded to the top and bottom end fittings. The approximate overall weight of the element is 16.6 kg, and the U-235 content is 37 g. Serial numbers scribed on the top end of the fixtures or spacer blocks are used to identify individual fuel elements.

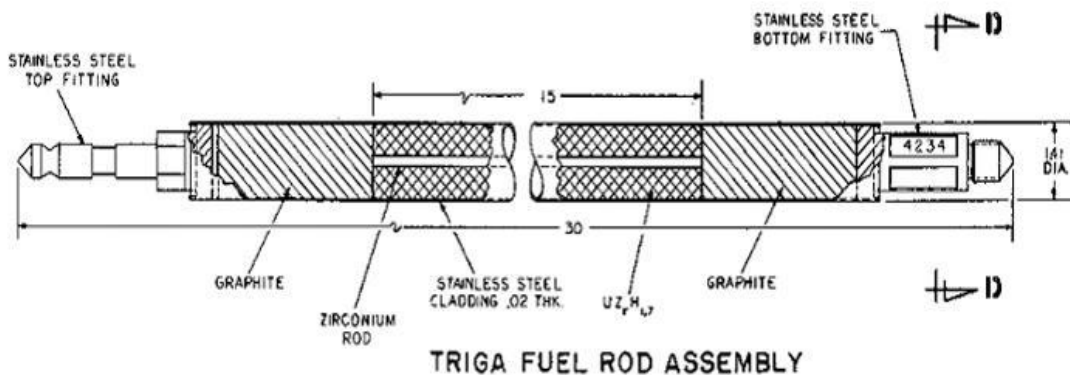


Figure 3.1: TRIGA Fuel-Moderator Element [31]

The MCNP model of the fuel element with geometry approximations, in comparison to the actual fuel element is shown in Figure 3.1. The fuel and moderator, the top and bottom graphite slugs, and the central zirconium rod, top and bottom fittings, the hexagonally shaped first part of the top fitting, top cones, were all modeled in detail according to engineering drawing [31]. All top fittings dimensions were measured from a replica dummy fuel element. The hexagonally shaped first top fitting measures 1.5 cm tall and 2.4 cm in diameter. The second top fitting, marked as

#1 (see Figure 3.3), is 1.57 cm in diameter and 2.4 cm high; the third top fitting, marked as #2, is 1.1 cm in diameter and 1.3 cm high; the fourth top fitting, marked as #3, is identical to the second top fitting. The fuel moderator, central zirconium rod, and cladding dimensions and specifications used in the MCNP model are shown in Figure 3.3. Minor geometry approximations were introduced in the MCNP model TRIGA fuel element described. The bottom end thread and cone were made part of the grid plate geometry and were not modeled separately. The effect of such approximations in geometry is discussed in the “Results” chapter in this document.

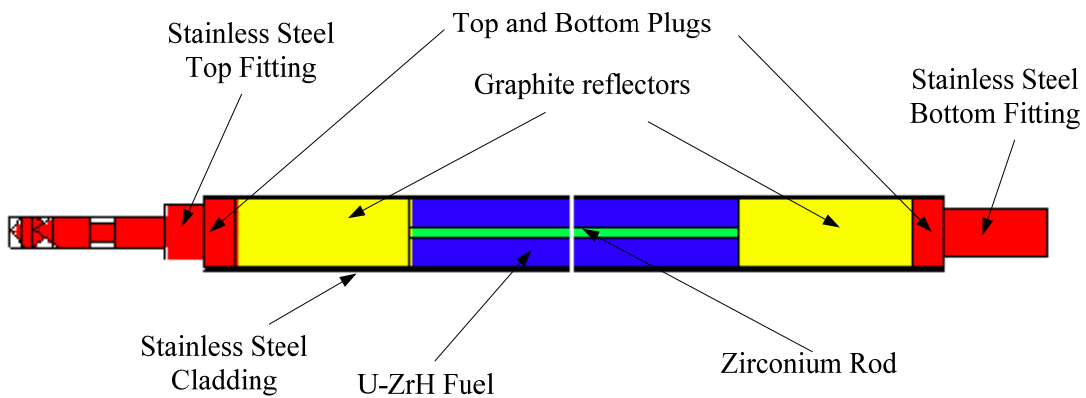


Figure 3.2: MCNP Model of the UMTR TRIGA Fuel Element

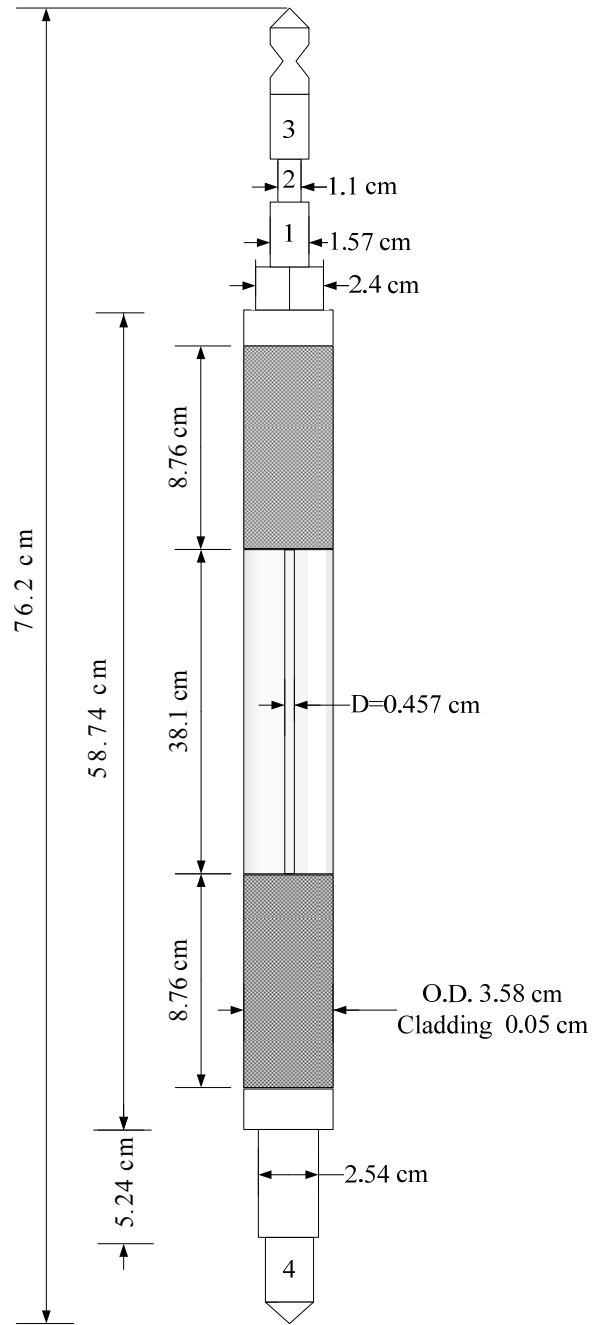


Figure 3.3: TRIGA Fuel Element Dimensions

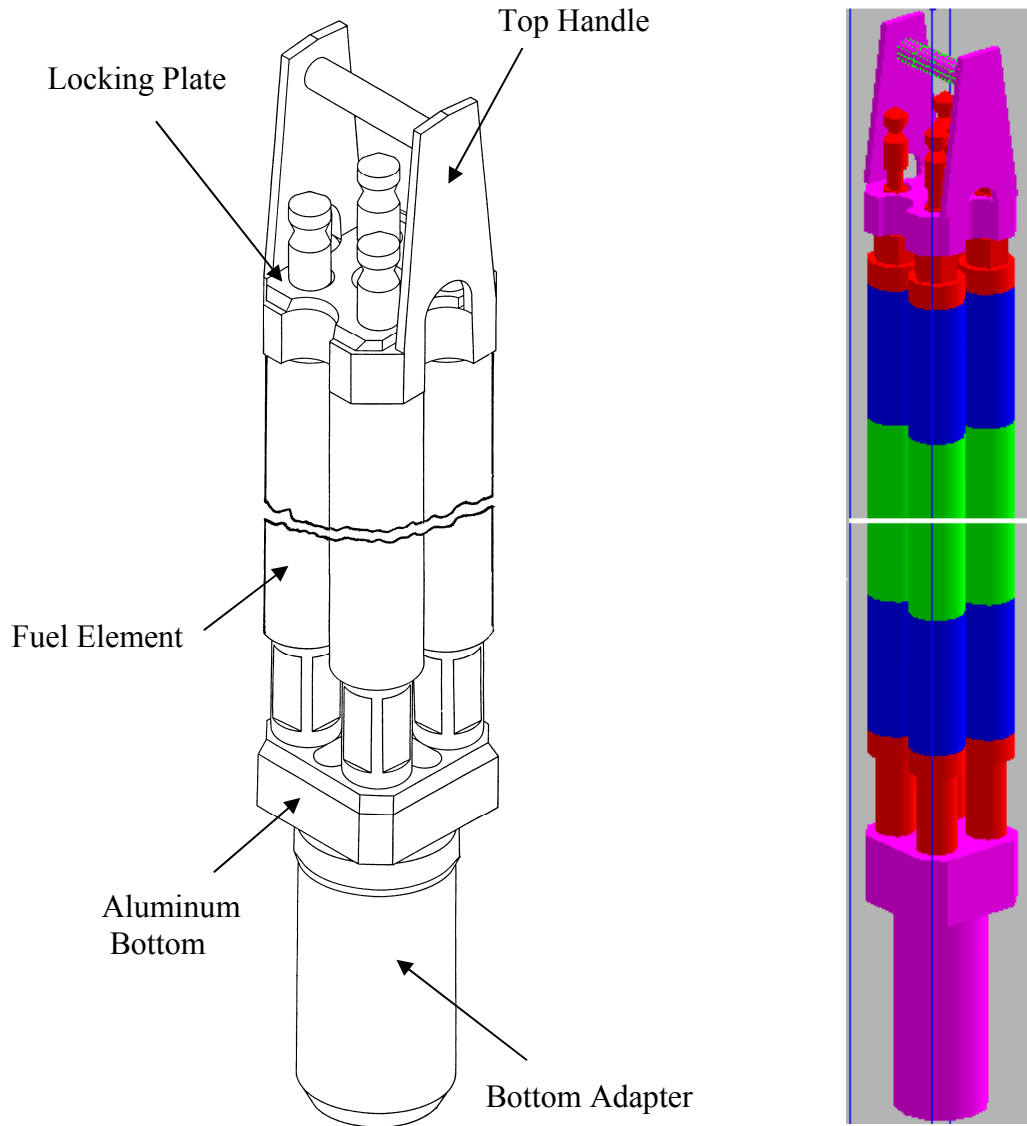


Figure 3.4: Four-Rod Fuel-Moderator Cluster
 Left, 3D sketch of actual cluster; right, 3D MCNP model.

3.3.3 Four-Rod Fuel Cluster Description

The 4-rod fuel cluster was developed to provide a simple means for converting MUTR-type reactors to TRIGA-fuel reactors. The 4-rod cluster consists of an aluminum bottom, 4 stainless steel clad fuel rods and aluminum top handle.

The bottom adapter is designed to fit into and rests on the existing MUTR-type grid plate which provides vertical support and spacing. The top of the adapter contains four tapped holes into which the fuel rods are threaded. The bottom end fitting on the fuel rod is provided with a flange at the base of the threads so that the fuel rod seats firmly on the adapter and is rigidly supported in cantilever fashion.

The top handle of the cluster, Figure 3.4, serves as a lifting fixture and a spacer for the upper ends of the fuel rods. A sliding fit is provided between the top handle and the fuel rod upper end fittings to accommodate differential expansion. A stainless-steel locking plate fastens the top handle to the fuel elements.

3.3.4 MCNP Model of the Four-Rod Fuel Cluster

The MCNP model of the fuel-rod fuel cluster consists of: four-rod fuel lattice elements, top handle, aluminum bottom, and a bottom adapter. The MCNP model of the fuel element lattice and the bottom adapter [32] were modeled in detail. Modeling the geometry of the top handle according to engineering drawings [33] posed the greatest challenge. Many geometry modeling attempts were tried until a final strategy was adopted to carry out the final four-rod fuel cluster and four-rod fuel and control rod cluster MCNP models. The repeated-structures capability of MCNP [28, 29] is used to build a lattice cell that comprises either a U-ZrH fuel element or a control element. The repeated structures capability extends the concept of an MCNP cell. The user can specify that a cell that is to be filled with something called a universe. The U statement in MCNP identifies the universe, to which a cell belongs, and the FILL statement specifies with which universe a cell is to be filled. As shown in Figure 3.5,

a “unit lattice cell” with its dimensions is created with fuel and moderator-coolant around it. A universe $U=1$ is assigned to the fuel-moderator unit cell. A two dimensional lattice of four elements in the range 0:1 0:1 0:0 in the X Y Z directions, respectively, is created. The lattice “keyword” LAT=1 [28] for tetrahedral or square lattice is assigned, and hence a four-rod lattice element is created. The four-rod lattice element is shown in Figure 3.6. This four-rod lattice is assigned a universe $U=2$. A “window” is created to house the four-rod cluster and filled with universe $U=2$. Because the lattice is always infinite, a window is necessary to draw the boundary of the final geometry. Now the window is filled with four-rod cluster which is $U=2$. This window is assigned a universe $U=4$, so as it can be used as a cell for a new lattice. The top handle and the square part of the bottom fitting, the aluminum bottom, are constructed inside the “window” that houses the four-rod cluster and they were also assigned a universe $U=4$. Now the four-rod fuel cluster, the top handle, aluminum bottom, and the bottom fitting are within a new window and all assigned the universe $U=4$. Later, this universe is used to fill the core lattice.

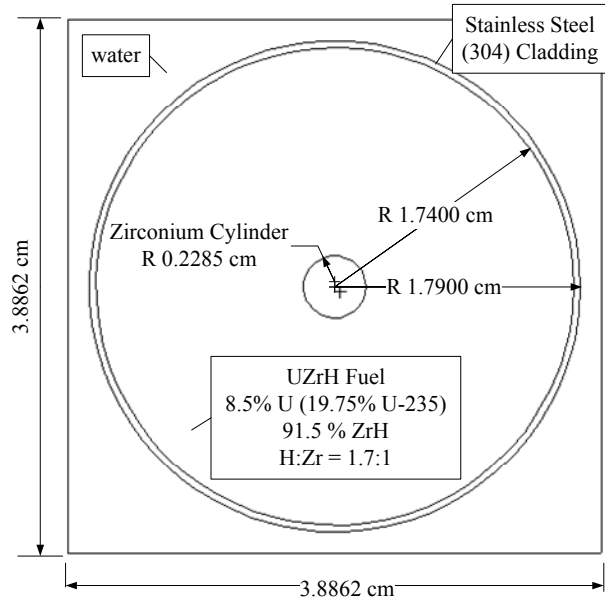


Figure 3.5: MCNP Model of the U-ZrH Fuel-Moderator Element Lattice Cell.

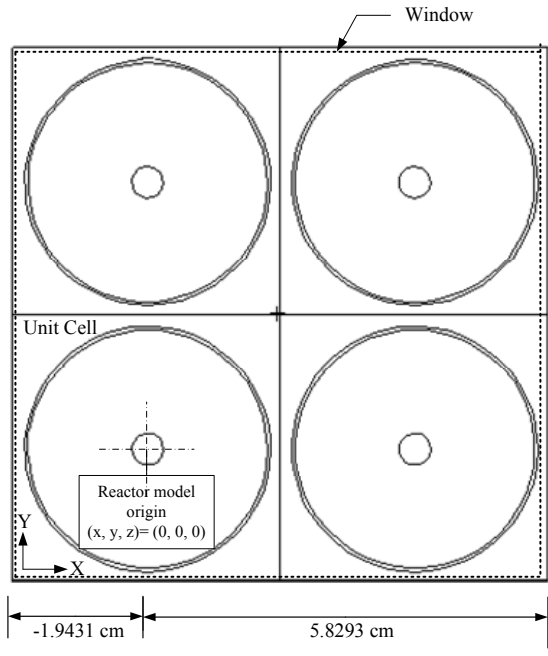


Figure 3.6: MCNP Model the Four-Rod Cluster Lattice

3.3.5 Control Rods

Reactivity control for the MUTR is done using three control rods. Each control rod, Figure 3.7, is 43.2 cm (17 in) in length and contains borated graphite, B_4C , in powder form. The top and bottom fittings are welded to an aluminum can which has a cladding thickness of 0.71 mm (0.028 in). The completed welded can is helium leak tested before B_4C is poured into the can through a sinkhole in the bottom fitting. The top fitting is threaded to accommodate a connecting rod extending from the fuel lattice to the rod drive mechanism.

3.3.6 Control Rod Fuel Cluster

To accommodate a control rod, one fuel rod in a cluster is replaced by a control rod guide tube that has the same outside diameter and screw end bottom fitting as a fuel rod. The aluminum handle and locking plate on the control rod cluster was modified to accommodate the guide tube.

3.3.7 MCNP Model of Control Rod Fuel Cluster

The three-rod fuel and control element, Figure 3.7, is constructed the same way as the four-rod fuel cluster except that one lattice cell is filled with the control element that is assigned the universe number $U=3$ rather than the fuel universe $U=1$. The geometry of the control rod, the boron carbide poison, aluminum cladding, and the top and bottom plugs, are modeled exactly according to engineering drawings [34].

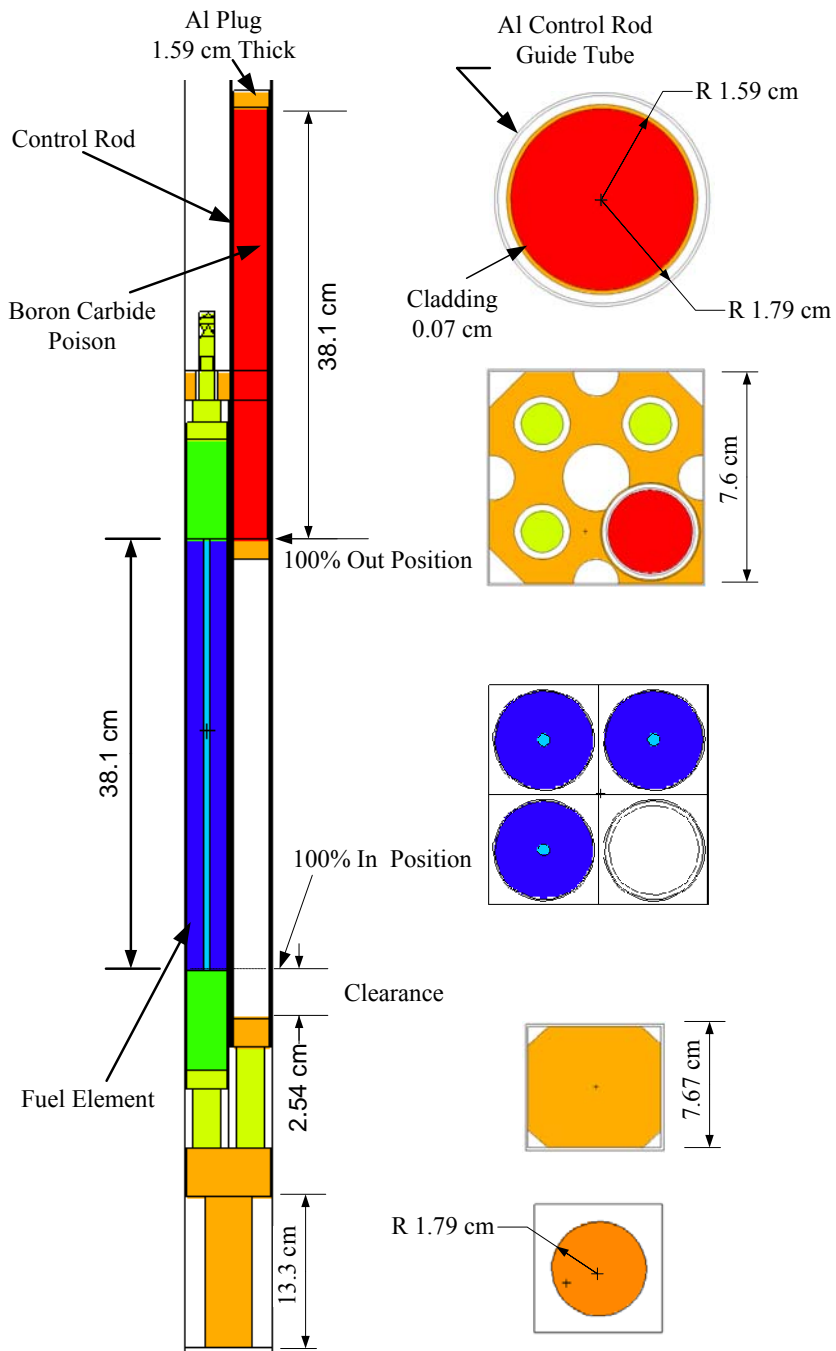


Figure 3.7 :MCNP Model of Control Rod Fuel Cluster

3.3.8 The Pneumatic Transfer System—the Rabbit

A pneumatic transfer system, the rabbit, provides a rapid and convenient means of transferring small samples between the hot room and the reactor core. The control system for the pneumatic transfer system is located in the control room. The driving force for this system is available pressurized CO₂. The transfer system consists of a pneumatic mechanism located in an exhaust hood, polyethylene tubing for transferring samples between the laboratory and core, and a terminus located in core position C-4. The MCNP model of the rabbit and a cut away drawing of the terminus are shown in Figure 3.8.

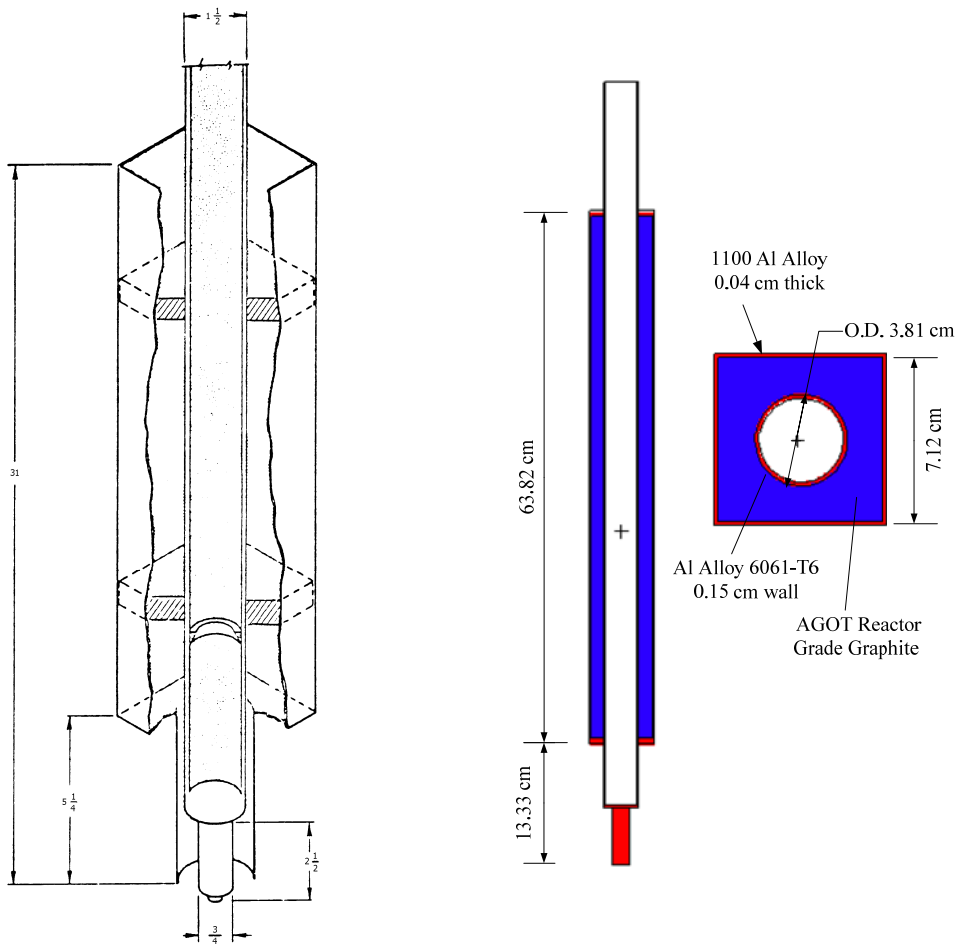


Figure 3.8: Pneumatic Transfer System Terminus: Rabbit left, schematic of actual drawings; right, MCNP model.

3.3.9 Neutron Moderator and Reflector

The MUTR has four types of neutron moderator and reflectors. The first is the reactor pool water that is used for both moderator and coolant. The second is in the form of graphite slugs located above and below the fuel region of each TRIGA fuel element, (see Figure 3.2). The third are two aluminum encapsulated graphite blocks located in grid positions D2 and E2, (see Reactor). The MCNP model of the graphite blocks is shown in Figure 3.9.

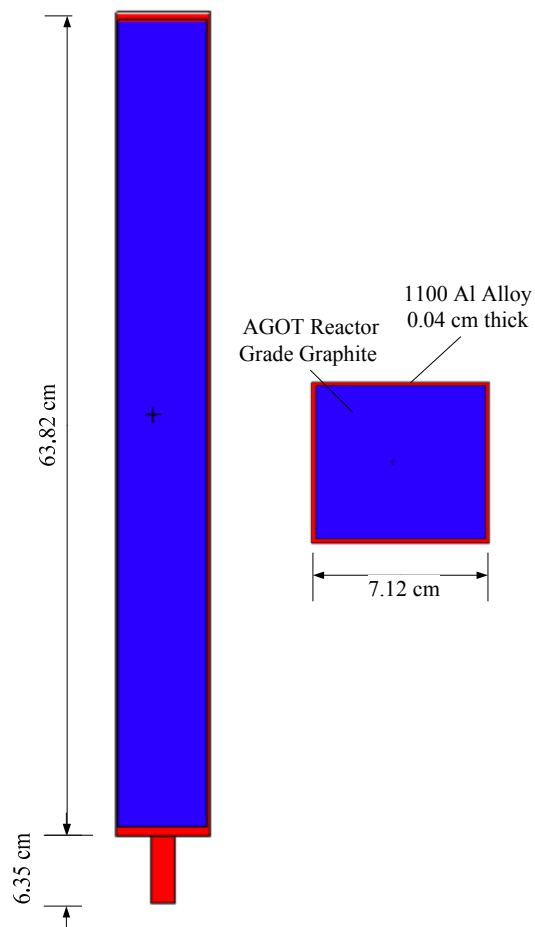


Figure 3.9: MCNP model of the Graphite Reflector Block

3.3.10 The Thermal Column

The thermal column, Figure 3.10, is a graphite filled housing extending from within 0.953 cm (0.375 in) of the back face of the core through the pool tank wall and the concrete shield. The core end of the housing is a 0.953 cm (0.375 in) thick aluminum sleeve that passes through an aluminum nozzle welded to the pool tank wall. The sleeve is bolted and gasketed to a flange, which connects the nozzle and the thermal column liner. The liner extends through the concrete shield and accommodates a steel-concrete shield plug at its outer end.

The graphite assembly, Figure 10.2, consists of 25.81 cm² (4 in²) graphite stringers arranged to form a stepped column 1.52 m (5 ft) long. The section forward of the step is 0.959 m (37.75 in) long and 0.610 m (2 ft) wide in which the stringers are arranged in a 6 x 6 pattern. The outer section of the graphite column is 0.565 m (22.25 in) long and 0.813 m (32 in) wide and its stringers are arranged in an 8 x 8 pattern surrounded with 0.318 cm (0.125 in) thick boral. There are small slots and holes in the stringers to accommodate experimental samples in the region of high thermal neutron flux. Lead bricks surround the outer end of the thermal column graphite for shielding. The thermal column shield plug at the outer end of the thermal column liner is 1.041 m (41 in) long and 1.010 m (39.75 in) on each edge. It consists of concrete covered on all sides with 1.27 cm (0.5 in) of carbon steel. On the core side, it is additionally covered with 0.318 cm (0.125 in) of boral. The plug rides within the liner on rollers and contains a smaller carbon steel-covered concrete access plug with 0.318 cm (0.125 in) of boral on its forward end. When the access plug is

removed, four stringers are exposed and may be removed in sections of different lengths to form experimental holes of various sizes.

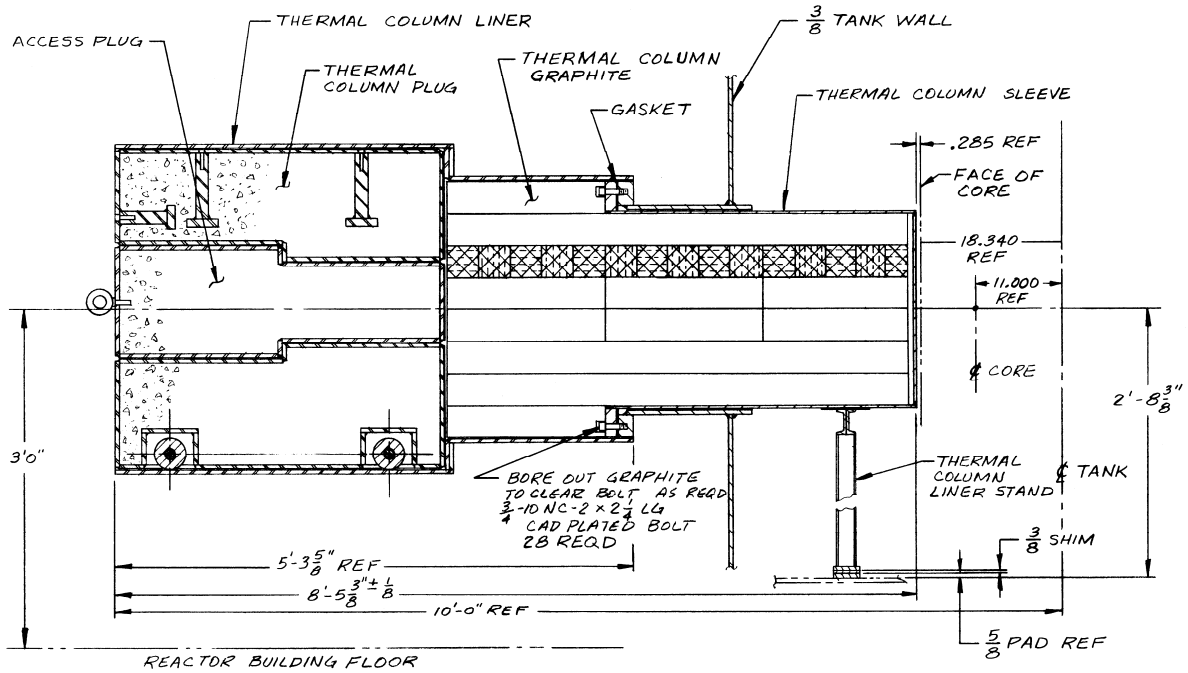


Figure 3.10: Thermal Column [27]

3.4 MCNP Geometry Model of MUTR

As was mentioned earlier, the MCNP model of the MUTR comprises several units: the core, peripheries and auxiliaries. The core was modeled as a one dimensional 9 x 6 lattice. Each core lattice element is either a four-rod fuel cluster or a three-rod fuel and control cluster. A schematic of the current layout of the core is shown in Figure 3.11. The MCNP model of the core layout during initial startup is shown in Figure 3.12.

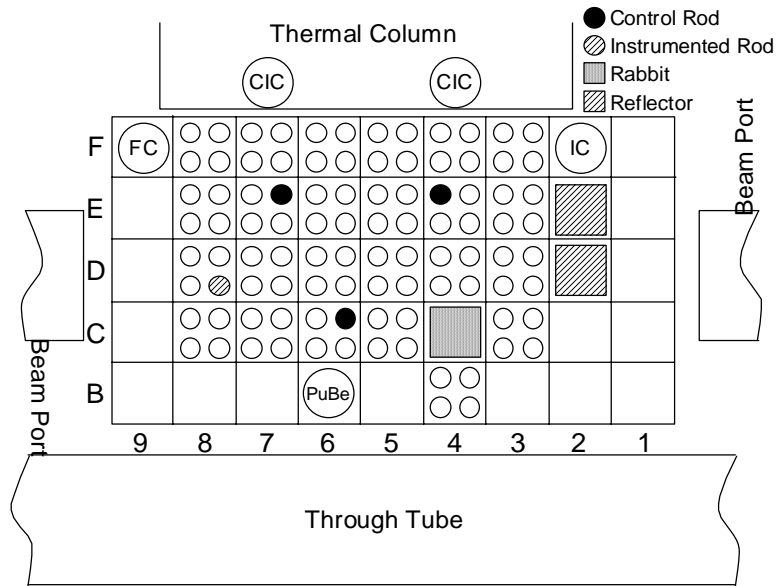


Figure 3.11: Current MUTR Core Layout

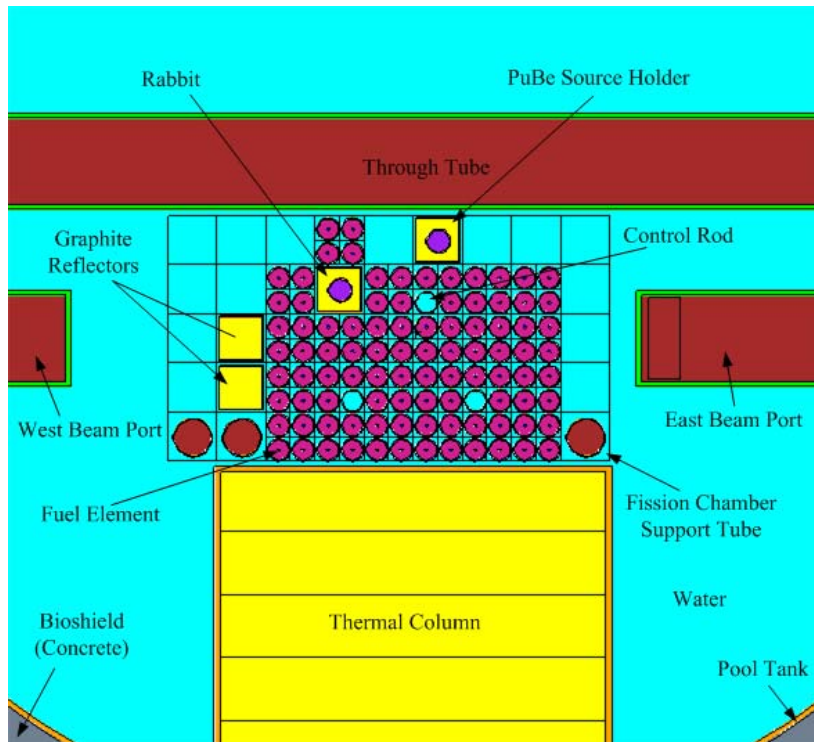


Figure 3.12: MCNP Model of MUTR

The four-rod fuel cluster is assigned universe U=4. Three four-rod fuel and control elements, named Shim I, Shim II, and Shim III are assigned universes U=8, 10, and 12, respectively. Shim III is the regulating rod. The reason for assigning three different universes for the control rods is to treat them independently so each can be inserted and removed without affecting the geometry of the other control rods. This is one of the powerful features of the repeated structure capability of MCNP. The graphite reflectors are assigned universe U=13. The pneumatic transfer system—the rabbit, is assigned universe U=18. The graphite PuBe source holder is assigned universe U=24. A core lattice element, which also serves as a universe to fill itself is assigned universe U=5. Now with all core elements are assigned distinct universes, the 9 x 6 core lattice ([1-9] x [A-F]) (see Figure 3.13) can be filled with the proper combination of the different universes to reflect a core condition at a point in time. The method thus outlined is adapted from [28, 29]. See Appendix A for the MCNP full model of the MUTR at initial startup.

| | | | | | | | | | |
|-------|---|----|----|----|----|----|---|---|------|
| ----- | | | | | | | | | |
| 5 | 5 | 4 | 4 | 4 | 4 | 4 | 4 | 5 | \$ F |
| 5 | 5 | 4 | 8 | 4 | 4 | 10 | 4 | 5 | \$ E |
| 5 | 5 | 4 | 4 | 4 | 4 | 4 | 4 | 5 | \$ D |
| 5 | 5 | 4 | 18 | 4 | 12 | 4 | 4 | 5 | \$ C |
| 5 | 5 | 13 | 4 | 13 | 24 | 5 | 5 | 5 | \$ B |
| 5 | 5 | 5 | 5 | 5 | 5 | 5 | 5 | 5 | \$ A |
| ----- | | | | | | | | | |
| 1 | 2 | 3 | 4 | 5 | 6 | 7 | 8 | 9 | \$ |
| ----- | | | | | | | | | |

Figure 3.13: Core Lattice Filled with Universes During Initial Startup

3.5 Materials Used in the MCNP Model

The composition of materials used in the MCNP model of the MUTR is listed in Table 3.1. The data used are extracted from Reference [35]. When materials are not found in Reference [35], their source is identified in the literature. The purpose of the development of Reference [35] is to provide standardization in transport calculations so as minimize results variations when benchmarks are done.

Table 3.1: Materials Composition used in MCNP Model of MUTR

| MCNP M# | Material | | Nuclide | Weight Fraction | Density (g/cm ³) |
|---------|---|-------------------------|------------------|-----------------|------------------------------|
| M1 | Fuel/Moderator | U-ZrH | ²³⁸ U | 0.068213 | 5.90-6.00 |
| | | | ²³⁵ U | 0.016788 | |
| | | | Zr | 0.898617 | |
| | | | H | 0.016383 | |
| M4 | Cladding (Stainless Steel 304) | | Fe | 0.695000 | 7.92 |
| | | | Cr | 0.190000 | |
| | | | Ni | 0.095000 | |
| | | | Mn | 0.020000 | |
| M3 | Reflector [36] (AGOT Nuclear Grade Graphite) | | C | 1.000000 | 1.60-1.75 |
| M2 | Zirconium Rod | | Zr | 1.000000 | 6.50 |
| M4 | Top/Bottom fittings | | M4 | | |
| M7 | Control Rod | B ₄ C Poison | C | 0.782610 | 2.51 |
| | | | B | 0.217390 | |
| M6 | Cladding [37] (Al Alloy 6061) | | Al | 0.975114 | 2.7 |
| | | | Cu | 0.005861 | |
| | | | Si | 0.006218 | |
| | | | Mg | 0.008970 | |
| | | | Cr | 0.003837 | |
| M5 | Moderator/Coolant | Water | H | 0.11 | 1.0 |

| | | | O | 0.89 | | |
|-----|---------------------------|--|----------|----------|----------|---|
| M6 | Graphite Reflector Blocks | (AGOT) Nuclear Grade Graphite | C | 1.000000 | 1.6-1.75 | |
| | | | Al | 0.992120 | | |
| | | | Cu | 0.004455 | 2.7 | |
| | | | Mn | 0.001013 | | |
| | | | Zn | 0.002412 | | |
| | PuBe Source Holder | Graphite Cladding [37] (Al Alloy 1100) | M6 M6 | | | |
| | Pneumatic Transfer System | Graphite | M3 | | | |
| | | Cladding (Al Alloy 1100) | M6 | | | |
| M16 | Thermal Column | Graphite | C | 1.000000 | 1.6-1.75 | |
| | | Cladding (Al Alloy 1100) | M6 | | | |
| M10 | Beam Tubes | Plugs (Concrete) | H | 0.022100 | 2.25 | |
| | | | C | 0.002484 | | |
| | | | O | 0.574930 | | |
| | | | Na | 0.015208 | | |
| | | | Mg | 0.001266 | | |
| | | | Al | 0.019953 | | |
| | | | Si | 0.304627 | | |
| | | | K | 0.010045 | | |
| | | | Ca | 0.042951 | | |
| | | | | Air | | C |
| | | | | N | 0.755268 | |
| | | | | O | 0.231781 | |
| | | | | Ar | 0.012827 | |
| | | Wall (Stainless Steel 304) | M4 | | | |

3.6 MCNP Criticality Calculation Setup

3.6.1 Structure of the MCNP Input File

The MCNP input file [6] describes the problem geometry, specifies the materials and the source, and defines the results desired, and the output quantities, such as flux dose, spectrum, and so forth. These output quantities are known as tallies. The geometry is built by defining cells that are bound by one or more surfaces, and combinatorial geometry logic (union, intersection, and complement) is applied to assign materials to cells (Figure 3.14). The union operation may be thought of as a logical OR, in that the union of A and B is a new region containing all space either in region A OR region B. The intersection operation may be thought of as a logical AND, in that the result is a region that contains only space common to both A AND B. The complement operator # plays the roll of a logical NOT. For example # (A:B) represents all space outside the union of A and B. With these three logical operations—OR, AND, and #, the complement operator—any conceivable geometry can be defined.

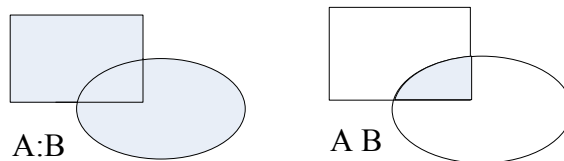


Figure 3.14: Combinatorial Geometry Logic
Left: the union A:B or “A or B”. Right: the intersection A B or “A and B”.

An MCNP input file has three major sections: cell cards (lines of input), surface cards, data cards. A single (line) data card precedes the cell card section. In MCNP, lines of input are referred to as cards; the term is historical, and was carried over from

the “early days” of computer punch cards. Figure 3.15 shows the MCNP input file structure.

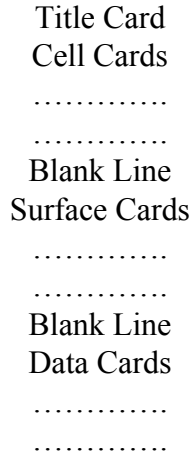


Figure 3.15: MCNP Input File Structure

An example Figure 3.16 shows an actual and complete MCNP input file for criticality problem of a 5 cm radius sphere of uranium enriched to 90%.

```

Title: Simple MCNP Input File
C      Cell Cards
C      Mat# g/cm3
1      M1 -p -1 imp:n=1
2      0      1 imp:n=0

C      Surface Cards
1      SO 5

C      Data Cards
C      Source Specification
C      Criticality Source
C      nsrck rkk ikz ket
Kcode 1000 1.0 15 100
Ksrc 0 0 0
C      Tallies
F4      1
C      Materials Specification
C      ZZZAAA W/O
M1      92235.66c -0.900000 92238.66c -0.100000

```

Figure 3.16: A Simple MCNP Input File

The first line of input file is the optional problem title. Cell cards follow the title card and at any place in the input file, a comment card can be inserted. The comment card starts with a “C.” Both upper and lower case characters are allowed in all input. In the cell definition, the first entry is the material number for the material defined in the data card section; the second entry is the density, followed by the combinatorial geometry specification of the cell, and an importance (imp:p=k) is assigned to each cell in the problem except the outer space surrounding the geometry, which is known as the “outside world.” A blank line is inserted after the cell cards section. In the surface cards section, the geometry is defined by using special symbols for the surfaces. For Example, in Figure 3.16 the uranium sphere is defined as “SO,” which is a sphere centered at the origin of the problem’s coordinate system. With the sphere, a single parameter defines the radius. In the data cards section, the source (for the type of transport, whether criticality or otherwise), cross sections libraries, and tallies are specified. Cross sections specification takes the format “ZZZAAA.LIBx,” where the first three digits represent the “Z” number of the nuclide in question, and A identifies its “A” number. LIB is the library from a particular evaluation (e.g. ENDF VI, VII), “x” signal whether continuous energy (c) or discrete (d) data should be used. In the input example, continuous cross sections evaluated at room temperature are used.

3.6.2 Setup of the MCNP Criticality Calculations

The criticality calculation must have a “kcode” card set in the data section of the MCNP input file (Figure 3.16). In this case, the criticality problem is run with 1000 neutrons per cycle (nsrck), and an initial guess of k_{eff} of 1.0 (rkk). Fifteen cycles

(ikz) are skipped before k_{eff} data tallying begins, and a total of 100 cycles (kct) are run.

3.7 Precision of the Monte Carlo Calculations

MCNP tally results are normalized to be per starting particle and accompanied by the estimated relative error R defined to be one estimated standard deviation of the mean $S_{\bar{x}}$ divided by the estimated mean \bar{x} [6]. Because the relative error is not fixed, it appropriate to call it “uncertainty.” For a well-behaved tally, R will be proportional to $1/\sqrt{N}$ where N is the number of histories. Thus, to reduce R by half, the total number of histories must be increased fourfold. For a poorly behaved tally, R may increase as the number of histories increases. The estimated relative error can be used to form confidence intervals about the estimated mean, allowing one to make a statement about what the true result is. The Central Limit Theorem states that as N approaches infinity there is a 68% chance that the true result is in the range $\bar{x}(1 \pm R)$ and a 95% chance in the range $\bar{x}(1 \pm 2R)$. These confidence statements refer only to the precision of the Monte Carlo calculation itself and not to the accuracy of the result compared to the true physical value. A statement regarding accuracy requires a detailed analysis of the uncertainties in the physical data, modeling, sampling techniques, and approximations, etc., used in a calculation.

3.8 Variance Reduction

Since R (the estimated relative error) is proportional to $1/\sqrt{N}$, where N is the number of histories, for a given MCNP run, the computer time expended T is proportional to N . Thus $R = C/\sqrt{T}$, where C is a positive constant. There are two

ways to reduce R : either increase T and/or decrease C . Computer budgets often limit the utility of the first approach. For example, if it has taken 2 hours to obtain $R = 0.10$, then 200 are required to obtain $R = 0.01$. For this reason MCNP has special variance reduction techniques for decreasing C . The constant C depends on the tally choice and/ or the sampling choices.

3.9 Analog and Non Analog Monte Carlo Sampling

To explain how sampling affects C it is necessary to understand the nonanalog Monte Carlo technique. The simplest Monte Carlo model for particle transport problems is the analog model that uses the natural probabilities that various events occur (for example, collision, fission, capture, etc.). Particles are followed from event to event by a computer, and the next event is always sampled (using the random number generator) from a number of possible next events according to the natural event probabilities. This is called the analog Monte Carlo technique because it is directly analogous to the naturally occurring transport [6, 38].

The analog Monte Carlo model works well when a significant fraction of the particles contribute to the tally estimate and can be compared to detecting a significant fraction of the particles in the physical situation. There are many cases for which the fraction of particles detected is very small (less than one in a million). For these problems analog Monte Carlo fails because few, if any, of the particles reach their intended target, and the statistical uncertainty in the answer is unacceptable.

Although the analog Monte Carlo model is the simplest conceptual probability model, there are other probability models for particle transport that estimate the same average value as the analog Monte Carlo model, while often making the variance

(uncertainty) of the estimate much smaller than the variance for the analog estimate. In this case problems that would be impossible to solve in days of computer time with analog methods can be solved in minutes of computer time with nonanalog methods.

A nonanalog Monte Carlo model attempts to follow “interesting” particles more often than “uninteresting” ones. An “interesting” particle is one that contributes a large amount to the quantity (or quantities) that needs to be estimated. There are many nonanalog techniques, and all are meant to increase the odds that a particle scores (contributes). To ensure that the average score is the same in the nonanalog model as in the analog model, the score is modified to remove the effect of biasing (changing) the natural odds. Thus, if a particle is artificially made q times as likely to execute a given random walk, then the particle’s score is weighted by (multiplied by) $1/q$. The average score is thus preserved because the average score is the sum, over all random walks, of the probability of a random walk multiplied by the score resulting from that random walk. A nonanalog Monte Carlo technique will have the same expected tallies as an analog technique if the expected weight executing any given random walk is preserved. For example, a particle can be split into two identical pieces and the tallies of each piece are weighted by $1/2$ of what the tallies would have been without the split. Such nonanalog, or variance reduction, techniques can often decrease the relative error by sampling naturally rare events with an unnaturally high frequency and weighting the tallies appropriately.

Variance reduction techniques, used correctly, can tremendously help the user obtain a more efficient calculation. If however, used poorly, they can result in a wrong answer with good statistics. Some variance reduction methods have general

application and are not easily misused. Others are more specialized and attempts to use them carry high risk. For example, weight windows are the most powerful variance reduction method to obtain precise results in the shortest possible time, but their use requires more input data and more insight into the problem.

For many problems, variance reduction is not just a way to speed up the problem but is absolutely necessary to get any answer at all. Deep penetration problems, such as the calculation of neutron flux deep into the thermal column access plug or deep inside the beam ports, will run too slowly by factors of trillions without adequate variance reduction.

3.10 Validity of the Monte Carlo Precision

To have confidence in the results of the Monte Carlo calculations, MCNP performs ten statistical checks of the tally. The quantities involved in these checks are the estimated mean, R (relative error), VOV (variance of the variance), FOM (figure of merit) $=1/(R^2T)$ where T is the simulation time, and the large history score behavior of the history probability density functions, $f(x)$.

There are several variance reduction techniques available, but for this particular reactor problem weight windows are used, in spite of their notorious nature and the lack of literature about their use—that is because weight windows are highly dependent on the particular problem at hand and only general instruction is provided in the MCNP manual. Only after many failures successful implementation of the weight windows was achieved.

Chapter 4: Results and Discussion

4.1 Summary of the Results

The objective of this work was: first, to investigate whether approximations or simplification in the MCNP geometry model of the University of Maryland TRIGA Reactor has any bearing on the calculated fluxes in the experimental facilities of the reactor; namely, the thermal column, beam ports, through tube, and the pneumatic transfer system rabbit; second, to benchmark the reactor model against available experimental data; and third, to use the MCNP model to plan future experiments performed in the various experimental facilities of the reactor. Two models for the reactor were created: a detailed model and a simplified model. The detailed model attempted to create the MCNP geometry according to detailed engineering specifications. The simplified model includes only basic geometrical details deemed necessary for a realistic reactor; however, as shown below, these approximations do not alter results when both models are run at full reactor power, 250 kW. Table 3.1 shows the summary of the results of the Monte Carlo calculations as compared to available experimental data obtained at various locations of the reactor experimental facilities.

Table 4.1: Comparison of Experimental and MCNP Calculated Flux Data

| | Face of Thermal Colum Access Plug | ¹ Pneumatic Transfer System (Rabbit) | ² Pneumatic Transfer System (Rabbit) | Through Tube | Center of Fuel |
|-------------------------|-----------------------------------|---|---|---------------------------|------------------------|
| Thermal Flux | n/cm ² /sec/W | n/cm ² /sec | n/cm ² /sec/kW | n/cm ² /sec/kW | n/cm ² /sec |
| MCNP Detailed | 4.6262×10^3 | 4.38×10^{12} | 1.75×10^{10} | 1.67×10^9 | 6.04×10^{12} |
| MCNP Approx | 4.6215×10^3 | 4.16×10^{12} | 1.66×10^{10} | N/A | N/A |
| Experiment | 4.4203×10^3 | 5.39×10^{12} | 1.60×10^{10} | 1.60×10^9 | 5.70×10^{12} |
| ³ Difference | 4.4 % | 18.8% | 9.7% | 4.4% | 6.0% |
| Fast Flux | | > 1 MeV | > 0.1 MeV | > 0.1 MeV | |
| MCNP Detailed | 4.4205×10^3 | 1.52×10^{12} | 1.36×10^{10} | 1.02×10^9 | 6.04×10^{12} |
| MCNP Approx | 4.4205×10^3 | 1.42×10^{12} | 1.25×10^{10} | N/A | N/A |
| Experiment | 4.6459×10^3 | 1.12×10^{12} | 8.00×10^9 | 1.10×10^9 | N/A |
| Difference | 4.9 % | 35.9% | 69.6% | 7.6% | |
| Total Flux | | | | | |
| MCNP Detailed | 4.4205×10^3 | 6.14×10^{12} | 3.11×10^{10} | 2.69×10^9 | 6.04×10^{13} |
| MCNP Approx | 4.4205×10^3 | 5.58×10^{12} | 2.92×10^{10} | N/A | N/A |
| Experiment | 4.6408×10^3 | 6.51×10^{12} | 2.40×10^{10} | 2.70×10^9 | N/A |
| Difference | 4.7 % | 5.7% | 29.7% | 0.5% | |

¹ Belcher, R. L., Final Startup Report, University of Maryland TRIGA Fueled Reactor, 1974.

² Gavrillas, Mirela, The Gospel, MUTR Neutron Flux Measurement, University of Maryland, College Park, Maryland, 1987.

³ The difference is between the detailed model and experimental results.

4.2 Reactor Core Criticality Calculations

The method showing how the reactor geometry model is built is described in Sections 3.4; the criticality model setup is described in Section 3.6.

MCNP code (version 5) and MCNPX (version 2.6D) were used interchangeably to model the core configuration with continuous energy neutron cross-section data evaluations from ENDF/B-VI and VII libraries [51]. As far as criticality calculations are concerned, both MCNP and MCNPX are identical except that burnup calculations can only be performed with MCNPX. The free gas scattering kernel model was chosen, except for hydrogen in light water; hydrogen and zirconium in zirconium hydride, and graphite, for which the appropriate $S(\alpha,\beta)$ data at the appropriate temperatures (300-600 K) were employed to account for chemical molecular binding and crystalline effects that become important as neutron energy becomes sufficiently low—below 4 eV.

Most of MCNP calculations used 2000-5000 starting fission neutrons, 100 cycle were skipped to improve the spatial distribution of the source in the core, an initial guess of $k_{\text{eff}} = 1.0$ was used. The total number of histories is the total number per cycle multiplied by the number of active cycles. MCNP tallies three basic k_{eff} estimators (track-length, collision and absorption) and reports a best estimate of combined k_{eff} value together with the estimated standard deviation. The MCNP simulations were run on 3.2 Dell Xeon Work Station and it took at most 48 hours to achieve adequate statistical convergence in the calculations. Parameters of each set of

calculations together with the standard error associated with each specific calculation are listed separately.

Although a step-by-step method was adopted to build the core geometry, the whole process did not go without problems. One particular fatal error (MCNP can not proceed if it encounters a fatal error) in the first MCNP full core required a tremendous effort to discover and fix. That error is the “zero lattice element hit.” When MCNP encounters this fatal error, the error message that MCNP gives does not tell the user how to fix the problem. This is an exception, since MCNP has a very rich error message database and in most cases the error message is self descriptive. However with the “zero lattice element hit” fatal error, the MCNP manual describes it as a “bug,” when it is in fact a geometry error. Without a step-by-step model-built process that keeps track of the input files at various stages of the model development, this type of error can be catastrophic; it can not be fixed in a reasonable time and the user is forced to start all over again. However, if a user keeps track of previous stages, only one step is lost. The “zero lattice element hit” fatal error and how it was fixed is described. As has been described in Section 3.3.1, the core is an infinite lattice that is housed in a window. The window dimensions must be a tiny fraction smaller than the desired lattice dimensions. For example if there is a 2 x 2 lattice, with the lattice element dimensions 1 cm x 1 cm, and a fill (u=3) 3 3 3 3 in the x-y directions, then this four element lattice is 2 cm x 2 cm. The window should be 1.999999 cm x 1.999999 cm. As a rule, the window surfaces can not coincide with the problem geometry surfaces that it encloses. If the window is larger, then another lattice element starts, which does not have a fill (u=3)! That leads to the fatal error.

4.3 Calculation of the Neutron Flux Spectrum at the Thermal Column

The detailed reactor core model (Figure 4.1, and Figure 4.2) was used to compute the neutron flux in the thermal column access plug face. Figure 4.4 shows a top view of the MUTR reactor core and all experimental facilities: through tube, beam ports, rabbit system, and the thermal column.

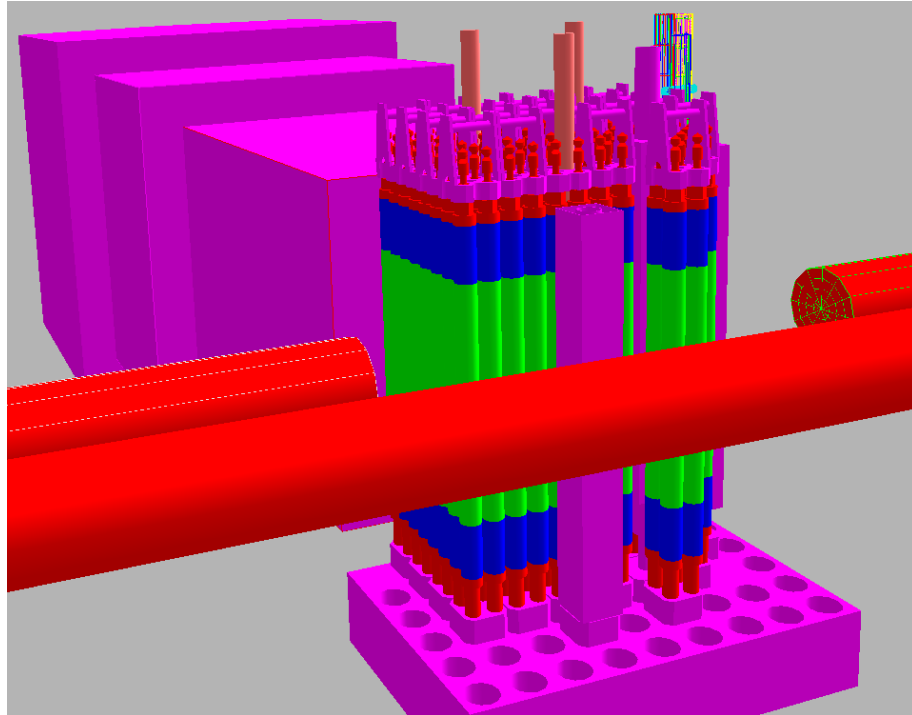


Figure 4.1: MCNP Model of UMD Reactor Core, Grid Plates, Beam Tubes, Thermal Column

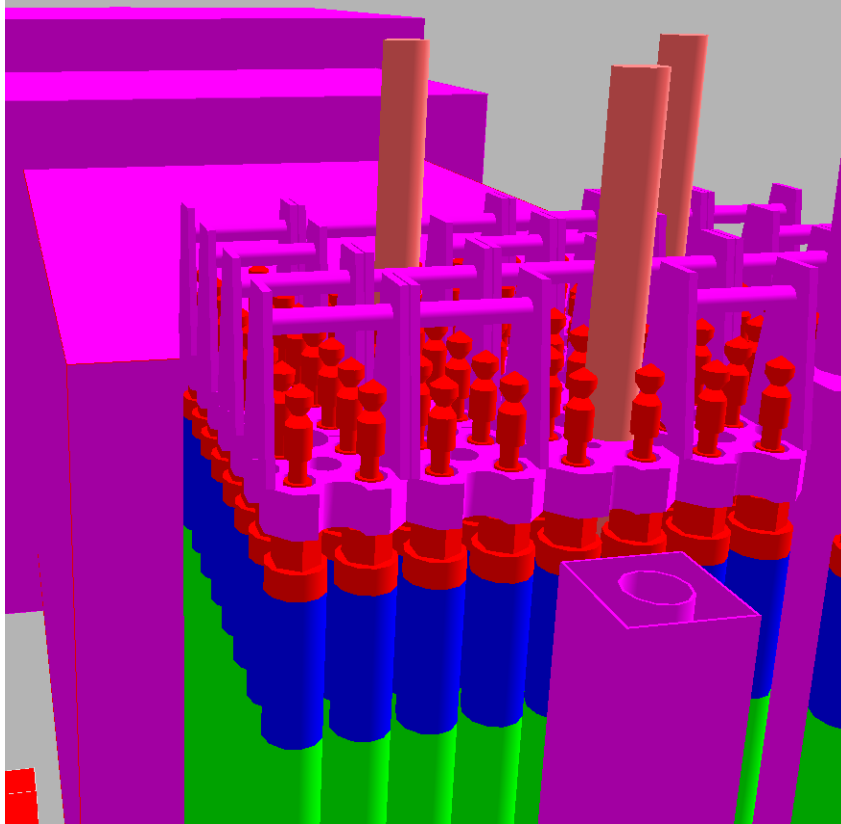


Figure 4.2: A Close-up view of the UMD Reactor Detailed Core Model

It was first attempted to get results by performing analog calculations but results with very poor statistics were obtained. It was apparent that an analog calculation to compute the neutron flux far deep in the thermal column at the face of the access plug (where most bio-sample irradiations occur) would never converge in a reasonable time. Hence a non-analog calculation must be performed.

4.4 Weight Windows

To fully describe the weight windows variance reduction technique, another variance reduction method essential to the understanding of weight windows, “geometry splitting and Russian roulette,” is explained. Geometry splitting/Russian roulette is a widely used variance reduction techniques. It is objective is to spend

more time sampling important (spatial) cells and less time sampling unimportant cells.

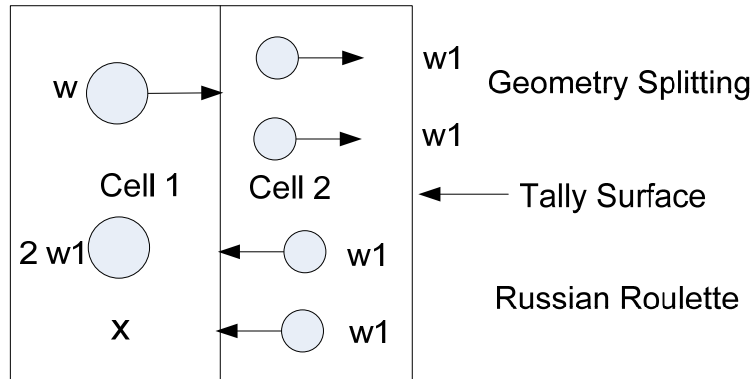


Figure 4.3: Geometry Splitting and Russian Roulette

In the geometry splitting and Russian roulette the technique (Figure 4.3) the following is performed:

1. The problem geometry is divided into cells;
2. An importance value, I_n , is assigned to each cell; and
3. when crossing from cell m to cell n (cell 1 to cell 2 in Figure 4.3), the ratio

$\zeta = I_n / I_m$ is computed. If

- a. $\zeta = 1$, continue particle transport
- b. $\zeta < 1$, play Russian roulette,
- c. $\zeta > 1$, split the particle into $\zeta = I_n / I_m$ tracks.

The Russian roulette is played as follows: if $\zeta < 1$, the particle is entering an “unimportant” cell and less sampling in it is desired, so the particle plays a Russian roulette. That is, with probability ζ , the particle avoids death, and its weight (w_1) is multiplied by $\zeta - 1$, or with probability $1 - \zeta$, the particle is killed (shown by X in Figure 4.3).

The weight window is a space-energy-dependent splitting and Russian roulette technique. For each space-energy phase-space cell, a lower and upper weight bounds are supplied to MCNP manually by the user, or automatically by the weight window generator. If a particle is below the weight lower weight bound, Russian roulette is played and the particle weight is either increased to be within the window, or the particle is killed. If the particle is above the upper weight bound, the particle is split so as all the split particle are within the window. No action is taken on the particle if it is found within the window. A detailed analysis for some weight windows examples is found in the literature [38, 39].

4.5 The Thermal Column Flux Calculation Optimization

After the detailed core model was successfully run, the thermal column was constructed and an analog calculation was run. The results obtained showed poor statistics and it was apparent that an analog calculation would not work for a tally region far from the source. The face of the thermal column plug is the intended tally region (see Figure 4.4). The geometry of the thermal column is constructed separately and a fixed photon source was tried first. Figure 4.5 shows particle tracks for the analog and non analog calculations of the same number of histories. It was clear that by using weight windows, more particles are being transported to the tally region efficiently.

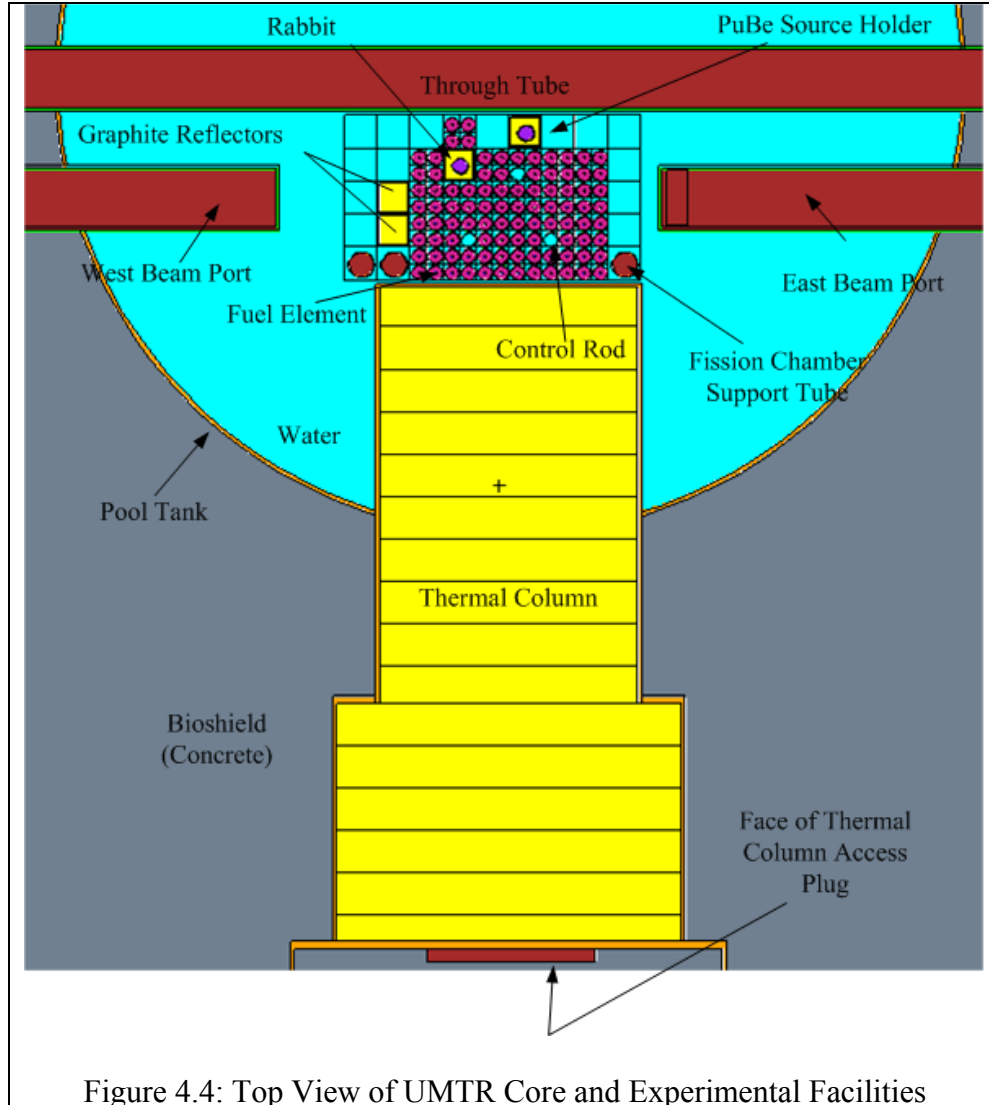


Figure 4.4: Top View of UMTR Core and Experimental Facilities

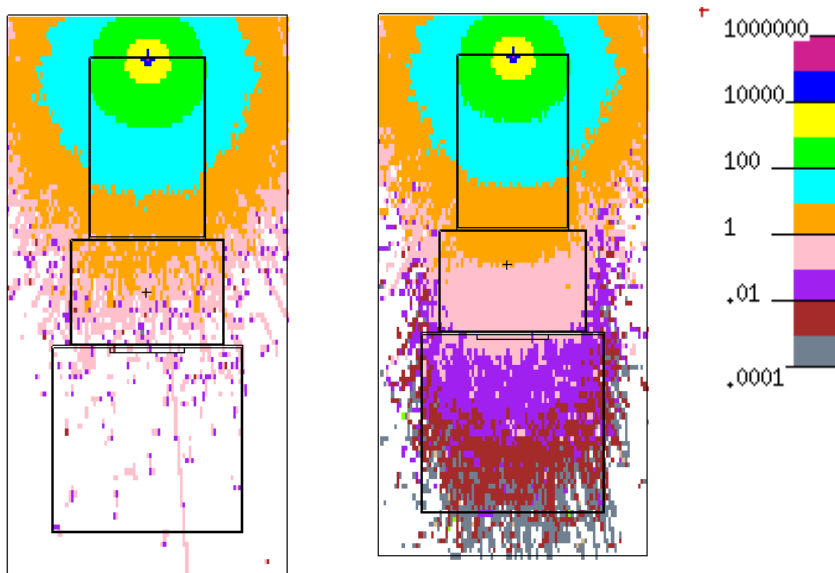


Figure 4.5: Particle Tracks for Analog and Non Analog Transport
 Left: analog—photons. Right: nonanalog weight windows mesh.
 Both runs are for 1,000,000 histories.

4.6 Results of the thermal Column Calculations

The criticality calculation was run for 2000 neutrons per cycle, with an initial k_{eff} guess of 1.0, 100 cycles were skipped, and a total of 4000 cycles (8,000,000 histories) were run. Delayed neutrons production was turned on, and an automatic weight window generator is used to produce the weight window importance mesh. The mesh was constructed in such a way to avoid the core entirely; otherwise MCNP issues a “bad trouble” error message which is fatal. The mesh is shown in Figure 4.6. The reactor was run at 250 kW, the pool, fuel temperatures were 15 °C and 101 °C, respectively. $S(\alpha,\beta)$ cross sections for both hydrogen and zirconium in zirconium hydride, were used with ENDF/B VII (Evaluated Nuclear Data File version B) continuous energy cross section data evaluated at 400 K. $S(\alpha,\beta)$ cross sections for the

thermal column's graphite evaluated at 293 K were used. The results of the MCNP calculations are always normalized to per source particle; thus, the criticality calculation must be normalized by the steady-state power of 250 kW. Therefore, to produce P watts, $3.467 \times 10^{10} P$ fissions per second are needed [6]. This power level produces $3.467 \times 10^{10} P \times \nu$ neutrons/sec, which is the neutron source strength per second for power level P . The average neutrons produced per fission, ν , is calculated by MCNP and printed in the output.

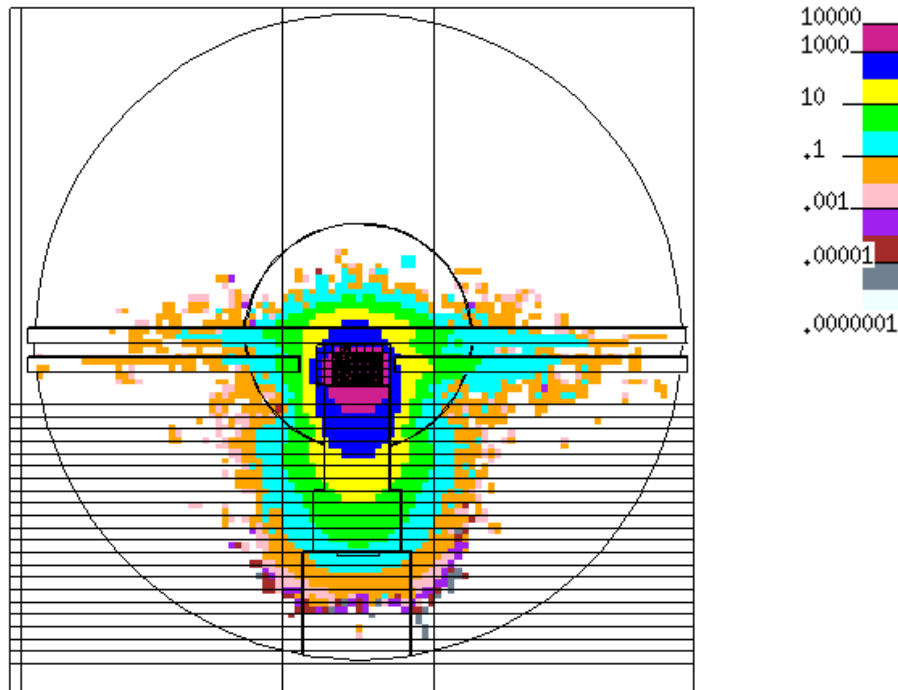


Figure 4.6: Weight Window Mesh for Thermal Column
Legend color indicates number of neutrons.

The flux was calculated at the thermal column's access plug face inside a volume filled with air which measures 40 cm x 40 cm x 3 cm. Figure 4.4 shows the face of

the access plug. Results of the neutron flux spectrum at the thermal column access plug calculations are shown in Figure 4.7. The unfolded spectrum is the measured result, which compares well with the detailed MCNP calculations within a 5% uncertainty for both the thermal (< 3 eV) and the total flux. The large ($> 100\%$) uncertainty at the lower end of the spectrum can be attributed to several factors: approximation in modeling details of the access plug, the temperature at the access plug, temperature at the thermal column near the face of the core, and uncertainty in cross sections evaluations at low energy. As seen in Figure 4.7, core geometry approximations were not found to alter the results (MCNP detailed vs MCNP approximated at 300 K). The temperature here is related to $S(\alpha, \beta)$ cross sections evaluations of graphite. It is safe to assume that the thermal column temperature was in equilibrium with the pool temperature, which was at $15\text{ }^{\circ}\text{C}$ (288 K). The cross sections used in the calculations are evaluated at 300 K. To see the effect of temperature, an $S(\alpha, \beta)$ cross sections for graphite evaluated at 400 K is used and the results are shown in Figure 4.7 (MCNP detailed at 400 K). The spectrum clearly is hardened or shifted to the higher energy region. The right (presumably correct) spectrum is in between. In the MCNP calculations, an increase in the temperature of the thermal column because of heating due to gamma rays was not taken into account, and that could be the source of the spectrum shift. Uncertainty in the experimental results is estimated to be around 5%. Presence of steel walls in the actual thermal column access plug might also contribute to this uncertainty. In the actual measurement, flux is measured inside a steel chamber at the face of the access plug, but in the MCNP calculations that was not taken into account because it would take

too long to produce acceptable statistics; therefore an approximation to the target geometry was made. In this work it was found that, and it was also reported [5], approximation in target geometry leads to discrepancy between experimental and calculated data. The focus of the measurements were to evaluate the neutron energy spectrum in the region < 3 eV, so the measurements were not optimized beyond that range; however, the uncertainty in the total flux (thermal and fast) for the entire spectrum (10^{-9} to 16 MeV) was less than 5%. In the thermal spectrum energy range (10^{-7} - 10^{-6} MeV) the uncertainty in the dose response is noticeable only in the energy bin 10^{-7} - 10^{-6} MeV (Table 4.2) and it is found to be about 17%. The quality factor corresponding to neutron energies up to 1 eV is 2.0. It is apparent that in the worse case scenario (all neutrons in the energy range 10^{-7} - 10^{-6} are shifted up or down) the uncertainty in the calculated dose can reach 22% if the uncertainty in the total thermal flux is at 5%.

Table 4.2: Neutron Flux-to-Dose Rate Conversion Factors [6]

| Energy (MeV) | Response (rem/hr)/(n/cm ² -s) |
|--------------|---|
| 2.5E-08 | 3.67E-06 |
| 1.0E-07 | 3.67E-06 |
| 1.0E-06 | 4.46E-06 |

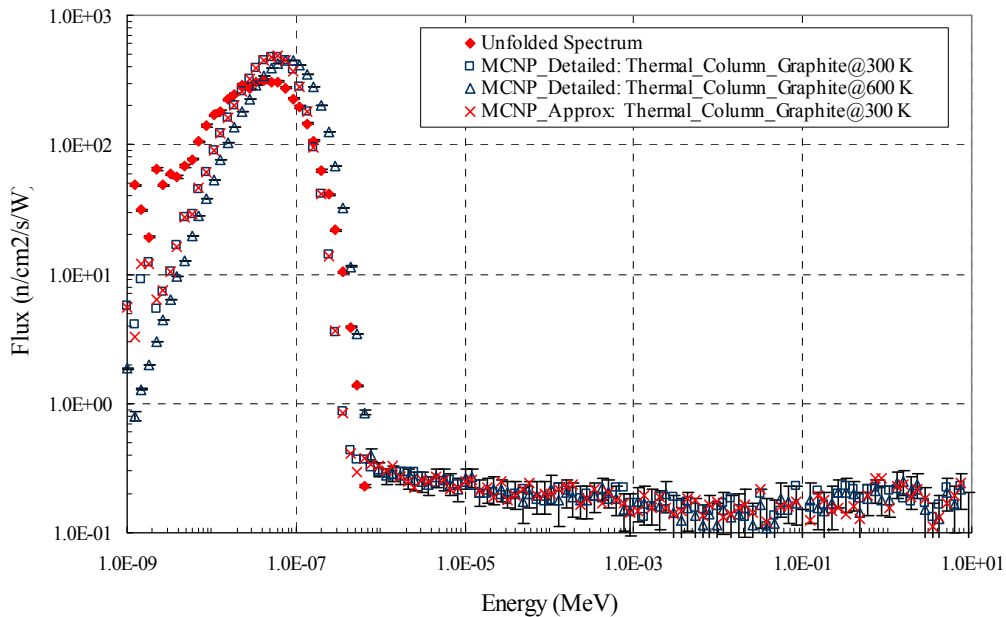


Figure 4.7: Neutron Spectrum Computed at the Thermal Column Access Plug

4.7 Neutron Spectrum Unfolding Measurements

Thermal and epithermal neutron fluxes are measured by foils (or monitors) that become radioactive by the (n, γ) reactions; this known as the foil activation method. If a foil is placed in a neutron flux composed of both thermal and epithermal neutrons, the monitor will be activated by both thermal and epithermal neutrons. These two activations may be distinguished by so called cadmium ratio or difference measurements. When a foil or monitor is placed in cadmium container, the monitor will be shielded from the thermal neutrons but not from the epithermal neutrons, because cadmium has a very large thermal absorption cross section, but very small cross section in epithermal region. The thermal component of the flux can be evaluated as [40]:

$$\phi_{th} = \frac{A}{N(1 - e^{-\lambda_i})\sigma_{th}} \left(1 - \frac{1}{CR}\right)$$

where A is the saturation activity due to both thermal and epithermal fluxes as is written as:

$$A = N\phi_{th}\sigma_{th}(1 - e^{-\lambda_i}) + N\phi_r I_0(1 - e^{-\lambda_i})$$

Where ϕ_r is the epithermal flux, I_0 is activation cross section for epithermal neutrons, and N is the number of atoms of the monitor. The cadmium ration, CR, is defined as the ratio of the saturation activity per atom of the bare monitor to saturation activity per atom of shielded monitor.

After acquiring the activation rates of the irradiated foils, these results are unfolded.

A passive neutron energy spectral unfolding technique [41] is used to unfold the thermal, and epithermal neutron spectrum at the thermal column access plug. Unfolding of the neutron spectra is accomplished by using both a Bayesian Estimator program in concert with a Maximum Entropy [42, 43] unfolding code (MAXED) to produce accurate and precise measurements of the neutron energy.

Unfolding of the foil data was performed using the MXD_FC33 code [2, 3]. In principle, the solution of the following equations yields the neutron flux spectrum.

$$\dot{P}_j(k) + \varepsilon_j(k) = \sum_{l=1}^n \phi_l R_{lj}(k) \quad (1)$$

$$\sum_k \sum_j \frac{\varepsilon_j(k)^2}{\sigma_j(k)^2} = \Omega \quad (2)$$

where $\dot{P}_j(k)$ is the measured activation rate (Bq/g per kW-sec); $\varepsilon_j(k)$ is the difference between the predicted value and the measured value of radionuclide j for set k ; $\sigma_j(k)$ is

the estimated standard uncertainty, ϕ_l is the neutron flux in energy group l (cm^{-2} per kW-sec); $R_{lj}(k)$ is the yield of radionuclide j for set k of neutrons in energy group l (Bq/g per n/cm^2), and Ω is a parameter set by the user (typically, Ω is set to the number of detectors).

The numbers of equations are less than the unknowns in equation (1) so a unique solution does not exist. The Bayesian statistics estimator is used to create the initial starting spectrum. Several key parameters are iterated on and a best fit to the data is made. This relies on having some understanding or *a priori* information about the system; the system in this instance is the MUTR thermal column neutron spectrum. Neutron peaks are added according to the neutron spectrum predicted. Key aspects about the neutron spectrum are iterated on until a best fit of the data has been achieved. These aspects include the energy of the peak, the width of the peak, the slope and height of the continuum connecting these peaks.

The experimental method for this type of unfolding involves combining several components whose energy response region is specific to specific neutron energy spectral regions. Resonance absorbers are used to provide energy information between 100 keV down to 0.01 eV. Several resonance absorbers commonly used for this method, available forms, and resonance energies are shown in Table 2. The resonance absorbers produce large depressions in the neutron energy spectrum incident on the neutron detector materials. Thermal neutron activation monitors together with the resonance absorbers provide the remainder of the energy information below 1 eV. Several common thermal neutron target materials used,

their half lives, relative abundances, and resulting decay products are shown in Table 3.

Table 4.3. Thermal Neutron Activation Reactions.

| Target Material | Target Isotope | Abundance | Reaction | Cross Section (barns) | Isotope | T _{1/2} | Decay Mode | Decay Energy | Decay Probability |
|-----------------|-------------------|-----------|----------|-----------------------|--------------------|------------------|------------|--------------|-------------------|
| Gold | ¹⁹⁷ Au | 100.0% | (n, γ) | 98.6 | ¹⁹⁸ Au | 2.7 d | γ | 411 | 95.6 |
| Copper | ⁶³ Cu | 69.2% | (n, γ) | 3.9 | ⁶⁴ Cu | 12.7 h | γ | 0.511 | 35.2 |
| Scandium | ⁴⁵ Sc | 100.0% | (n, γ) | 24.1 | ⁴⁶ Sc | 83.8 d | γ | 0.889 | 1 |
| | | | | | | | | 1.121 | 1 |
| Indium | ¹¹⁵ In | 95.7% | (n, γ) | 181.6 | ^{116m} In | 54.3 m | γ | 1.294 | 84.4 |
| | | | | | | | | 2.112 | 15.5 |
| Iron | ⁵⁸ Fe | 0.28% | (n, γ) | 1.2 | ⁵⁹ Fe | 44.5 d | γ | 0.143 | 1.02 |
| Silver | ¹⁰⁷ Ag | 51.8% | (n, γ) | 34.2 | ¹⁰⁸ Ag | 2.37 m | beta | 1.649 | 97.2 |
| | ¹⁰⁹ Ag | 48.2% | (n, γ) | 80.7 | ¹¹⁰ Ag | 24.6 s | beta | 2.892 | 99.7 |

4.8 Results and Analysis of Core Geometry Approximations

As mentioned in the summary of this chapter (Section 4.1) that to study core geometry approximations and their influence on the results, two models, one detailed and another stripped-down with severe approximations were created. Figure 4.8 shows both models. In the approximate model, structures above and below the core were entirely eliminated. The k_{eff} for both models are compared and found to differ only by < 0.4%; the results are listed in Table 4.5. Core geometry approximations clearly did not produce any noticeable effects. The reason is that the graphite reflectors above and below the fuel meat act as “neutron regulators,” and the

absorption properties of water and aluminum are similar (see Table 4.4). The effect of fuel upper and lower graphite reflectors is discussed in Section 4.8.

In Table 4.5, k_{eff} for the detailed model differs by 2.13% from the critical value. That is attributed to fission products poisoning, especially xenon. Fuel burnup and fission products poisoning is discussed in Section 4.10.

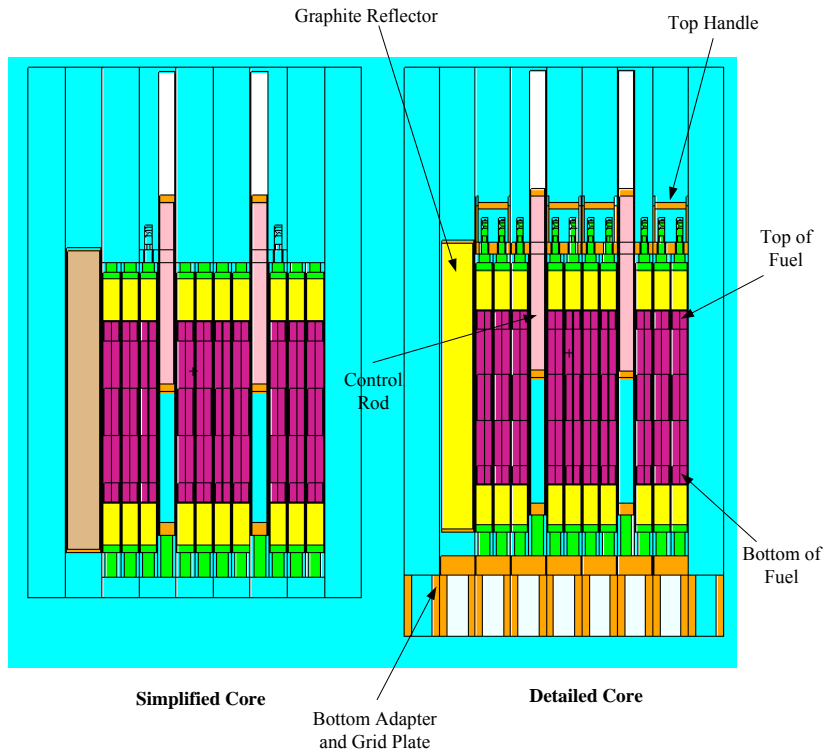


Figure 4.8: Side View of Simplified and Detailed Cores

It was observed that the neutron energy spectrum at the top and bottom of the fuel is not symmetric (Figure 4.10). This is due to the presence of the control rods near the center of the fuel (Figure 4.8). This lead to more neutron absorption at the top of the fuel and contributed to spectrum asymmetry.

Table 4.4: Scattering and Absorption Cross Sections For Water and Aluminum [44]

| Element | σ_s | σ_a |
|----------|------------|------------|
| Water | 103 | 0.664 |
| Aluminum | 1.49 | 0.230 |

Table 4.5 :Multiplication factor benchmarks during initial reactor startup

| Model | Rod Position (% removed) | | | Power | k_{eff} | |
|------------|--------------------------|---------|----------------|---------|-----------------------|-----------------------|
| | Shim I | Shim II | Regulating Rod | | Without Poisons | With Poisons |
| Detailed | 65.4 | 65.3 | 40.4 | 5 watts | 1.02113 ± 0.00020 | 1.00613 ± 0.00020 |
| Approx | “ | “ | “ | 5 watts | 1.01720 ± 0.00017 | |
| Difference | | | | | 0.4% | |
| Detailed | 65.4 | 65.3 | 70.1 | 250 kW | $1.01073+0.00021$ | 1.00527 ± 0.00021 |
| Approx | “ | “ | “ | 250 kW | $1.00872+0.00031$ | |
| Difference | | | | | 0.2% | |

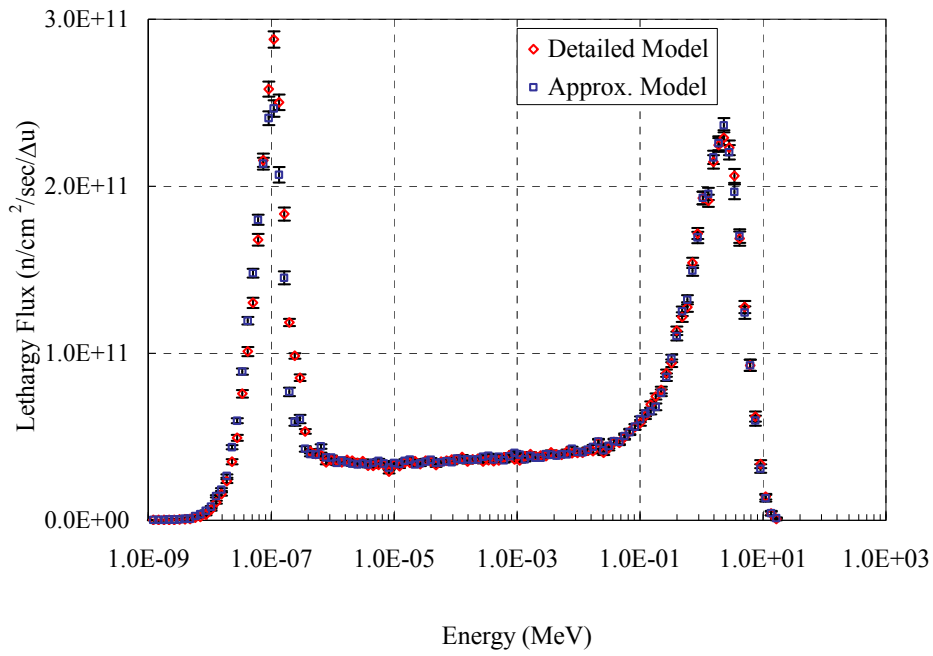


Figure 4.9: Neutron Spectrum at Top of Most Center Fuel

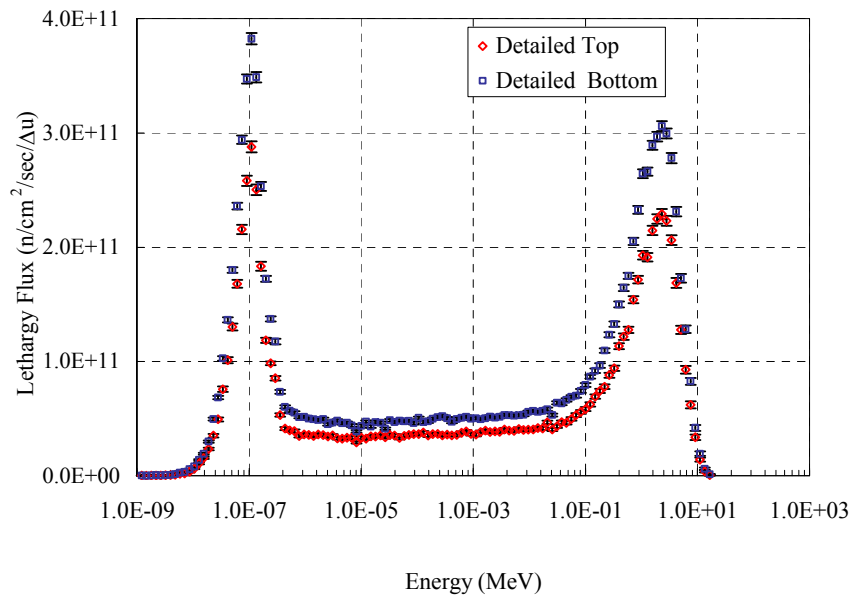


Figure 4.10: Neutron Energy Spectrum at the Top and Bottom of Fuel

The results thus obtained can be extended to TRIGA reactors equipped with standard TRIGA fuel elements having properties identical or similar to MUTR standard fuel element. Because this is a far reaching conclusion, further analysis is warranted to verify that the graphite reflectors above and below the core act as neutron energy regulators. An analysis of the effect of changing the graphite reflector length on the neutron flux spectrum in the fuel is studied.

4.8.1 Survey of TRIGA Fuels

Operating TRIGA reactors, worldwide, are equipped with TRIGA fuels [21, 45, 46, 47] of four types: Standard Fuel Element (SFE), Instrumented Fuel Element (IFE), Fuel Follower Control Rod (FFCR), and Rods for Cluster Assembly (4-rods, 16-rods, or 25 rods). The uranium weight percent varies from 8.0 to 45.0, and U-235 enrichment (%) is 20 [45, 46] or 70 [47]. The cladding of the standard (single) fuel rod is 0.05 cm, and either stainless steel or aluminum. The length of the active fuel region is 38.1 cm. The standard fuel rod upper and lower graphite reflectors lengths range from 8.7 to 8.97 cm depending on the fuel type.

An extensive search has been conducted using the IAEA (International Atomic Energy Agency) database of the world research reactors [48] to obtain the fuel data of operating TRIGA Mark I, Mark II, and TRIGA conversion reactors equipped with fuel enriched to 20 percent. Although the database is missing information about the fuel's upper and lower graphite reflectors, other fuel parameters were found consistent with the published literature. Validity of the data obtained from the IAEA database in regard to the standard TRIGA fuel rod (dimensions, type, density) was

confirmed by the fuel manufacturer, General Atomics [49], which also provided the dimensions and density of the upper and lower graphite reflectors. Dimensions of the standard TRIGA fuel rod and the graphite reflectors are listed in Table 4.6.

Table 4.6: Standard TRIGA Fuel Element Dimensions

| | Dimensions (cm) | Al Clad | SS Clad |
|--------------------------------------|-----------------|---------|-----------|
| Fuel | Diameter | 3.59 | 3.47-3.64 |
| | Height | 38.1 | 38.1 |
| Cladding | Thickness | 0.05 | 0.05 |
| Graphite Reflectors Lower & Upper | Diameter | 3.39 | 3.44 |
| | Height | 8.97 | 8.68 |

4.8.2 Graphite Reflectors Neutronic Effects

A unit cell (Figure 4.15) and a detailed (with all structures) 4-rod fuel assembly were used to analyze the effect of varying the upper and lower graphite reflector thickness of the standard TRIGA fuel element. The results of the calculations are listed in Table 4.7 and are shown in Figure 4.11. The thickness (8.7 cm) of the graphite reflector of the MUTR was selected as a reference; it is then increased and decreased by 2 and 6 cm. Although graphite reflectors having length greater than 10.2 or less than 8.7 cm are not among the surveyed standard TRIGA fuels, graphite reflectors lengths in the range 2.7-14.7 cm are analyzed. At upper and lower graphite reflector lengths of less than 3 cm, a change of slightly more than half a percent in k_{eff} is observed. At representative upper and lower graphite lengths (8.7-10.7 cm), the change in the k_{eff} is relatively small—within the uncertainty bounds of

k_{eff} . This small change is attributed to the relatively high moderating ratio of graphite. It takes only about 29 collisions for a neutron to lose 99% of an initial energy of 2 MeV. This is seen from the following:

$$n = \frac{1}{\xi} \ln\left(\frac{E_0}{E}\right) = \frac{\ln(100/1)}{0.158} \approx 29.$$

Thus, the graphite reflector thicknesses encountered in TRIGA standard fuels are quite sufficient to quickly moderate neutrons whose energies are altered due to approximations or eliminations of structures above and below the core to thermal energies. In such instance, these neutrons, when reflected back into the fuel, are indistinguishable from other neutrons that did not experience change in energy due to structural approximations.

Table 4.7: Change of k_{eff} with Graphite Reflector Thickness

| Graphite Reflector Length (cm) | k_{eff} (Pin Cell) | Difference (%) | k_{eff} (Detailed Assembly) | Difference (%) |
|--------------------------------|-----------------------------|----------------|--------------------------------------|----------------|
| 2.7 | 1.26676 ± 0.00042 | -0.66 | 1.26660 ± 0.00040 | -0.67 |
| 6.7 | 1.27354 ± 0.00042 | -0.13 | | |
| 8.7 | 1.27515 ± 0.00044 | 0.00 | 1.27517 ± 0.00041 | 0.00 |
| 10.7 | 1.27662 ± 0.00040 | 0.12 | | |
| 14.7 | 1.27798 ± 0.00041 | 0.22 | 1.27767 ± 0.00040 | 0.19 |

Figure 4.11 shows the pin cell, or unit cell neutron energy spectrum computed at different lengths of the standard TRIGA fuel element graphite reflectors. It is seen from Table 4.8 that the neutron energy spectrum shows a measurable change (< 8%) at graphite reflectors lengths below 3 cm. Between 6.7 and 10.7 cm, the change in the spectrum is up to 3%. Looking at Table 4.6, it can be concluded that the small difference in lengths (< 1 cm) of the standard TRIGA fuel graphite reflectors, found

in the literature, is not sufficient to produce a noticeable change in the neutron energy spectrum; therefore, the results obtained in this work my strongly suggest that structures above and below the core has little effect on the neutron energy spectrum in the fuel.

Table 4.8: Flux for Graphite Reflectors with at Different Lengths

| Flux | 2.7 cm | Diff. (%) | 6.7 cm | Diff. (%) | 8.7 cm | 10.7 cm | Diff. (%) | 14.7 cm | Diff. (%) |
|------------|---------|-----------|---------|-----------|---------|---------|-----------|---------|-----------|
| Thermal | 3.7E+09 | -7.5 | 4.0E+09 | -0.1 | 4.1E+09 | 4.2E+09 | 3.3 | 4.2E+09 | 3.3 |
| Epithermal | 4.0E+09 | -3.4 | 4.2E+09 | 0.6 | 4.2E+09 | 4.3E+09 | 2.8 | 4.3E+09 | 2.4 |
| Fast | 5.1E+09 | -4.2 | 5.3E+09 | 0.7 | 5.3E+09 | 5.5E+09 | 2.9 | 5.4E+09 | 2.5 |
| Total | 1.3E+10 | -4.9 | 1.4E+10 | 0.4 | 1.4E+10 | 1.4E+10 | 3.0 | 1.4E+10 | 2.7 |

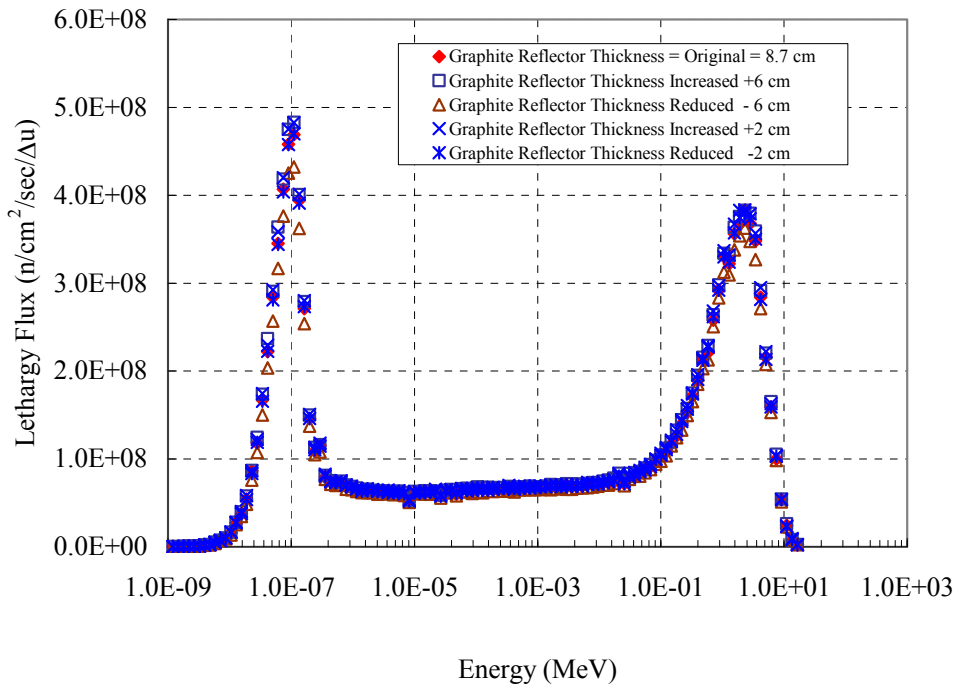


Figure 4.11: Pin Cell Neutron Energy Spectrum

4.9 Results of Uncertainty Calculations

A three-parameter uncertainty calculation to assess the extreme values of the MUTR core k_{eff} is conducted. The three parameters that affect the multiplication factor are: U-ZrH fuel density, hydrogen-to-zirconium ratio (H:Zr), and the density of the upper and lower graphite reflectors of the standard TRIGA fuel element. The core k_{eff} is directly proportional to all three parameters. Calculations are performed for the detailed core at a power of 5 watts, without including xenon and fission product poisoning. The results are listed in Table 4.9. Only three calculations are performed; and sensitivity analysis, to assess individual parameter contribution to the k_{eff} uncertainty, is not performed. However, maximum uncertainty ((minimum-maximum)/nominal) for the core k_{eff} is found to be less than 0.6%.

Table 4.9: Three-parameter Uncertainty Matrix

| Parameter | Value | | |
|--|-----------------------|-----------------------|-----------------------|
| | Minimum | Nominal | Maximum |
| U-ZrH Density (g/cm ³) | 5.90 | 5.95 | 6.00 |
| H:Zr Ratio | 1.60 | 1.65 | 1.70 |
| Graphite Density (g/cm ³) | 1.60 | 1.67 | 1.75 |
| k_{eff} | 1.01628 ± 0.00042 | 1.02026 ± 0.00039 | 1.02270 ± 0.00041 |

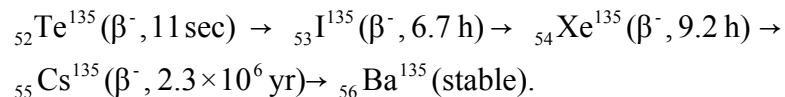
4.10 Fuel Burnup Effect

The changes in the composition of the fuel as it undergoes depletion or “burnup,” produce a number of effects which may include the following:

- 1) Transient or short term reactivity effects
- 2) Long term reactivity effects
- 3) Reactor kinetics effects
- 4) Neutron flux distribution effects

4.11 Short Term Reactivity Effects—Fission Products Poisoning

Although all fission products absorb neutrons to some extent, xenon-135, ^{135}Xe , has the most negative effect on reactivity during reactor startup or operation because of its large thermal absorption cross section and fission yield (direct and indirect). The thermal absorption cross section for ^{135}Xe is 2.65×10^6 barns. ^{135}Xe is formed as a result of ^{135}I decay and also produced directly in fission. The total yield of ^{135}Xe is up to 6%. The decay chain that leads to ^{135}Xe production is:



The fission products poisoning or the negative reactivity insertion during reactor operation due ^{135}Xe is known as xenon loading or equilibrium xenon and is estimated as follows [44, 17]:

$$\rho = -\frac{\gamma_I + \gamma_X}{\nu p \epsilon}$$

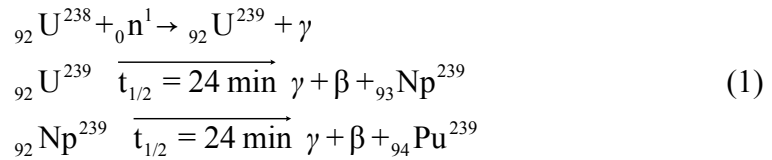
where γ_I , γ_X are the ^{135}I , and ^{135}Xe yields, respectively; ν , p , and ϵ are the average number of neutrons produced in fission, the resonance escape probability, and the fast

fission factor, respectively. Conservatively assuming that there is no resonance absorption, and $p=\epsilon=1$, the reactivity due ^{135}X poisoning is

$$\rho = -\frac{\gamma_I + \gamma_X}{\nu} = -0.066/2.438 = -2.7\%.$$

4.12 Long Term Reactivity Effects

The composition of the fuel changes substantially during the lifetime of the reactor. There are two predominant effects: the burnup of U-235 and the conversion of U-238 into plutonium as follows:



The Pu-239 that is produced can capture a neutron and transmutes to Pu-240. The Pu-240, formed by neutron capture, has properties very similar U-238 (see Table 4.10) so if it captures another neutron, it will form fissile Pu-241. Therefore, during reactor operation power is produced from fission of U-235, Pu-239, and Pu-241 (Figure 4.12). The buildup of Pu-240 and neutron absorbing fission products is of equal importance to overall long term reactivity.

At the beginning, the burnup of U-235 and its replacement by Pu-239 leads to an increase in reactivity. This is due to the higher fission cross section of Pu-239 (see Table 4.10). At higher burnup, the U-235 still being consumed, but the buildup of Pu-239 becomes less rapid as it approaches its equilibrium level, when production of Pu-239 equals its removal by fission and radiative capture. At high burnup, the reduction in fissile nuclei causes a reduction in reactivity.

The buildup of Pu-240 produces a large negative reactivity contribution due significant neutron absorption ($\sigma_a = 287$ b). This is partially offset by the buildup of Pu-241. There is an initial rapid increase in fission products negative reactivity due Sm-149 ($\sigma_a = 41,800$ b) which reaches an equilibrium after 300 hours of operation. This is followed by nearly linear decrease in reactivity due to the continued formation of mildly neutron absorbing fission products.

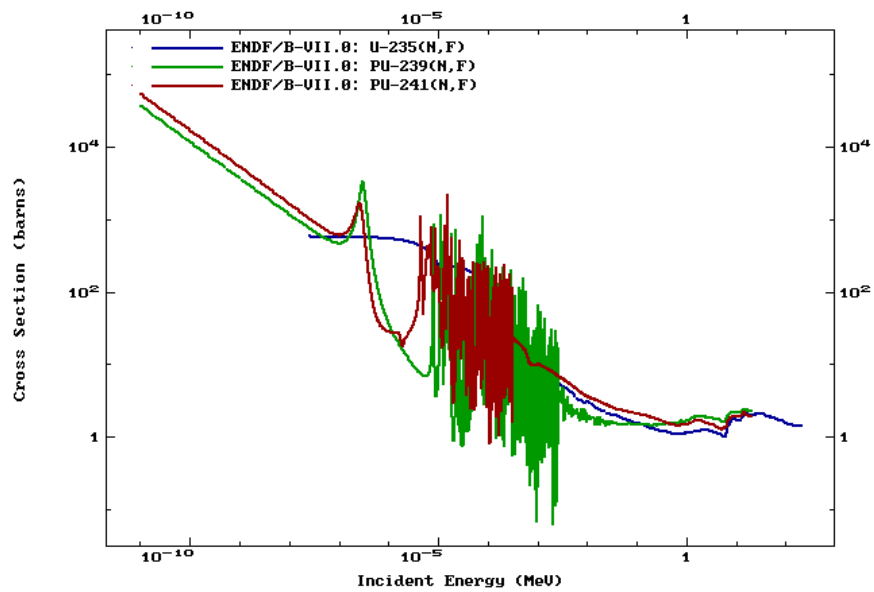


Figure 4.12: Fission Cross Section for Fissile Materials

Table 4.10: Thermal Cross Sections Data (0.0253 eV) for Fissile and Fertile Nuclides [50, 51, 52].

| Nuclide | σ_c | σ_f | $\sigma_a = \sigma_c + \sigma_f$ |
|---------|------------|------------|----------------------------------|
| U-235 | 98.7 | 585.1 | 683.8 |
| U-238 | 2.7 | 1.7E-05 | 2.7 |
| Pu-239 | 270.7 | 747.9 | 1018.6 |
| Pu-240 | 287.6 | 6.4E-02 | 287.7 |
| Pu-241 | 363.1 | 1012.3 | 1375.4 |

4.13 MCNPX Burnup Process

MCNPX depletion is a linked process involving steady-state flux calculations in MCNPX and nuclide depletion calculations in CINDER90 [53], a neutron transmutation code. MCNPX runs a steady-state calculation to determine the system eigenvalue, 63-group fluxes, energy integrated reaction rates, average fission neutrons (ν), and recoverable energy per fission (Q values). CINDER90 then takes those MCNPX-generated values and carries out the depletion calculation to generate new number densities at the following time step. MCNPX then takes those new number densities and generates another set of fluxes and reaction rates; the process repeats itself until after the final time step.

CINDER90 uses decay and energy integrated reaction rate probabilities along with fission yield information to calculate the temporal nuclide buildup and depletion. The library of data in CINDER90 includes isotope decay and interaction probability data for 3456 isotopes including, ~30 fission yield sets, and yield data for 1325 fission products.

4.14 Results of Flux Calculations in The Rabbit System

The uncertainty in the results of the MCNP calculations for the empty rabbit as compared to previously obtained experimental results [54] (see Table 4.1) is more 35%. Reason could be attribution to lack of details of the experimental arrangement when the flux is calculated in the Rabbit system. In the MCNP calculations, the flux is calculated in air inside the Rabbit (Figure 4.13). In the actual measurement, it could be calculated within a foil. In this case it shows that target geometry and materials might have contributed to the high uncertainty.

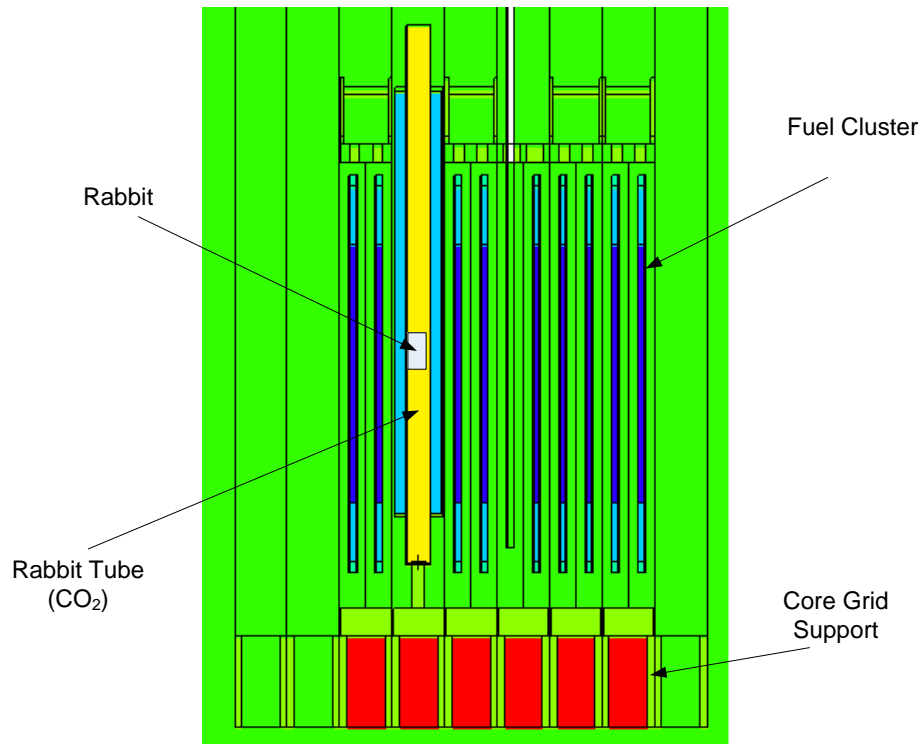


Figure 4.13: Rabbit in the Core

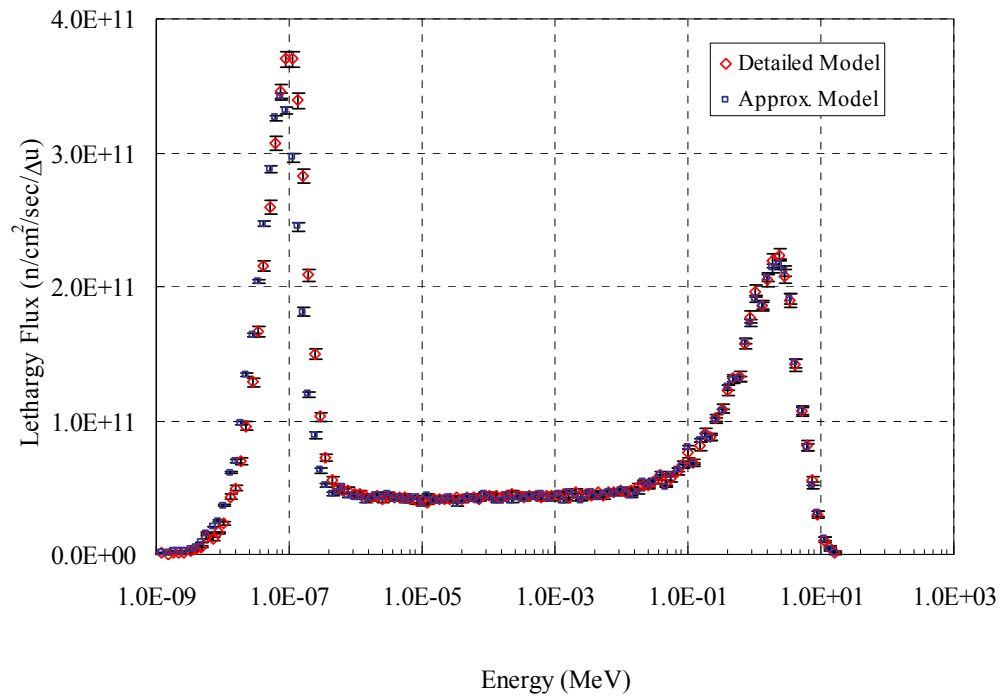


Figure 4.14: Neutron Flux at The Pneumatic Tube Transfer System Rabbit

4.15 Study of Fuel Burnup Using Cell Calculations

One of the powerful features of MCNP is the ability to perform cell and assembly calculation without running a full simulation. A unit cell (Figure 4.15) is created and a reflective boundary condition is assigned to four surfaces along the x-y directions and an infinite boundary condition in the axial direction. Two single step burnup calculations, one for a single step of 8 hours and another for 40 days at 250 kW, were run. The second calculation approximated the up-to-date burnup of the fuel (15 grams consumed out of a total of 3400 grams). The only difference seen is that the thermal peak is increased while the fast peak of the spectrum remained unchanged. The 8 hour burnup calculations showed a negative reactivity due to fission product poisoning of 2.68%. For the 8 hour burnup calculation, k_{eff} at the beginning of life and at 40 days at 250 kW are 1.25511 ± 0.00062 and 1.22823 ± 0.00067 , respectively. It is seen that the cell is supercritical and it overestimate the flux and consequently the poisoning. Therefore, it is expected that if the cell density is lowered until the initial k_{eff} is about only 3% supercritical, then the value of the negative reactivity due to fission products poisoning simulates that of the reactor during startup or operation.

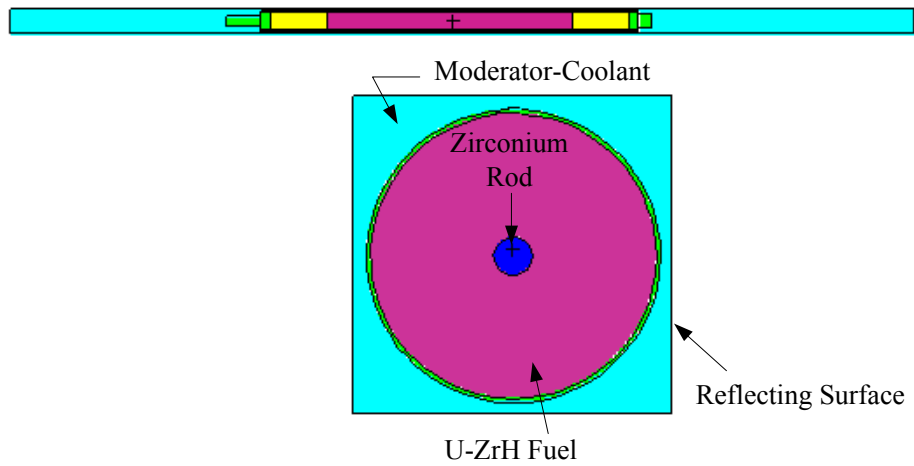


Figure 4.15: MCNP Model of A Unit Cell

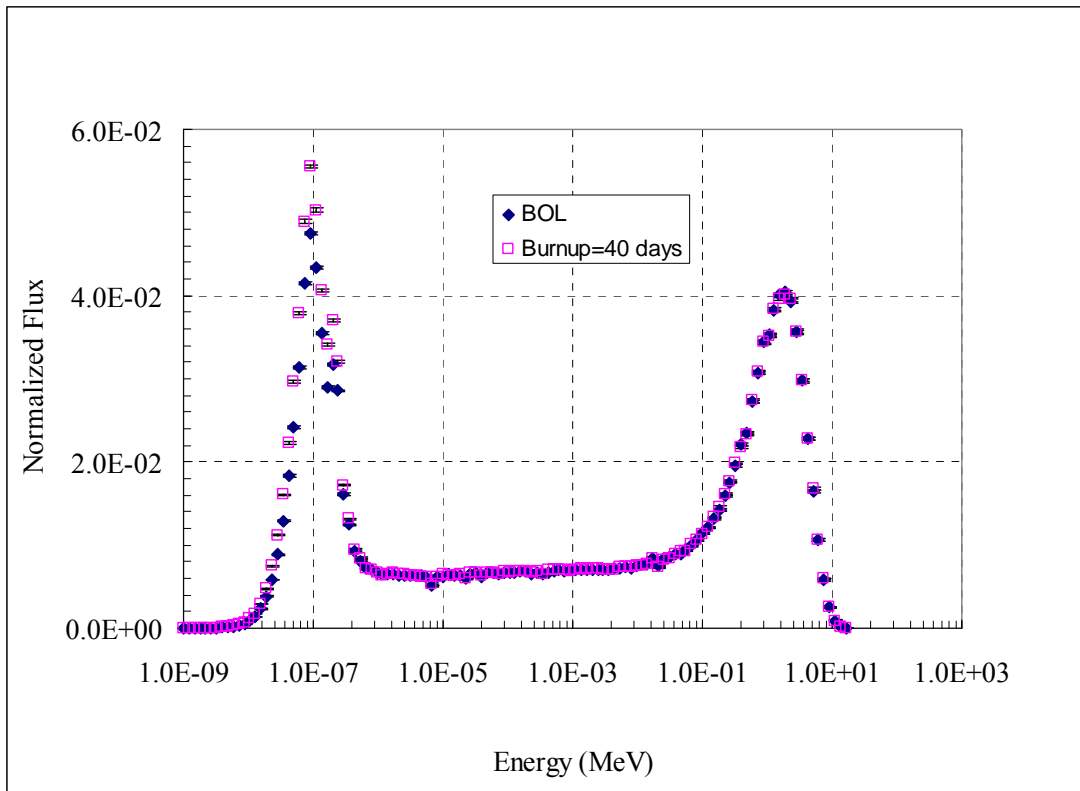


Figure 4.16: Neutron spectrum inside a Unit Cell After 40 MWD Irradiation

Chapter 5: Conclusions and Future Work

Two MCNP models of the University of the Maryland Training Reactor (MUTR) were successfully created and benchmarked against experimental data. The first model created a detailed core with minimal approximations to the core geometrical arrangements. The simplified model is stripped from all structural materials above and below the core. Core geometry approximations were found to contribute little to flux profiles in and out of the core. MCNP calculations of the thermal and total flux in the thermal column access plug agreed with experiment within 5% uncertainty. The uncertainty in dose rate calculated in the thermal region of the spectrum is dependent on the uncertainty of neutron energies in range $1e-7$ to $1e-6$ and was estimated to be up to 22%. Results of the flux calculated in the pneumatic rabbit system were found to agree with experiment within 35% uncertainty. The relatively large uncertainty was attributed to approximation in the geometry and composition of the target in the Rabbit. Geometrical details and experimental conditions of the target were found to be important and the lack of details on the conditions of the experiments was found to have major contribution to the calculated flux uncertainty. The contribution of this work to the TRIGA research reactor community could not be underestimated. Research reactors equipped with standard TRIGA fuels can be modeled with core geometry approximations, such as the approximations modeled in this work, without affecting the precision of the Monte Carlo calculations. The uncertainty due to modeling simplifications due to the elimination of structural

materials above and below would amount to less than half a percent increase in the uncertainty. Major modeling efforts could be saved by adopting such simplified TRIGA reactor models.

Modeling of targets with minimum geometry approximations is crucial to finding good agreement with experimental results. In Future work, cross sections will be evaluated, using a special code, at the reactor operating conditions to obtain better results.


```

1 1
1 1
1 1
41 5 -1.0 -74 75 -76 77 78 -79 imp:n,p=1 u=4 fill=2
42 5 -1.0 (74:-75:76:-77:-78:79)
(470:-471:472:-473:-474:(475 510 511 512 513):535)
(600:-601:602:-603:-604:605) (476:-471:-473:472:-475:478)
(470:-477:-473:472:-475:478) (570)
imp:n,p=1 u=4 $(74:-75:76:-77:-51:52 )
c
c -----
c Bottom adapter and grid plate
c -----
54 5 -1.0 -50 u=14 imp:n,p=1$
55 6 -2.70 50 u=14 imp:n,p=1$
56 12 -2.70 -50 u=17 imp:n,p=1$
57 6 -2.70 50 u=17 imp:n,p=1$
c
c -----
c Grid plate
c 51 6 -2.70 -74 75 -76 77 51 -52 50 u=4 imp:n,p=1$
c
c -----
c Bottom adapter and holes
c -----
58 6 -2.70 -53 54 -55 56 imp:n,p=1 u=15 lat=1 fill=0:8 0:5 0:0
c
c -----
c 17 17 17 17 17 17 17 17 17 17 $ F
c 14 17 17 17 17 17 17 17 14 $ E
c 14 17 17 17 17 17 17 17 14 $ D
c 14 14 17 17 17 17 17 17 14 $ C
c 14 14 14 17 14 17 14 14 14 $ B
c 14 14 14 14 14 14 14 14 14 $ A
c
c -----
c
c -----
c Bottom adapter window
c -----
60 5 -1.0 62 -61 -63 64 51 -52 imp:n,p=1 fill=15
c
c =====
c Core lattice
c -----
80 5 -1.0 -81 82 -83 84 imp:n,p=1 tmp=2.4829e-8
u=5 lat=1 fill=0:8 0:4 0:0
c
c -----
c 25 25 4 4 4 4 4 4 25 $ F
c 5 5 4 8 4 4 10 4 5 $ E
c 5 5 4 4 4 4 4 4 5 $ D
c 5 5 4 18 4 12 4 4 5 $ C
c 5 5 13 4 13 24 5 5 5 $ B
c
c -----
c 1 2 3 4 5 6 7 8 9 $
c
c -----
81 5 -1.0 94 -93 96 -95 91 -92 tmp=2.4829e-8 imp:n,p=1 fill=5
c
c -----
c Outside window
c -----
99 5 -1.0 (-100 -102 103) (-94:93:-96:95:-91:92) (630) (640)
(-62:61:63:-64:-51:52) (650) (700)
imp:n,p=2 tmp=2.4829e-8
c
c -----
c Reactor Pool Tank wall
c -----
100 6 -2.70 -101 100 -102 103 (630) (640) (650) (700)
imp:n,p=1
c
c -----
c Bioshield (concrete)
c -----
110 11 -2.25 101 -110 103 -111 (630) (640) (650) (700) (722)
(-733:734:736:-737:738) imp:n,p=1
c
c -----
c Outside World

```

```

c -----
c 199      0 99  imp:n,p=0 $
199      0      (110:(111 101):102:-103) (630:632:-633) (640) (650)
              imp:n,p=0 $
c =====
c
c Shim I (control rod)
c -----
200      5 -1.0 -1 32 -15 206      u=20  imp:n,p=1 $ guide tube
201      6 -2.70 -2 1 -15 32      u=20  imp:n,p=1 $ tube wall
202      4 -7.92 -10 -32 11      u=20  imp:n,p=1 $ bottom fitting
203      5 -1.0 2:(-32 10):-11:15 u=20  imp:n,p=1 $ exterior of tube
c -----
204      7 -2.51 -205 207 -15      u=20  imp:n,p=1 $ B4C
205      6 -2.70 -206 205 207 -15 u=20  imp:n,p=1 $ Al clad
206      5 -1.0 -206 33 -34      u=20  imp:n,p=1 $ void below B4C
c -----
c Shim I Cluster
c -----
c Fuel-Control assembly lattice cell and exterior of cell
c -----
207      5 -1.0 -70 71 -72 73      imp:n,p=1 lat=1 u=7 fill=0:1 0:1 0:0 $
              1 20
              1 1
208      5 -1.0 -74 75 -76 77 78 -79 imp:n,p=1 u=8 fill=7
209      5 -1.0 (74:-75:76:-77:-78:79)
              (470:-471:472:-473:-474:(475 510 512 513):535) (275)
              (600:-601:602:-603:-604:605) (74:-75:76:-77:-51:52 )
              imp:n,p=1 u=8
c =====
c Shim II (control rod)
c -----
210      5 -1.0 -1 32 -15 206      u=21  imp:n,p=1 $ guide tube
211      6 -2.70 -2 1 -15 32      u=21  imp:n,p=1 $ tube wall
212      4 -7.92 -10 -32 11      u=21  imp:n,p=1 $ bottom fitting
213      5 -1.0 2:(-32 10):-11:15 u=21  imp:n,p=1 $ exterior of tube
c -----
214      7 -2.51 -205 217 -15      u=21  imp:n,p=1 $ B4C
215      6 -2.70 -206 205 217 -15 u=21  imp:n,p=1 $ Al clad
216      5 -1.0 -206 33 -35      u=21  imp:n,p=1 $ void below B4C
c -----
c Shim II Cluster
c -----
c Fuel-Control assembly lattice cell and exterior of cell
c -----
217      5 -1.0 -70 71 -72 73      imp:n,p=1 lat=1 u=9 fill=0:1 0:1 0:0 $
              21 1
              1 1
218      5 -1.0 -74 75 -76 77 78 -79 imp:n,p=1 u=10 fill=9
219      5 -1.0 (74:-75:76:-77:-78:79)
              (470:-471:472:-473:-474:(475 511 512 513):535) (335)
              (600:-601:602:-603:-604:605) (74:-75:76:-77:-51:52 )
              imp:n,p=1 u=10
c =====
c Shim III (control rod)
c -----
220      5 -1.0 -1 32 -15 206      u=22  imp:n,p=1 $ guide tube
221      6 -2.70 -2 1 -15 32      u=22  imp:n,p=1 $ tube wall
222      4 -7.92 -10 -32 11      u=22  imp:n,p=1 $ bottom fitting
223      5 -1.0 2:(-32 10):-11:15 u=22  imp:n,p=1 $ exterior of tube
c -----
224      7 -2.51 -205 227 -15      u=22  imp:n,p=1 $ B4C
225      6 -2.70 -206 205 227 -15 u=22  imp:n,p=1 $ Al clad
226      5 -1.0 -206 33 -36      u=22  imp:n,p=1 $ void below B4C
c -----
c Shim III Cluster
c -----
c Fuel-Control assembly lattice cell and exterior of cell
c -----
227      5 -1.0 -70 71 -72 73      imp:n,p=1 lat=1 u=11 fill=0:1 0:1 0:0 $
              22 1

```

```

1 1
228 5 -1.0 -74 75 -76 77 78 -79 imp:n,p=1 u=12 fill=11
229 5 -1.0 (74:-75:76:-77:-78:79)
      (470:-471:472:-473:-474:(475 511 512 513):535) (385)
      (600:-601:602:-603:-604:605) (74:-75:76:-77:-51:52 )
      imp:n,p=1 u=12
c -----
c =====
c Top handle and holes for control element Shim I
c -----
230 6 -2.70 -470 471 -472 473 474 -475 501 (238)
      (607 -608 -609) 503 504 245 240 241 242 243
      u=8 imp:n,p=1
231 5 -1.0 -501 -475 474 510 u=8 imp:n,p=1
232 6 -2.70 -235 -475 474 232 u=8 imp:n,p=1 $ cladd
233 5 -1.0 -503 -475 474 512 u=8 imp:n,p=1
234 5 -1.0 -504 -475 474 513 u=8 imp:n,p=1
c -----
235 5 -1.0 -245 -475 474 u=8 imp:n,p=1 $ cener hole
c -----
236 0 -237 -475 474 235 u=8 imp:n,p=1 $ guide tube
237 6 -2.70 -238 -475 474 237 u=8 imp:n,p=1 $ guide tube wall
c -----
c Side trims of top handle
c -----
240 0 -470 473 -606 474 -475 u=8 imp:n,p=1
241 5 -1.0 471 473 -607 474 -475 u=8 imp:n,p=1
242 5 -1.0 -470 -472 608 474 -475 u=8 imp:n,p=1
243 5 -1.0 471 -472 609 474 -475 u=8 imp:n,p=1
c -----
c Fuel element top fittings (part of top handle geometry)
c -----
250 4 -7.92 -510 -475 474 u=8 imp:n,p=1
251 7 -2.51 -232 -475 474 u=8 imp:n,p=1 $ B4C
252 4 -7.92 -512 -475 474 u=8 imp:n,p=1
253 4 -7.92 -513 -475 474 u=8 imp:n,p=1
c -----
c Shim I top handle side holes
c -----
260 5 -1.0 -240 -475 474 473 u=8 imp:n,p=1
261 5 -1.0 -241 -475 474 -472 u=8 imp:n,p=1
262 5 -1.0 -242 -475 474 471 u=8 imp:n,p=1
263 5 -1.0 -243 -475 474 -470 u=8 imp:n,p=1
c -----
c Shim I second top fittings (top of top handle)
c -----
271 4 -7.92 -510 545 -546 u=8 imp:n,p=1
272 7 -2.51 -272 u=8 imp:n,p=1
273 4 -7.92 -512 545 -546 u=8 imp:n,p=1
274 4 -7.92 -513 545 -546 u=8 imp:n,p=1
275 6 -2.70 -273 272 u=8 imp:n,p=1 $cladd for control
c -----
276 0 -274 273 u=8 imp:n,p=1 $guide tube
277 6 -2.70 -275 274 u=8 imp:n,p=1 $guide tube wall
c -----
c Shim I third top fittings
c -----
281 4 -7.92 -531 475 -545 u=8 imp:n,p=1
c 282 7 -2.51 -232 475 -535 u=8 imp:n,p=1 $ B4C
283 4 -7.92 -533 475 -545 u=8 imp:n,p=1
284 4 -7.92 -534 475 -545 u=8 imp:n,p=1
c -----
c
286 5 -1.0 -510 475 -545 531 u=8 imp:n,p=1
c 547 0 -235 475 -535 232 u=8 imp:n,p=1 cladd
288 5 -1.0 -512 475 -545 533 u=8 imp:n,p=1
289 5 -1.0 -513 475 -545 534 u=8 imp:n,p=1
c -----
290 5 -1.0 -510 548 -535 549 u=8 imp:n,p=1

```

```

c      551      0      -511 548 -535 550      u=8 imp:n,p=1
292    5 -1.0    -512 548 -535 551      u=8 imp:n,p=1
293    5 -1.0    -513 548 -535 552      u=8 imp:n,p=1
c
-----
294    5 -1.0    -510 546 -547 553 554      u=8 imp:n,p=1
c      555      0      -511 546 -547 555 556      u=8 imp:n,p=1
296    5 -1.0    -512 546 -547 557 558      u=8 imp:n,p=1
297    5 -1.0    -513 546 -547 559 560      u=8 imp:n,p=1
c
-----
298    4 -7.92   -510 547 -548      u=8 imp:n,p=1
c      559      4      -7.92 -511 547 -548      u=8 imp:n,p=1
300    4 -7.92   -512 547 -548      u=8 imp:n,p=1
301    4 -7.92   -513 547 -548      u=8 imp:n,p=1
c
-----
c      Fuel element top cones
c
-----
302    4 -7.92   -549 548      u=8 imp:n,p=1
c      563      4      -7.92 -550 548      u=8 imp:n,p=1
304    4 -7.92   -551 548      u=8 imp:n,p=1
305    4 -7.92   -552 548      u=8 imp:n,p=1
c
-----
c      Middle cones (top fittings)
c
-----
306    4 -7.92   -553 -547 554      u=8 imp:n,p=1
307    4 -7.92   -554 546      u=8 imp:n,p=1
c
-----
c      568      4      -7.92 -555 -547 556      u=8 imp:n,p=1
c      569      4      -7.92 -556 546      u=8 imp:n,p=1
c
-----
310    4 -7.92   -557 -547 558      u=8 imp:n,p=1
311    4 -7.92   -558 546      u=8 imp:n,p=1
c
-----
312    4 -7.92   -559 -547 560      u=8 imp:n,p=1
313    4 -7.92   -560 546      u=8 imp:n,p=1
c
-----
c      Square above bottom adapter for Shim I
c
-----
320    6 -2.70   -600 601 -602 603 604 -605 606 607 -608 -609
                                           u=8 imp:n,p=1
326    5 -1.0    -600 603 -606 604 -605      u=8 imp:n,p=1
327    5 -1.0     601 603 -607 604 -605      u=8 imp:n,p=1
328    5 -1.0    -600 -602 608 604 -605      u=8 imp:n,p=1
329    5 -1.0     601 -602 609 604 -605      u=8 imp:n,p=1
c
=====
c      Top handle and holes for control element Shim II
c
-----
340    6 -2.70   -470 471 -472 473 474 -475 (606 -608 -609)
                                           502 503 504 (247) 245 240 241 242 243
                                           u=10 imp:n,p=1
341    6 -2.70   -236 -475 474 231      u=10 imp:n,p=1 $ cladd
342    5 -1.0    -502 -475 474 511      u=10 imp:n,p=1
343    5 -1.0    -503 -475 474 512      u=10 imp:n,p=1
344    5 -1.0    -504 -475 474 513      u=10 imp:n,p=1
c
-----
345    5 -1.0    -245 -475 474      u=10 imp:n,p=1 $ center hole
c
-----
c      Side trims of top handle
c
-----
346    5 -1.0    -470 473 -606 474 -475      u=10 imp:n,p=1
c      347      0      471 473 -607 474 -475      u=10 imp:n,p=1
348    5 -1.0    -470 -472 608 474 -475      u=10 imp:n,p=1
349    5 -1.0     471 -472 609 474 -475      u=10 imp:n,p=1
c
-----
c      Fuel element top fittings (part of top handle geometry)
c
-----
350    7 -2.51   -231 -475 474      u=10 imp:n,p=1 $ B4C
351    4 -7.92   -511 -475 474      u=10 imp:n,p=1
352    4 -7.92   -512 -475 474      u=10 imp:n,p=1
353    4 -7.92   -513 -475 474      u=10 imp:n,p=1
c
-----

```

```

c      Guide tube (top handle)
c      -----
355    0          -246 -475 474 236          u=10  imp:n,p=1 $ air
356    6  -2.70   -247 -475 474 246          u=10  imp:n,p=1 $ cladd
c      -----
c      Shim II top handle side holes
c      -----
360    5  -1.0    -240 -475 474  473          u=10  imp:n,p=1
361    5  -1.0    -241 -475 474 -472          u=10  imp:n,p=1
362    5  -1.0    -242 -475 474  471          u=10  imp:n,p=1
363    5  -1.0    -243 -475 474 -470          u=10  imp:n,p=1
c      -----
c      Shim II second top fittings (top of top handle)
c      -----
371    7  -2.51   -331                    u=10  imp:n,p=1
372    4  -7.92   -511 545 -546          u=10  imp:n,p=1
373    4  -7.92   -512 545 -546          u=10  imp:n,p=1
374    4  -7.92   -513 545 -546          u=10  imp:n,p=1
375    6  -2.70   -332 331          u=10  imp:n,p=1 $ cladd for control
c      -----
c      Guide tube (very top section)
c      -----
376    0          -334 332          u=10  imp:n,p=1 $ air
377    6  -2.70   -335 334          u=10  imp:n,p=1 $ wall
c      -----
c      Shim II third top fittings
c      -----
381    4  -7.92   -531 475 -545          u=10  imp:n,p=1
382    4  -7.92   -532 475 -545          u=10  imp:n,p=1 $
383    4  -7.92   -533 475 -545          u=10  imp:n,p=1
384    4  -7.92   -534 475 -545          u=10  imp:n,p=1
c      -----
c      386    0  -510 475 -545 531          u=10  imp:n,p=1
387    5  -1.0    -511 475 -545 532          u=10  imp:n,p=1
388    5  -1.0    -512 475 -545 533          u=10  imp:n,p=1
389    5  -1.0    -513 475 -545 534          u=10  imp:n,p=1
c      -----
c      390    0  -510 548 -535 549          u=10  imp:n,p=1
391    5  -1.0    -511 548 -535 550          u=10  imp:n,p=1
392    5  -1.0    -512 548 -535 551          u=10  imp:n,p=1
393    5  -1.0    -513 548 -535 552          u=10  imp:n,p=1
c      -----
c      394    0  -510 546 -547 553 554          u=10  imp:n,p=1
395    5  -1.0    -511 546 -547 555 556          u=10  imp:n,p=1
396    5  -1.0    -512 546 -547 557 558          u=10  imp:n,p=1
397    5  -1.0    -513 546 -547 559 560          u=10  imp:n,p=1
c      -----
c      398    4  -7.92   -510 547 -548          u=10  imp:n,p=1
399    4  -7.92   -511 547 -548          u=10  imp:n,p=1
400    4  -7.92   -512 547 -548          u=10  imp:n,p=1
401    4  -7.92   -513 547 -548          u=10  imp:n,p=1
c      -----
c      Fuel element top cones
c      -----
402    4  -7.92   -549 548          u=10  imp:n,p=1
403    4  -7.92   -550 548          u=10  imp:n,p=1
404    4  -7.92   -551 548          u=10  imp:n,p=1
405    4  -7.92   -552 548          u=10  imp:n,p=1
c      -----
c      Middle cones (top fittings)
c      -----
406    4  -7.92   -553 -547 554          u=10  imp:n,p=1
407    4  -7.92   -554  546          u=10  imp:n,p=1
c      -----
408    4  -7.92   -555 -547 556          u=10  imp:n,p=1
409    4  -7.92   -556  546          u=10  imp:n,p=1
c      -----
410    4  -7.92   -557 -547 558          u=10  imp:n,p=1
411    4  -7.92   -558  546          u=10  imp:n,p=1

```

```

c -----
412 4 -7.92 -559 -547 560 u=10 imp:n,p=1
413 4 -7.92 -560 546 u=10 imp:n,p=1
c -----
c Square above bottom adapter for Shim II
c -----
415 6 -2.70 -600 601 -602 603 604 -605 606 607 -608 -609
u=10 imp:n,p=1
416 5 -1.0 -600 603 -606 604 -605 u=10 imp:n,p=1
417 5 -1.0 601 603 -607 604 -605 u=10 imp:n,p=1
418 5 -1.0 -600 -602 608 604 -605 u=10 imp:n,p=1
419 5 -1.0 601 -602 609 604 -605 u=10 imp:n,p=1
c -----
c =====
c Top handle and holes for control element Shim III
c -----
425 6 -2.70 -470 471 -472 473 474 -475 (606 -608 -609)
502 503 504 (247) 245 240 241 242 243
u=12 imp:n,p=1
426 6 -2.70 -236 -475 474 231 u=12 imp:n,p=1 $ cladd
427 5 -1.0 -502 -475 474 511 u=12 imp:n,p=1
428 5 -1.0 -503 -475 474 512 u=12 imp:n,p=1
429 5 -1.0 -504 -475 474 513 u=12 imp:n,p=1
c -----
430 5 -1.0 -245 -475 474 u=12 imp:n,p=1 $ center hole
c -----
c Guide tube (top handle)
c -----
431 0 -246 -475 474 236 u=12 imp:n,p=1 $ air
432 6 -2.70 -247 -475 474 246 u=12 imp:n,p=1 $ cladd
c -----
c Side trims of top handle
c -----
435 5 -1.0 -470 473 -606 474 -475 u=12 imp:n,p=1
c 436 0 471 473 -607 474 -475 u=12 imp:n,p=1
437 5 -1.0 -470 -472 608 474 -475 u=12 imp:n,p=1
438 5 -1.0 471 -472 609 474 -475 u=12 imp:n,p=1
c -----
c Fuel element top fittings (part of top handle geometry)
c -----
440 7 -2.51 -231 -475 474 u=12 imp:n,p=1 $ B4C
441 4 -7.92 -511 -475 474 u=12 imp:n,p=1
442 4 -7.92 -512 -475 474 u=12 imp:n,p=1
443 4 -7.92 -513 -475 474 u=12 imp:n,p=1
c -----
c Shim III top handle side holes
c -----
450 5 -1.0 -240 -475 474 473 u=12 imp:n,p=1
451 5 -1.0 -241 -475 474 -472 u=12 imp:n,p=1
452 5 -1.0 -242 -475 474 471 u=12 imp:n,p=1
453 5 -1.0 -243 -475 474 -470 u=12 imp:n,p=1
c -----
c Shim III second top fittings (part of top handle geometry)
c -----
454 7 -2.51 -381 u=12 imp:n,p=1
455 4 -7.92 -511 545 -546 u=12 imp:n,p=1
456 4 -7.92 -512 545 -546 u=12 imp:n,p=1
457 4 -7.92 -513 545 -546 u=12 imp:n,p=1
458 6 -2.70 -382 381 u=12 imp:n,p=1 $ cladd for control
c -----
c Guide tube (very top section)
c -----
459 0 -384 382 u=12 imp:n,p=1 $ air
460 6 -2.70 -385 384 u=12 imp:n,p=1 $ wall
c -----
c Shim III third top fittings
c -----
c 381 4 -7.92 -531 475 -545 u=12 imp:n,p=1
462 4 -7.92 -532 475 -545 u=12 imp:n,p=1 $

```

```

463 4 -7.92 -533 475 -545 u=12 imp:n,p=1
464 4 -7.92 -534 475 -545 u=12 imp:n,p=1
-----
c
c
c 386 0 -510 475 -545 531 u=12 imp:n,p=1
465 5 -1.0 -511 475 -545 532 u=12 imp:n,p=1
466 5 -1.0 -512 475 -545 533 u=12 imp:n,p=1
467 5 -1.0 -513 475 -545 534 u=12 imp:n,p=1
-----
c
c 390 0 -510 548 -535 549 u=12 imp:n,p=1
471 5 -1.0 -511 548 -535 550 u=12 imp:n,p=1
472 5 -1.0 -512 548 -535 551 u=12 imp:n,p=1
473 5 -1.0 -513 548 -535 552 u=12 imp:n,p=1
-----
c
c 394 0 -510 546 -547 553 554 u=12 imp:n,p=1
476 5 -1.0 -511 546 -547 555 556 u=12 imp:n,p=1
477 5 -1.0 -512 546 -547 557 558 u=12 imp:n,p=1
478 5 -1.0 -513 546 -547 559 560 u=12 imp:n,p=1
-----
c
c 398 4 -7.92 -510 547 -548 u=12 imp:n,p=1
480 4 -7.92 -511 547 -548 u=12 imp:n,p=1
481 4 -7.92 -512 547 -548 u=12 imp:n,p=1
482 4 -7.92 -513 547 -548 u=12 imp:n,p=1
-----
c
c Fuel element top cones
-----
c
c 402 4 -7.92 -549 548 u=12 imp:n,p=1
484 4 -7.92 -550 548 u=12 imp:n,p=1
485 4 -7.92 -551 548 u=12 imp:n,p=1
486 4 -7.92 -552 548 u=12 imp:n,p=1
-----
c
c Middle cones (top fittings)
-----
c
c 406 4 -7.92 -553 -547 554 u=12 imp:n,p=1
c 407 4 -7.92 -554 546 u=12 imp:n,p=1
-----
c
c 489 4 -7.92 -555 -547 556 u=12 imp:n,p=1
490 4 -7.92 -556 546 u=12 imp:n,p=1
-----
c
c 491 4 -7.92 -557 -547 558 u=12 imp:n,p=1
492 4 -7.92 -558 546 u=12 imp:n,p=1
-----
c
c 493 4 -7.92 -559 -547 560 u=12 imp:n,p=1
494 4 -7.92 -560 546 u=12 imp:n,p=1
-----
c
c Square above bottom adapter for Shim III
-----
c
c 495 6 -2.70 -600 601 -602 603 604 -605 606 607 -608 -609
u=12 imp:n,p=1
496 5 -1.0 -600 603 -606 604 -605 u=12 imp:n,p=1
497 5 -1.0 601 603 -607 604 -605 u=12 imp:n,p=1
498 5 -1.0 -600 -602 608 604 -605 u=12 imp:n,p=1
499 5 -1.0 601 -602 609 604 -605 u=12 imp:n,p=1
-----
c
c =====
c
c Top handle and holes for Fuel elements
-----
c
c 500 6 -2.70 -470 471 -472 473 474 -475 (606 607 -608 -609)
501 502 503 504 505 520 521 522 523
u=4 imp:n,p=1
501 5 -1.0 -501 -475 474 510 u=4 imp:n,p=1
502 5 -1.0 -502 -475 474 511 u=4 imp:n,p=1
503 5 -1.0 -503 -475 474 512 u=4 imp:n,p=1
504 5 -1.0 -504 -475 474 513 u=4 imp:n,p=1
-----
c
c 505 5 -1.0 -505 -475 474 u=4 imp:n,p=1
-----
c
c Side trims of top handle
-----
c
c 506 5 -1.0 -470 473 -606 474 -475 u=4 imp:n,p=1

```



```

507 5 -1.0 471 473 -607 474 -475 u=4 imp:n,p=1
508 5 -1.0 -470 -472 608 474 -475 u=4 imp:n,p=1
509 5 -1.0 471 -472 609 474 -475 u=4 imp:n,p=1
c
-----
c Fuel element top fittings (part of top handle geometry)
c
-----
510 4 -7.92 -510 -475 474 u=4 imp:n,p=1
511 4 -7.92 -511 -475 474 u=4 imp:n,p=1
512 4 -7.92 -512 -475 474 u=4 imp:n,p=1
513 4 -7.92 -513 -475 474 u=4 imp:n,p=1
c
-----
c Top handle side holes
c
-----
520 5 -1.0 -520 -475 474 473 u=4 imp:n,p=1
521 5 -1.0 -521 -475 474 -472 u=4 imp:n,p=1
522 5 -1.0 -522 -475 474 471 u=4 imp:n,p=1
523 5 -1.0 -523 -475 474 -470 u=4 imp:n,p=1
c
-----
c Top handle arm support side holes
c
-----
524 5 -1.0 -524 471 -476 475 u=4 imp:n,p=1
525 5 -1.0 -525 477 -470 475 u=4 imp:n,p=1
c
-----
c Fuel element second top fittings (part of top handle geometry)
c
-----
531 4 -7.92 -510 545 -546 u=4 imp:n,p=1
532 4 -7.92 -511 545 -546 u=4 imp:n,p=1
533 4 -7.92 -512 545 -546 u=4 imp:n,p=1
534 4 -7.92 -513 545 -546 u=4 imp:n,p=1
c
-----
c Fuel element Third top fittings
c
-----
541 4 -7.92 -531 475 -545 u=4 imp:n,p=1
542 4 -7.92 -532 475 -545 u=4 imp:n,p=1
543 4 -7.92 -533 475 -545 u=4 imp:n,p=1
544 4 -7.92 -534 475 -545 u=4 imp:n,p=1
c
-----
c
546 5 -1.0 -510 475 -545 531 u=4 imp:n,p=1
547 5 -1.0 -511 475 -545 532 u=4 imp:n,p=1
548 5 -1.0 -512 475 -545 533 u=4 imp:n,p=1
549 5 -1.0 -513 475 -545 534 u=4 imp:n,p=1
c
-----
c
550 5 -1.0 -510 548 -535 549 u=4 imp:n,p=1
551 5 -1.0 -511 548 -535 550 u=4 imp:n,p=1
552 5 -1.0 -512 548 -535 551 u=4 imp:n,p=1
553 5 -1.0 -513 548 -535 552 u=4 imp:n,p=1
c
-----
c
554 5 -1.0 -510 546 -547 553 554 u=4 imp:n,p=1
555 5 -1.0 -511 546 -547 555 556 u=4 imp:n,p=1
556 5 -1.0 -512 546 -547 557 558 u=4 imp:n,p=1
557 5 -1.0 -513 546 -547 559 560 u=4 imp:n,p=1
c
-----
c
558 4 -7.92 -510 547 -548 u=4 imp:n,p=1
559 4 -7.92 -511 547 -548 u=4 imp:n,p=1
560 4 -7.92 -512 547 -548 u=4 imp:n,p=1
561 4 -7.92 -513 547 -548 u=4 imp:n,p=1
c
-----
c Fuel element top cones
c
-----
562 4 -7.92 -549 548 u=4 imp:n,p=1
563 4 -7.92 -550 548 u=4 imp:n,p=1
564 4 -7.92 -551 548 u=4 imp:n,p=1
565 4 -7.92 -552 548 u=4 imp:n,p=1
c
-----
c Middle cones (top fittings)
c
-----
566 4 -7.92 -553 -547 554 u=4 imp:n,p=1
567 4 -7.92 -554 546 u=4 imp:n,p=1
c
-----
568 4 -7.92 -555 -547 556 u=4 imp:n,p=1

```

```

569 4 -7.92 -556 546 u=4 imp:n,p=1
c
-----
570 4 -7.92 -557 -547 558 u=4 imp:n,p=1
571 4 -7.92 -558 546 u=4 imp:n,p=1
c
-----
572 4 -7.92 -559 -547 560 u=4 imp:n,p=1
573 4 -7.92 -560 546 u=4 imp:n,p=1
c
-----
c Top handle arm
c
-----
581 6 -2.70 -476 471 480 -481 475 -478 524 u=4 imp:n,p=1
582 6 -2.70 -470 477 480 -481 475 -478 525 u=4 imp:n,p=1
c
-----
584 5 -1.0 -476 471 473 -480 475 -478 u=4 imp:n,p=1
585 5 -1.0 -476 471 -472 481 475 -478 u=4 imp:n,p=1
c
-----
586 5 -1.0 -470 477 473 -480 475 -478 u=4 imp:n,p=1
587 5 -1.0 -470 477 -472 481 475 -478 u=4 imp:n,p=1
c
-----
590 6 -2.70 -570 u=4 imp:n,p=1
c
-----
c Square above bottom adapter
c
-----
600 6 -2.70 -600 601 -602 603 604 -605 606 607 -608 -609
u=4 imp:n,p=1
606 5 -1.0 -600 603 -606 604 -605 u=4 imp:n,p=1
607 5 -1.0 601 603 -607 604 -605 u=4 imp:n,p=1
608 5 -1.0 -600 -602 608 604 -605 u=4 imp:n,p=1
609 5 -1.0 601 -602 609 604 -605 u=4 imp:n,p=1
c
-----
c Rabbit
c
-----
610 3 -1.60 -610 613 imp:n,p=1 u=18
611 6 -2.70 -611 610 613 imp:n,p=1 u=18
612 5 -1.0 611 (600:-601:602:-603:-604:605) 612 613
imp:n,p=1 u=18
c
-----
613 6 -2.70 -612 u=18 imp:n,p=1 $ bottom fitting
c
-----
c Rabbit tube
c
-----
614 6 -2.70 -613 614 u=18 imp:n,p=1 $ wall
615 9 -1.9769e-3 -614 830 u=18 imp:n,p=1 $ CO2
c
-----
c Square above bottom adapter for Rabbit
c
-----
616 6 -2.70 -600 601 -602 603 604 -605 606 607 -608 -609
u=18 imp:n,p=1
617 5 -1.0 -600 603 -606 604 -605 u=18 imp:n,p=1
618 5 -1.0 601 603 -607 604 -605 u=18 imp:n,p=1
619 5 -1.0 -600 -602 608 604 -605 u=18 imp:n,p=1
620 5 -1.0 601 -602 609 604 -605 u=18 imp:n,p=1
c
-----
c =====
c Graphite reflectors
c
-----
621 3 -1.60 -620 imp:n,p=1 u=13 $ graphite
622 6 -2.70 -621 620 imp:n,p=1 u=13 $ Al wall
623 5 -1.0 621 (600:-601:602:-603:-604:605) 622
imp:n,p=1 u=13 $ outside
c
-----
c graphite reflectors bottom fitting
c
-----
624 6 -2.70 -622 imp:n,p=1 u=13 $ Al wall
c
-----
c Square above bottom adapter for graphite reflectors
c
-----
625 6 -2.70 -600 601 -602 603 604 -605 606 607 -608 -609
u=13 imp:n,p=1
626 5 -1.0 -600 603 -606 604 -605 u=13 imp:n,p=1
627 5 -1.0 601 603 -607 604 -605 u=13 imp:n,p=1

```

```

628 5 -1.0 -600 -602 608 604 -605 u=13 imp:n,p=1
629 5 -1.0 601 -602 609 604 -605 u=13 imp:n,p=1
c
c
c Through tube
c
c
630 4 -7.92 -630 631 -632 633 imp:n,p=2 $ wall
631 10 -1.205e-3 -631 -632 633 634 imp:n,p=4 $ air
c
c
c Through tube tally
c
c
634 10 -1.205e-3 -634 imp:n,p=8 $ air
c
c
c
c
c Graphite PuBe source holder
c
c
635 3 -1.60 -625 627 imp:n,p=1 u=24 $ graphite
636 6 -2.70 -626 625 imp:n,p=1 u=24 $ Al wall
637 5 -1.0 626 (600:-601:602:-603:-604:605)
imp:n,p=1 u=24 $ outside
c
c
c PuBe source tube
c
c
638 6 -2.70 -627 628 u=24 imp:n,p=1 $
639 9 -1.9769e-3 -628 u=24 imp:n,p=1 $
c
c
c Square above bottom adapter for PuBe source
c
c
645 6 -2.70 -600 601 -602 603 604 -605 606 607 -608 -609
u=24 imp:n,p=1
646 5 -1.0 -600 603 -606 604 -605 u=24 imp:n,p=1
647 5 -1.0 601 603 -607 604 -605 u=24 imp:n,p=1
648 5 -1.0 -600 -602 608 604 -605 u=24 imp:n,p=1
649 5 -1.0 601 -602 609 604 -605 u=24 imp:n,p=1
c
c
c Beam ports
c
c
650 4 -7.92 -640 641 imp:n,p=2 $ beam port 1 wall East
651 10 -1.205e-3 -641 642 imp:n,p=4 $ beam port 1 air
652 10 -1.205e-3 -642 imp:n,p=8 $ Bp1 Flux tally
c
c
662 4 -7.92 -650 651 imp:n,p=2 $ beam port 2 wall West
663 10 -1.205e-3 -651 652 imp:n,p=4 $ beam port 2 air
664 10 -1.205e-3 -652 imp:n,p=8 $ beam port 2 air
c
c
c Fission chamber support tube
c
c
670 6 -2.70 -615 616 u=25 imp:n,p=1 $
671 10 -1.205e-3 -616 u=25 imp:n,p=1 $
672 5 -1.0 615 (600:-601:602:-603:-604:605)
u=25 imp:n,p=1 $
c
c
c Square above bottom adapter for PuBe source
c
c
675 6 -2.70 -600 601 -602 603 604 -605 606 607 -608 -609
u=25 imp:n,p=1
676 5 -1.0 -600 603 -606 604 -605 u=25 imp:n,p=1
677 5 -1.0 601 603 -607 604 -605 u=25 imp:n,p=1
678 5 -1.0 -600 -602 608 604 -605 u=25 imp:n,p=1
679 5 -1.0 601 -602 609 604 -605 u=25 imp:n,p=1
c
c
c Thermal column
c
c
c First part
670 6 -2.70 -700 (-701:702:-703:704:-705:706) imp:n,p=1
701 16 -1.60 701 -702 703 -704 705 -706 imp:n,p=1
c
c Second part
722 6 -2.70 -722 700 (-723:724:-725:726:-727:728)

```

```

                                imp:n,p=1
723 16 -1.60          723 -724 725 -726 727 -728 imp:n,p=1
c
c -----
c Third part
734 6 -2.70  733 -734 -110 -736 737 -738
      (-743:744:746:-747:748)      imp:n,p=1
735 11 -2.25  743 -744 -110 -746 747 -748 750 imp:n,p=1
750 10 -1.205e-3 -750      imp:n,p=1
c
c -----
c repeated structure tally
c
c -----
800 1 -5.95 -800 9 u=1 vol=80.424 imp:n,p=1 $
c Top of fuel tally
802 1 -5.95 -802 9 u=1 vol=1      imp:n,p=1 $
c Bottom of fuel tally
803 1 -5.95 -803 9 u=1 vol=1      imp:n,p=1 $
c
c -----
c Rabbit and cadmium covered cylinder
c
c -----
c Rabbit
830 9 -1.9769e-3 -830 831      u=18 imp:n,p=1 $ Polyethylene
831 9 -1.9769e-3 -831 832      u=18 imp:n,p=1 $ CO2
c Cadmium Cylinder
832 9 -1.9769e-3 -832 833      u=18 imp:n,p=1 $ Cadmium
833 9 -1.9769e-3 -833      u=18 imp:n,p=1 $ CO2
c
c -----
c
c =====
c Surface cards
c
c =====
c Fuel element
c
c -----
1 cz 1.740 $ fuel cylinder
2 cz 1.790 $ cladding cylinder
5 pz 0.001 $ bottom of lower graphite plug
6 pz 8.811 $ top of lower graphite plug
7 pz 46.911 $ top of UZrH active fuel
8 pz 55.671 $ top of upper graphite plug
9 cz 00.2285 $ Zr cylinder
10 cz 1.25 $ bottom fitting
11 pz -6.788 $ bottom surface for bottom fitting
c 14 cz 1.374 $ first top fitting's cylinder [dummy]
15 pz 59.221 $ top of 'first top fitting' cylinder
c
c -----
16 pz 57.221 $ top of cladd's top thickness
17 pz -1.55 $ bottom of cladd's bottom thickness
18 pz 8.891 $ Mo disk 0.08 cm thick below fuel
19 pz 46.831 $ Mo disk 0.08 cm thick above fuel
c
c -----
c Hexagonal first top fitting
c
c -----
20 p 1 1.73205 0 2.400
21 px 1.200
22 p -1 1.73205 0 -2.400
23 p 1 1.73205 0 -2.400
24 px -1.200
25 p -1 1.73205 0 2.400
c
c -----
c Control element
c
c -----
32 pz 2.102 $ top of bottom fitting for Shim
33 pz 4.642 $ guide tube bottom steel plug
34 pz 32.137 $ bottm poison plug Shim I, thick=1.59 cm
35 pz 32.099 $ bottm poison plug Shim II
36 pz 33.928 $ bottm poison plug Shim III
c
c -----
c Bottom adpater and grid plate lattice
c
c -----
50 c/z 1.9431 1.9431 2.86 $ 5.72 diameter hole
51 pz -24.416
52 pz -11.081 $ relates to sur 604--increaase/decrease

```

```

53 px 5.82939 $
54 px -1.94319
55 py 5.82939
56 py -1.94319
c -----
c Bottom adapter window
c -----
61 px 68.0100 $13.60196$ 5.82938 $
62 px -1.94318
63 py 44.6922
64 py -1.94318
c -----
c Lattice cell surfaces
c -----
70 px 1.9431 $
71 px -1.9431
72 py 1.9431
73 py -1.9431
c -----
c Cluster (Assembly) boundary surfaces
c -----
74 px 5.8292 $
75 px -1.9430
76 py 5.8292
77 py -1.9430
78 pz -6.7879 $ less than surf 11 by 0.0001
79 pz 59.220
c -----
c Core lattice
c -----
81 px 5.8294 $
82 px -1.9432
83 py 5.8294
84 py -1.9432
c -----
c Core window
c -----
91 pz -11.0809 $ -40.441 $ was bottom of pool
92 pz 100 $ 85.6721
93 px 68.0101 $ 5.829399
94 px -1.94311
95 py 36.91970 $
96 py -1.94311
c -----
c 99 rpp -1.9531 68.02 -1.9531 44.7 -41.441 86.6721
c -----
c Reactor Pool Tank: 3/8 in Al plate on side and 1/2 in on bottom
c Diameter: 2.13 m (7 ft): 6.48 m High
c Al 6061 T6
c -----
100 c/z 37.0089 45.5379 106.5 $ tank actual radius is 106.5
101 c/z 37.0089 45.5379 107.45 $ tank wall radius is 107.45
102 pz 200.30 $ (was 602) top surface 6.48 m -45.70 cm
103 pz -45.70 $ bottom surface
c -----
c Bioshield (concrete)
c -----
c Lower part: 1.98 m (6.5 ft) thick and 3.35 m (11 ft) high
c First upper part:1.52 m (5 ft) thick and 0.61 m (2 ft)
c Second upper part:0.91 thick and 2.52 m
c Tank heigh is 6.48 m -(1.52 + 1.98 = 2.52
c -----
110 c/z 37.0089 45.5379 305.45 $ radius = 107.45 + 198
111 pz 140.3 $ = -45.7+335
c =====
c Shim I
c -----
c 100% removed is at pz=46.91 $ B4C
205 cz 1.52 $ B4c
206 cz 1.59 $ Al cladd

```

```

c      Rod position at 65.4%--sur 475 pz =61.7621 (for top B4C)
207   pz      33.727 $ increase/decrease surf 34 also by 1.59 cm
c     208     pz      44.36  $
c     -----
c     Shim II
c     -----
c     Poison and cladd are surfs 205 and 206 for Shim II, III
c     Rod position at 65.3%
217   pz      33.689 $ increase/decrease surf 35 also by 1.59 cm
c     -----
c     Shim III 70.1%
c     -----
227   pz      35.518 $ increase/decrease surf 36 also by 1.59 cm
c     -----
c     Top handle holes for control element
c     -----
231   cz              1.52 $ hole for element [0 0 0]
232   c/z  3.8862 0      1.52 $ hole for element [1 0 0]
233   c/z  0      3.8862 1.00 $ hole for element [0 1 0]
234   c/z  3.8862 3.8862 1.00 $ hole for element [1 1 0]
c     -----
c     Cladd of Shim in top handle
c     -----
235   c/z  3.8862 0      1.59 $ cladd for element [1 0 0]
236   cz              1.59 $ cladd for element [0 0 0]
c     -----
c     Guide tube (top handle) Shim I
c     -----
237   c/z  3.8862 0      1.740 $ cladd for element [1 0 0]$ guide
238   c/z  3.8862 0      1.790 $ cladd for element [1 0 0]$ guide
c     -----
c     Top handle side holes for control element
c     -----
240   c/z  1.9431 -1.8000 0.8 $
241   c/z  1.9431  5.7000 0.8 $
242   c/z -1.8000  1.9431 0.8 $
243   c/z  5.7000  1.9431 0.8 $
c     -----
245   c/z  1.9431 1.9431 0.50 $ top handle center hole for control
c     -----
c     Guide tube (top handle) Shim II
c     -----
246   cz              1.740 $ hole for element [0 0 0]
247   cz              1.790 $ hole for element [0 0 0]
c     -----
c     Poison and cladd for Shim I very top section
c     -----
272   rcc 3.8862 0 61.7621 0 0 10.065 1.52 $ [1 0 0] see surf 475
273   rcc 3.8862 0 61.7621 0 0 11.655 1.59 $ [1 0 0] see surf 475
c     -----
c     Guide tube (top section) Shim I
c     -----
274   rcc 3.8862 0 61.7621 0 0 37.5336 1.740 $ [1 0 0] see surf 475
275   rcc 3.8862 0 61.7621 0 0 37.5337 1.790 $ [1 0 0] see surf 475
c     -----
c     Poison and cladd for Shim II very top section
c     -----
331   rcc 0 0 61.7621 0 0 10.027 1.52 $ see surf 475
332   rcc 0 0 61.7621 0 0 11.617 1.59 $ see surf 475
c     -----
c     Guide tube (top section) Shim II
c     -----
334   rcc 0 0 61.7621 0 0 37.5334 1.740 $ see surf 475
335   rcc 0 0 61.7621 0 0 37.5335 1.790 $ see surf 475
c     -----
c     Poison and cladd for Shim III very top section
c     -----
381   rcc 0 0 61.7621 0 0 11.856 1.52 $ see surf 475
382   rcc 0 0 61.7621 0 0 13.446 1.59 $ see surf 475
c     -----
c

```

```

c      Guide tube (top section) Shim III
384   rcc 0 0 61.7621 0 0 37.5338 1.740 $ see surf 475
385   rcc 0 0 61.7621 0 0 37.5339 1.790 $ see surf 475
c
c      Top handle
c
c      -----
470   px 5.7785 $
471   px -1.8923
472   py 5.7785
473   py -1.8923
474   pz 59.2221
475   pz 61.7621
c
c      -----
c      Top handle arm support
476   px -1.3905
477   px 5.2767
478   pz 71.7865
480   p 0 1 -.14 -9.55
481   p 0 1 .14 13.436
c
c      -----
c      Top handle holes
c
c      -----
501   cz                1.00 $ hole for element [0 0 0]
502   c/z 3.8862 0          1.00 $ hole for element [1 0 0]
503   c/z 0 3.8862 1.00 $ hole for element [0 1 0]
504   c/z 3.8862 3.8862 1.00 $ hole for element [1 1 0]
c
c      -----
505   c/z 1.9431 1.9431 1.00 $ top handle center hole
c
c      -----
510   cz                0.751 $ second top fitng for element [0 0 0]
511   c/z 3.8862 0.0       0.751 $ second top fitng for element [1 0 0]
512   c/z 0.0 3.8862 0.751 $ second top fitng for element [0 1 0]
513   c/z 3.8862 3.8862 0.751 $ second top fitng for element [1 1 0]
c
c      -----
c      Top handle side holes
c
c      -----
520   c/z 1.9431 -1.8000 1.3 $
521   c/z 1.9431 5.7000 1.3 $
522   c/z -1.8000 1.9431 1.3 $
523   c/z 5.7000 1.9431 1.3 $
c
c      -----
c      Top handle arm support side holes
c
c      -----
524   c/x 1.9431 61.7621 1.3000 $
525   c/x 1.9431 61.7621 1.3001 $
c
c      -----
c      Third top fitting cylinder
c
c      -----
531   cz                0.5 $ element [0 0 0]
532   c/z 3.8862 0.0       0.5 $ element [1 0 0]
533   c/z 0.0 3.8862 0.5 $ element [0 1 0]
534   c/z 3.8862 3.8862 0.5 $ element [1 1 0]
535   pz 67.0721 $ was 61.9721
c
c      -----
545   pz 63.0621
546   pz 64.8621
547   pz 65.9621
548   pz 66.5121
c
c      -----
c      Cone on top of element
c
c      -----
549   kz 67.0721                1.79 -1 $ element [0 0 0]
550   k/z 3.8862 0.0 67.0721 1.79 -1 $ element [1 0 0]
551   k/z 0.0 3.8862 67.0721 1.79 -1 $ element [0 1 0]
552   k/z 3.8862 3.8862 67.0721 1.79 -1 $ element [1 1 0]
c
c      -----
c      Middle cones (top fittings)
c
c      -----
553   kz 64.8621                0.45 1 $ element [0 0 0]
554   kz 65.9621                0.45 -1 $ element [0 0 0]

```

```

c -----
555 k/z 3.8862 0.0 64.8621 0.45 1 $ element [1 0 0]
556 k/z 3.8862 0.0 65.9621 0.45 -1 $ element [1 0 0]
c -----
557 k/z 0.0 3.8862 64.8621 0.45 1 $ element [0 1 0]
558 k/z 0.0 3.8862 65.9621 0.45 -1 $ element [0 1 0]
c -----
559 k/z 3.8862 3.8862 64.8621 0.45 1 $ element [1 1 0]
560 k/z 3.8862 3.8862 65.9621 0.45 -1 $ element [1 1 0]
c -----
c Top handle arm
c -----
c -----
570 rcc -1.3904 1.9431 69.7865 6.6670 0 0 0.70 $middle bar
c -----
c Top of square part of bottom adapter
c -----
600 px 5.7000 $
601 px -1.8000
602 py 5.7000
603 py -1.8000
604 pz -11.080 $ relates to surf 52-- increase/decrease
605 pz -6.7881
c -----
c Squarare part side trim planes
c -----
606 p -1 1 0 -6.386
607 p 1 1 0 -2.500
608 p 1 1 0 10.27
609 p -1 1 0 6.386
c =====
c Rabbit
c -----
610 rpp -1.4503 5.3365 -1.4503 5.3365 7.182 69.7295 $ Graphite
611 rpp -1.6154 5.5016 -1.6154 5.5016 6.547 70.3645 $ Al wall
c -----
c Rabbit bottom fitting
c -----
612 rcc 1.9431 1.9431 -6.788 0 0 6.35 0.9525 $ 3/4 in diameter
c -----
c Rabbit tube
c -----
613 rcc 1.9431 1.9431 -0.438 0 0 80.0 1.905 $ 3/4 in diameter
614 rcc 1.9431 1.9431 -0.197 0 0 79.759 1.739 $ air
c -----
c -----
c Fission chamber support tube
c -----
615 rcc 1.9431 1.9431 -6.788 0 0 70.8175 3.06 $ 3/4 in diameter
616 rcc 1.9431 1.9431 -6.788 0 0 70.8175 2.90 $ air
c -----
c Graphite reflectors
c -----
620 rpp -1.4503 5.3365 -1.4503 5.3365 -0.915 61.6325
621 rpp -1.6154 5.5016 -1.6154 5.5016 -1.55 62.2675
c -----
c graphite reflectors bottom fitting
c -----
622 rcc 1.9431 1.9431 -6.788 0 0 5.238 0.9525 $ 3/4 in diameter
c -----
c -----
c Graphite PuBe source holder
c -----
625 rpp -1.4503 5.3365 -1.4503 5.3365 -6.788 57.0295
626 rpp -1.6154 5.5016 -1.6154 5.5016 -6.788 57.0295
627 rcc 1.9431 1.9431 -6.788 0 0 63.8175 1.905 $ 3/4 in diameter
628 rcc 1.9431 1.9431 -6.788 0 0 63.8175 1.739 $ air
c -----
c -----
c Through tube
c -----

```



```

630 c/x 45.5379 30.2630 7.62
631 c/x 45.5379 30.2630 6.82
632 px 348.0
633 px -274.0
c -----
c Through tube flux tally
634 rcc 18.03 45.5379 30.2630 15 0 0 6.8
c -----
c Beam ports
c -----
640 rcc 72.2 17.5279 30.2630 276.0 0 0 7.62 $ beam port 1 wall
641 rcc 73.0 17.5279 30.2630 275.2 0 0 6.82 $ beam port 1
642 rcc 74.0 17.5279 30.2630 10.0 0 0 6.80 $ Flux tally
c -----
650 rcc -17.2 17.5279 30.2630 -257.8 0 0 7.62 $ beam port 2 wall
651 rcc -18.0 17.5279 30.2630 -257.0 0 0 6.82 $ beam port 2
652 rcc -19.0 17.5279 30.2630 -10.0 0 0 6.80 $ Flux tally
c =====
c Thermal column section
c -----
c Thermal column
c -----
c First part
700 rpp 5.4856 68.3516 -102.0460 -2.6670 -3.6230 59.2430 $
c -----
701 px 6.4386
702 px 67.3986
703 py -102.0460
704 py -3.6200
705 pz -2.6700
706 pz 58.2900
c -----
c Second part
722 rpp -4.6744 78.5116 -157.9261 -100.14 -13.7830 69.4030 $
c 723 rpp -3.8814 77.5586 -157.9261 -102.0460 -12.8300 68.4500 $
c -----
723 px -3.8814
724 px 77.5586
725 py -157.9261
726 py -102.0460
727 pz -12.8300
728 pz 68.4500
c -----
c Third part
c 734 rpp -14.6769 88.3541 -250.1617 -157.9261 -23.6255 79.2455 $
c -----
733 px -14.6769
734 px 88.3541
c 735 py -250.1617
736 py -157.9261
737 pz -23.6255
738 pz 79.2455
c -----
739 rpp -13.7239 87.4011 -249.2087 -159.8322 -22.6725 78.2925 $
743 px -13.7239
744 px 87.4011
c 745 py -249.2087
746 py -159.8322
747 pz -22.6725
748 pz 78.2925
c -----
c Front of access plug test zone
750 rpp 17.7239 57.4011 -162.8323 -159.8323 8.6725 48.2925 $
c -----
c repeated structure tally
c -----
800 rcc 0.0 0.0 22.86 0 0 10 1.6
c -----
c Top of fuel tally
802 rcc 0.0 0.0 42.70 0 0 4.00 1.6
c Bottom of fuel tally

```

```

803   rcc 0.0 0.0 9.00 0 0 4.00 1.6
c
c   Rabbit and Cadmium container
c
830   rcc 1.9431 1.9431 24.86 0 0 6.0 1.700 $ Polyethylene
831   rcc 1.9431 1.9431 25.06 0 0 5.6 1.500 $ air
c   Cadmium container
832   rcc 1.9431 1.9431 25.07 0 0 5.4 1.330 $ Cadmium
833   rcc 1.9431 1.9431 25.17 0 0 5.2 1.230 $ air
c
c
c   =====
c   Data cards
c   =====
mode  n p
kcode 3000 1.0 100 5000
ksrc  16.2 0.0 30
      39.6 8.5 30
      31.8 16.2 30
prtmp  0 0 1
phys:N 3j -1001 $ delayed neutron production is on
phys:P 5j -101  $ delayed gamma production is on
c
c   BURN      TIME=20,20
c   MAT=1
c   MATVOL=32981.75
c   POWER=0.25
c   PFRAC=1.0,1.0
c   BOPT=1.0, -14 1.0
c
c
c   =====
c   Tallies
c   =====
fc34   Neutron flux at the face of thermal column access plug
f34:n  750
sd34   1
e34    1e-9 120ilog 20 $
c
fc54   Neutron flux at rabbit
f54:n  833
sd54   1
e54    0.625E-6 0.1 20.0 T
c
fc64   Neutron flux spectrum at rabbit
f64:n  833
sd64   1
e64    1e-9 120ilog 20 $
c
c
fc124  Flux at Beam Port 1
f124:n 652
sd124  1
e124   1e-9 120ilog 20 $
c
fc134  Flux at Beam Port 2
f134:n 664
sd134  1
e134   1e-9 120ilog 20 $
c
fc144  Flux at Through Tube
f144:n 634
sd144  1
e144   1e-9 120ilog 20 $
c
c
c   =====
c   Materials
c   =====
Material #1: Uranium Zirconium Hydride--UZrH with H:Zr 1.65:1

```

```

c      U is 8.5 w/o , with U235 enriched to < 20% =19.75% rest is ZrH
c      S(alpha, beta) cross sections for both Hydrogen in ZrH and Zr
c      in ZrH are used. The specification is in ml card.
c      -----
m1     40000 -.898617 1001 -0.016383 92238 -0.068213 92235 -0.016788
mt1    zr/h.62t h/zr.62t
c      -----
c      Material #2: Zirconium
c      -----
m2     40000 -1.0 $
c      -----
c      Material #3:carbon
c      -----
m3     6000 -1.000000 $
mt3    grph.62t
c      -----
c      Material #4: stainless steel 304 (Fe Cr Ni Mn) density 7.92
c      Los Alamos data.
c      -----
m4     26000 -0.695000 24000 -0.190000 28000 -0.095000 25055
        -0.020000 $
c      -----
c      Material #5: water
c      -----
m5     1001 2 8016 1$
mt5    lwtr.61t
c      -----
c      Material #6: Al 6061 T6--Aluminum Tank
m6     13027 -0.97511 29000 -0.00586 14000 -0.00622
        12000 -0.00897 24000 -0.00384
c      -----
c      Material #7: Boron Carbide
m7     5011 3.2 5010 .8 6000 1 $
c      -----
c      Material #8: Al 1100
c      m8     13027.66c -0.992120 29000 -0.004455 25055 -0.001013
c           30000 -0.002412$
c      -----
c      Material #9: Carbon Dioxide $ density=1.9769e-3 revise and cite
m9     6000 -0.272919 8016 -0.727081 $
c      -----
c      Material #10: Standard Air (Attix page 531)
m10    7014 -0.752308 7015 -0.002960 8016 -0.231687
        8017 -0.000094 6000 -0.000124 18000 -0.012827
c      -----
c      Material #11: Concrete (from Los Alamos Criticallity Primer)
m11    1001 -0.00453 8016 -0.5126 14000 -.36036
        13027 -0.03555 11023 -0.01527 20000 -0.05791
        26000 -0.01378
c      -----
c      Material #6: Al 6061 T6--Bottom adapter
m12    13027 -0.97511 29000 -0.00586 14000 -0.00622
        12000 -0.00897 24000 -0.00384
c      -----
c      Material #13: Molybdenum
m13    42000 -1.0 $
c      -----
c      Material #14: Cadmium
m14    48000 -1.0 $
c      -----
c      Material #14: Polyethylene
m15    1001 -0.143716 6012 -0.856284 $
c      -----
c      Material #16: Graphite
m16    6000 -1.0 $
mt16   grph.60t
c      =====

```

A.2 MCNP Model of the Simplified Core of MUTR

```

MCNP      UMD Reactor Model (Core)
c      =====
c      =====
c
c              Ali Bellou Mohamed
c              10/19/2009
c              University of Maryland
c              College Park, Maryland
c              Property of the University of Maryland
c      =====
c              Cell cards
c      =====
c      Fuel element
c      -----
1      3      -1.60      -1      5      -6      u=1 imp:n=1 $ lower graphite plug
c              tmp=2.526e-8
2      1      -5.95      -1      9      18      -19      800 802 803
c              u=1 vol=1 imp:n=1 $ UZrH fuel
c              tmp=2.526e-8
3      3      -1.60      -1      7      -8      u=1 imp:n=1 $ upper graphite plug
c              tmp=2.526e-8
4      2      -6.53      -9      18      -19      u=1 imp:n=1 $ Zr rod in
c              tmp=2.526e-8
5      4      -7.92      -10      -17      11      u=1 imp:n=1 $ bottom fitting
c              tmp=2.526e-8
7      4      -7.92      (-21 24 -20 23 -25 22) 16 -15 u=1 imp:n=1
c              tmp=2.526e-8
c              $ First hexagonal top fitting
8      13      -10.2      -1      -18      6      u=1 imp:n=1 $ Molybdenum disk
c              tmp=2.526e-8
9      13      -10.2      -1      19      -7      u=1 imp:n=1 $ Molybdenum disk
c              tmp=2.526e-8
c      -----
10     4      -7.92      -1      8      -16      u=1 imp:n=1 $plug above top grap plg
c              tmp=2.526e-8
11     4      -7.92      -1      -5      17      u=1 imp:n=1 $ " below bttom grap plg
c              tmp=2.526e-8
c      -----
c      Interior and exterior of element
c      -----
20     4      -7.92      -2      1      17      -16      u=1 imp:n=1 $ cladding
c              tmp=2.526e-8
21     5      -1.0      2:(16 (21:-24:20:-23:25:-22)):(15):(-17 10):-11
c              u=1 imp:n=1 $ ouside element
c      -----
c      Control element (control rod guide)
c      -----
30     6      -2.70      -206      32      -33      u=20 imp:n=1 $ bottm plug
31     6      -2.70      -206      32      -33      u=21 imp:n=1 $
32     6      -2.70      -206      32      -33      u=22 imp:n=1 $
c      -----
34     6      -2.70      -206      -207      34      u=20 imp:n=1 $ Shim I bttm plg
35     6      -2.70      -206      -217      35      u=21 imp:n=1 $ Shim II bttm plg
36     6      -2.70      -206      -227      36      u=22 imp:n=1 $ Shim III bttm plg
c      -----
c      Fuel assembly lattice (four rods) cell and exterior of cell
c      -----

```

```

40 5 -1.0 -70 71 -72 73 imp:n=1 lat=1 u=2 fill=0:1 0:1 0:0 $
      1 1
      1 1
41 5 -1.0 -74 75 -76 77 78 -79 imp:n=1 u=4 fill=2
42 5 -1.0 (74:-75:76:-77:-78:79)
      imp:n=1 u=4 $
c -----
c -----
c =====
c Core lattice
c -----
80 5 -1.0 -81 82 -83 84 imp:n=1 tmp=2.4829e-8
      u=5 lat=1 fill=0:8 0:4 0:0
c -----
      5 5 4 4 4 4 4 4 5 $ F
      5 13 4 8 4 4 10 4 5 $ E
      5 13 4 4 4 4 4 4 5 $ D
      5 5 4 18 4 12 4 4 5 $ C
      5 5 5 4 5 5 5 5 5 $ B
c -----
c 1 2 3 4 5 6 7 8 9 $
c -----
81 5 -1.0 94 -93 96 -95 91 -92 tmp=2.4829e-8 imp:n=1 fill=5
c -----
c Outside window
c -----
99 5 -1.0 (-100 -102 103) (-94:93:-96:95:-91:92) (630) (640)
      (650) (700)
      imp:n=1 tmp=2.4829e-8
c -----
c Reactor Pool Tank wall
c -----
100 6 -2.70 -101 100 -102 103 (630) (640) (650) (700)
      imp:n=1
c -----
c Bioshield (concrete)
c -----
110 11 -2.25 101 -110 103 -111 (630) (640) (650) (700) (722)
      (-733:734:736:-737:738) imp:n=1
c -----
c Outside World
c -----
199 0 99 imp:n=0 $
199 0 (110:(111 101):102:-103) (630:632:-633) (640) (650)
      imp:n=0 $
c =====
c -----
c Shim I (control rod)
c -----
200 5 -1.0 -1 32 -15 206 u=20 imp:n=1 $ guide tube
201 6 -2.70 -2 1 -15 32 u=20 imp:n=1 $ tube wall
202 4 -7.92 -10 -32 11 u=20 imp:n=1 $ bottom fitting
203 5 -1.0 2:(-32 10):-11:15 u=20 imp:n=1 $ exterior of tube
c -----
204 7 -2.51 -205 207 -15 u=20 imp:n=1 $ B4C
205 6 -2.70 -206 205 207 -15 u=20 imp:n=1 $ Al clad
206 5 -1.0 -206 33 -34 u=20 imp:n=1 $ void below B4C
c -----
c Shim I Cluster
c -----
c Fuel-Control assembly lattice cell and exterior of cell
c -----
207 5 -1.0 -70 71 -72 73 imp:n=1 lat=1 u=7 fill=0:1 0:1 0:0 $
      1 20
      1 1
208 5 -1.0 -74 75 -76 77 78 -79 imp:n=1 u=8 fill=7
209 5 -1.0 (74:-75:76:-77:-78:79)
      (470:-471:472:-473:-474:(475 510 512 513):535) (275)
      (74:-75:76:-77:-51:52 )

```

```

                                imp:n=1 u=8
c =====
c Shim II (control rod)
c -----
210 5 -1.0 -1 32 -15 206 u=21 imp:n=1 $ guide tube
211 6 -2.70 -2 1 -15 32 u=21 imp:n=1 $ tube wall
212 4 -7.92 -10 -32 11 u=21 imp:n=1 $ bottom fitting
213 5 -1.0 2:(-32 10):-11:15 u=21 imp:n=1 $ exterior of tube
c -----
214 7 -2.51 -205 217 -15 u=21 imp:n=1 $ B4C
215 6 -2.70 -206 205 217 -15 u=21 imp:n=1 $ Al clad
216 5 -1.0 -206 33 -35 u=21 imp:n=1 $ void below B4C
c -----
c Shim II Cluster
c -----
c Fuel-Control assembly lattice cell and exterior of cell
c -----
217 5 -1.0 -70 71 -72 73 imp:n=1 lat=1 u=9 fill=0:1 0:1 0:0 $
      21 1
      1 1
218 5 -1.0 -74 75 -76 77 78 -79 imp:n=1 u=10 fill=9
219 5 -1.0 (74:-75:76:-77:-78:79)
      (470:-471:472:-473:-474:(475 511 512 513):535) (335)
      (74:-75:76:-77:-51:52 )
      imp:n=1 u=10
c =====
c Shim III (control rod)
c -----
220 5 -1.0 -1 32 -15 206 u=22 imp:n=1 $ guide tube
221 6 -2.70 -2 1 -15 32 u=22 imp:n=1 $ tube wall
222 4 -7.92 -10 -32 11 u=22 imp:n=1 $ bottom fitting
223 5 -1.0 2:(-32 10):-11:15 u=22 imp:n=1 $ exterior of tube
c -----
224 7 -2.51 -205 227 -15 u=22 imp:n=1 $ B4C
225 6 -2.70 -206 205 227 -15 u=22 imp:n=1 $ Al clad
226 5 -1.0 -206 33 -36 u=22 imp:n=1 $ void below B4C
c -----
c Shim III Cluster
c -----
c Fuel-Control assembly lattice cell and exterior of cell
c -----
227 5 -1.0 -70 71 -72 73 imp:n=1 lat=1 u=11 fill=0:1 0:1 0:0 $
      22 1
      1 1
228 5 -1.0 -74 75 -76 77 78 -79 imp:n=1 u=12 fill=11
229 5 -1.0 (74:-75:76:-77:-78:79)
      (470:-471:472:-473:-474:(475 511 512 513):535) (385)
      (74:-75:76:-77:-51:52 )
      imp:n=1 u=12
c -----
c =====
c Top handle and holes for control element Shim I
c -----
230 5 -1.0 -470 471 -472 473 474 -475 501 (238)
      (607 -608 -609) 503 504 245 240 241 242 243
      u=8 imp:n=1
231 5 -1.0 -501 -475 474 510 u=8 imp:n=1
232 6 -2.70 -235 -475 474 232 u=8 imp:n=1 $ cladd
233 5 -1.0 -503 -475 474 512 u=8 imp:n=1
234 5 -1.0 -504 -475 474 513 u=8 imp:n=1
c -----
235 5 -1.0 -245 -475 474 u=8 imp:n=1 $ cener hole
c -----
236 0 -237 -475 474 235 u=8 imp:n=1 $ guide tube
237 6 -2.70 -238 -475 474 237 u=8 imp:n=1 $ guide tube wall
c -----
c Side trims of top handle
c -----
240 0 -470 473 -606 474 -475 u=8 imp:n=1
241 5 -1.0 471 473 -607 474 -475 u=8 imp:n=1

```

```

242 5 -1.0 -470 -472 608 474 -475 u=8 imp:n=1
243 5 -1.0 471 -472 609 474 -475 u=8 imp:n=1
c
c Fuel element top fittings (part of top handle geometry)
c
250 5 -1.0 -510 -475 474 u=8 imp:n=1
251 7 -2.51 -232 -475 474 u=8 imp:n=1 $ B4C
252 5 -1.0 -512 -475 474 u=8 imp:n=1
253 5 -1.0 -513 -475 474 u=8 imp:n=1
c
c Shim I top handle side holes
c
260 5 -1.0 -240 -475 474 473 u=8 imp:n=1
261 5 -1.0 -241 -475 474 -472 u=8 imp:n=1
262 5 -1.0 -242 -475 474 471 u=8 imp:n=1
263 5 -1.0 -243 -475 474 -470 u=8 imp:n=1
c
c Shim I second top fittings (top of top handle)
c
271 5 -1.0 -510 545 -546 u=8 imp:n=1
272 7 -2.51 -272 u=8 imp:n=1
273 5 -1.0 -512 545 -546 u=8 imp:n=1
274 5 -1.0 -513 545 -546 u=8 imp:n=1
275 6 -2.70 -273 272 u=8 imp:n=1 $cladd for control
c
276 0 -274 273 u=8 imp:n=1 $guide tube
277 6 -2.70 -275 274 u=8 imp:n=1 $guide tube wall
c
c Shim I third top fittings
c
281 5 -1.0 -531 475 -545 u=8 imp:n=1
c 282 7 -2.51 -232 475 -535 u=8 imp:n=1 $ B4C
283 5 -1.0 -533 475 -545 u=8 imp:n=1
284 5 -1.0 -534 475 -545 u=8 imp:n=1
c
c
286 5 -1.0 -510 475 -545 531 u=8 imp:n=1
c 547 0 -235 475 -535 232 u=8 imp:n=1 cladd
288 5 -1.0 -512 475 -545 533 u=8 imp:n=1
289 5 -1.0 -513 475 -545 534 u=8 imp:n=1
c
290 5 -1.0 -510 548 -535 549 u=8 imp:n=1
c 551 0 -511 548 -535 550 u=8 imp:n=1
292 5 -1.0 -512 548 -535 551 u=8 imp:n=1
293 5 -1.0 -513 548 -535 552 u=8 imp:n=1
c
294 5 -1.0 -510 546 -547 553 554 u=8 imp:n=1
c 555 0 -511 546 -547 555 556 u=8 imp:n=1
296 5 -1.0 -512 546 -547 557 558 u=8 imp:n=1
297 5 -1.0 -513 546 -547 559 560 u=8 imp:n=1
c
298 5 -1.0 -510 547 -548 u=8 imp:n=1
c 559 4 -7.92 -511 547 -548 u=8 imp:n=1
300 5 -1.0 -512 547 -548 u=8 imp:n=1
301 5 -1.0 -513 547 -548 u=8 imp:n=1
c
c Fuel element top cones
c
302 5 -1.0 -549 548 u=8 imp:n=1
c 563 4 -7.92 -550 548 u=8 imp:n=1
304 5 -1.0 -551 548 u=8 imp:n=1
305 5 -1.0 -552 548 u=8 imp:n=1
c
c Middle cones (top fittings)
c
306 5 -1.0 -553 -547 554 u=8 imp:n=1
307 5 -1.0 -554 546 u=8 imp:n=1
c
c 568 4 -7.92 -555 -547 556 u=8 imp:n=1
c 569 4 -7.92 -556 546 u=8 imp:n=1

```

```

c -----
310 5 -1.0 -557 -547 558 u=8 imp:n=1
311 5 -1.0 -558 546 u=8 imp:n=1
c -----
c -----
312 5 -1.0 -559 -547 560 u=8 imp:n=1
313 5 -1.0 -560 546 u=8 imp:n=1
c -----
c -----
c =====
c Top handle and holes for control element Shim II
c -----
340 5 -1.0 -470 471 -472 473 474 -475 (606 -608 -609)
      502 503 504 (247) 245 240 241 242 243
      u=10 imp:n=1
341 6 -2.70 -236 -475 474 231 u=10 imp:n=1 $ cladd
342 5 -1.0 -502 -475 474 511 u=10 imp:n=1
343 5 -1.0 -503 -475 474 512 u=10 imp:n=1
344 5 -1.0 -504 -475 474 513 u=10 imp:n=1
c -----
345 5 -1.0 -245 -475 474 u=10 imp:n=1 $ center hole
c -----
c -----
c Side trims of top handle
c -----
346 5 -1.0 -470 473 -606 474 -475 u=10 imp:n=1
c 347 0 471 473 -607 474 -475 u=10 imp:n=1
348 5 -1.0 -470 -472 608 474 -475 u=10 imp:n=1
349 5 -1.0 471 -472 609 474 -475 u=10 imp:n=1
c -----
c Fuel element top fittings (part of top handle geometry)
c -----
350 7 -2.51 -231 -475 474 u=10 imp:n=1 $ B4C
351 5 -1.0 -511 -475 474 u=10 imp:n=1
352 5 -1.0 -512 -475 474 u=10 imp:n=1
353 5 -1.0 -513 -475 474 u=10 imp:n=1
c -----
c Guide tube (top handle)
c -----
355 0 -246 -475 474 236 u=10 imp:n=1 $ air
356 6 -2.70 -247 -475 474 246 u=10 imp:n=1 $ cladd
c -----
c Shim II top handle side holes
c -----
360 5 -1.0 -240 -475 474 473 u=10 imp:n=1
361 5 -1.0 -241 -475 474 -472 u=10 imp:n=1
362 5 -1.0 -242 -475 474 471 u=10 imp:n=1
363 5 -1.0 -243 -475 474 -470 u=10 imp:n=1
c -----
c -----
c Shim II second top fittings (top of top handle)
c -----
371 7 -2.51 -331 u=10 imp:n=1
372 5 -1.0 -511 545 -546 u=10 imp:n=1
373 5 -1.0 -512 545 -546 u=10 imp:n=1
374 5 -1.0 -513 545 -546 u=10 imp:n=1
375 6 -2.70 -332 331 u=10 imp:n=1 $ cladd for control
c -----
c Guide tube (very top section)
c -----
376 0 -334 332 u=10 imp:n=1 $ air
377 6 -2.70 -335 334 u=10 imp:n=1 $ wall
c -----
c Shim II third top fittings
c -----
381 4 -7.92 -531 475 -545 u=10 imp:n=1
382 5 -1.0 -532 475 -545 u=10 imp:n=1 $
383 5 -1.0 -533 475 -545 u=10 imp:n=1
384 5 -1.0 -534 475 -545 u=10 imp:n=1
c -----
c -----
386 0 -510 475 -545 531 u=10 imp:n=1
387 5 -1.0 -511 475 -545 532 u=10 imp:n=1

```



```

388 5 -1.0 -512 475 -545 533 u=10 imp:n=1
389 5 -1.0 -513 475 -545 534 u=10 imp:n=1
c
c 390 0 -510 548 -535 549 u=10 imp:n=1
391 5 -1.0 -511 548 -535 550 u=10 imp:n=1
392 5 -1.0 -512 548 -535 551 u=10 imp:n=1
393 5 -1.0 -513 548 -535 552 u=10 imp:n=1
c
c 394 0 -510 546 -547 553 554 u=10 imp:n=1
395 5 -1.0 -511 546 -547 555 556 u=10 imp:n=1
396 5 -1.0 -512 546 -547 557 558 u=10 imp:n=1
397 5 -1.0 -513 546 -547 559 560 u=10 imp:n=1
c
c 398 4 -7.92 -510 547 -548 u=10 imp:n=1
399 5 -1.0 -511 547 -548 u=10 imp:n=1
400 5 -1.0 -512 547 -548 u=10 imp:n=1
401 5 -1.0 -513 547 -548 u=10 imp:n=1
c
c Fuel element top cones
c
c 402 4 -7.92 -549 548 u=10 imp:n=1
403 5 -1.0 -550 548 u=10 imp:n=1
404 5 -1.0 -551 548 u=10 imp:n=1
405 5 -1.0 -552 548 u=10 imp:n=1
c
c Middle cones (top fittings)
c
c 406 4 -7.92 -553 -547 554 u=10 imp:n=1
c 407 4 -7.92 -554 546 u=10 imp:n=1
c
408 5 -1.0 -555 -547 556 u=10 imp:n=1
409 5 -1.0 -556 546 u=10 imp:n=1
c
410 5 -1.0 -557 -547 558 u=10 imp:n=1
411 5 -1.0 -558 546 u=10 imp:n=1
c
412 5 -1.0 -559 -547 560 u=10 imp:n=1
413 5 -1.0 -560 546 u=10 imp:n=1
c
c
c =====
c Top handle and holes for control element Shim III
c
425 5 -1.0 -470 471 -472 473 474 -475 (606 -608 -609)
502 503 504 (247) 245 240 241 242 243
u=12 imp:n=1
426 6 -2.70 -236 -475 474 231 u=12 imp:n=1 $ cladd
427 5 -1.0 -502 -475 474 511 u=12 imp:n=1
428 5 -1.0 -503 -475 474 512 u=12 imp:n=1
429 5 -1.0 -504 -475 474 513 u=12 imp:n=1
c
430 5 -1.0 -245 -475 474 u=12 imp:n=1 $ center hole
c
c Guide tube (top handle)
c
431 0 -246 -475 474 236 u=12 imp:n=1 $ air
432 6 -2.70 -247 -475 474 246 u=12 imp:n=1 $ cladd
c
c Side trims of top handle
c
435 5 -1.0 -470 473 -606 474 -475 u=12 imp:n=1
c 436 0 471 473 -607 474 -475 u=12 imp:n=1
437 5 -1.0 -470 -472 608 474 -475 u=12 imp:n=1
438 5 -1.0 471 -472 609 474 -475 u=12 imp:n=1
c
c Fuel element top fittings (part of top handle geometry)
c
440 7 -2.51 -231 -475 474 u=12 imp:n=1 $ B4C
441 5 -1.0 -511 -475 474 u=12 imp:n=1
442 5 -1.0 -512 -475 474 u=12 imp:n=1

```

```

443 5 -1.0 -513 -475 474 u=12 imp:n=1
c
c Shim III top handle side holes
c
450 5 -1.0 -240 -475 474 473 u=12 imp:n=1
451 5 -1.0 -241 -475 474 -472 u=12 imp:n=1
452 5 -1.0 -242 -475 474 471 u=12 imp:n=1
453 5 -1.0 -243 -475 474 -470 u=12 imp:n=1
c
c Shim III second top fittings (part of top handle geometry)
c
454 7 -2.51 -381 u=12 imp:n=1
455 5 -1.0 -511 545 -546 u=12 imp:n=1
456 5 -1.0 -512 545 -546 u=12 imp:n=1
457 5 -1.0 -513 545 -546 u=12 imp:n=1
458 6 -2.70 -382 381 u=12 imp:n=1 $ cladd for control
c
c Guide tube (very top section)
c
459 0 -384 382 u=12 imp:n=1 $ air
460 6 -2.70 -385 384 u=12 imp:n=1 $ wall
c
c Shim III third top fittings
c
381 4 -7.92 -531 475 -545 u=12 imp:n=1
462 5 -1.0 -532 475 -545 u=12 imp:n=1 $
463 5 -1.0 -533 475 -545 u=12 imp:n=1
464 5 -1.0 -534 475 -545 u=12 imp:n=1
c
c 386 0 -510 475 -545 531 u=12 imp:n=1
465 5 -1.0 -511 475 -545 532 u=12 imp:n=1
466 5 -1.0 -512 475 -545 533 u=12 imp:n=1
467 5 -1.0 -513 475 -545 534 u=12 imp:n=1
c
c 390 0 -510 548 -535 549 u=12 imp:n=1
471 5 -1.0 -511 548 -535 550 u=12 imp:n=1
472 5 -1.0 -512 548 -535 551 u=12 imp:n=1
473 5 -1.0 -513 548 -535 552 u=12 imp:n=1
c
c 394 0 -510 546 -547 553 554 u=12 imp:n=1
476 5 -1.0 -511 546 -547 555 556 u=12 imp:n=1
477 5 -1.0 -512 546 -547 557 558 u=12 imp:n=1
478 5 -1.0 -513 546 -547 559 560 u=12 imp:n=1
c
c 398 4 -7.92 -510 547 -548 u=12 imp:n=1
480 5 -1.0 -511 547 -548 u=12 imp:n=1
481 5 -1.0 -512 547 -548 u=12 imp:n=1
482 5 -1.0 -513 547 -548 u=12 imp:n=1
c
c Fuel element top cones
c
402 4 -7.92 -549 548 u=12 imp:n=1
484 5 -1.0 -550 548 u=12 imp:n=1
485 5 -1.0 -551 548 u=12 imp:n=1
486 5 -1.0 -552 548 u=12 imp:n=1
c
c Middle cones (top fittings)
c
406 4 -7.92 -553 -547 554 u=12 imp:n=1
407 4 -7.92 -554 546 u=12 imp:n=1
c
489 5 -1.0 -555 -547 556 u=12 imp:n=1
490 5 -1.0 -556 546 u=12 imp:n=1
c
491 5 -1.0 -557 -547 558 u=12 imp:n=1
492 5 -1.0 -558 546 u=12 imp:n=1
c
493 5 -1.0 -559 -547 560 u=12 imp:n=1
494 5 -1.0 -560 546 u=12 imp:n=1

```

```

c -----
c -----
c Rabbit
c -----
610 16 -1.60 -610 613      imp:n=1 u=18
611 6 -2.70 -611 610 613  imp:n=1 u=18
612 5 -1.0 611 612 613
      imp:n=1 u=18
c -----
613 6 -2.70 -612      u=18 imp:n=1 $ bottom fitting
c -----
c Rabbit tube
c -----
614 6 -2.70 -613 614      u=18 imp:n=1 $ wall
615 9 -1.9769e-3 -614 830  u=18 imp:n=1 $ CO2
c -----
c =====
c Graphite reflectors
c -----
621 16 -1.60 -620      imp:n=1 u=13 $ graphite
622 6 -2.70 -621 620      imp:n=1 u=13 $ Al wall
623 5 -1.0 621 622
      imp:n=1 u=13 $ outside
c -----
c graphite reflectors bottom fitting
c -----
624 6 -2.70 -622      imp:n=1 u=13 $ Al wall
c -----
c =====
c Through tube
c -----
630 4 -7.92 -630 631 -632 633      imp:n=1 $ wall
631 10 -1.205e-3 -631 -632 633 634  imp:n=1 $ air
c -----
c Through tube tally
c -----
634 10 -1.205e-3 -634      imp:n=1 $ air
c -----
c =====
c Graphite PuBe source holder
c -----
635 16 -1.60 -625 627      imp:n=1 u=24 $ graphite
636 6 -2.70 -626 625      imp:n=1 u=24 $ Al wall
637 5 -1.0 626 (600:-601:602:-603:-604:605)
      imp:n=1 u=24 $ outside
c -----
c PuBe source tube
c -----
638 6 -2.70 -627 628      u=24 imp:n=1 $
639 9 -1.9769e-3 -628      u=24 imp:n=1 $
c -----
c Square above bottom adapter for PuBe source
c -----
645 6 -2.70 -600 601 -602 603 604 -605 606 607 -608 -609
      u=24 imp:n=1
646 5 -1.0 -600 603 -606      604 -605      u=24 imp:n=1
647 5 -1.0 601 603 -607      604 -605      u=24 imp:n=1
648 5 -1.0 -600 -602 608      604 -605      u=24 imp:n=1
649 5 -1.0 601 -602 609      604 -605      u=24 imp:n=1
c -----
c =====
c Beam ports
c -----
650 4 -7.92 -640 641      imp:n=1 $ beam port 1 wall East
651 10 -1.205e-3 -641      imp:n=1 $ beam port 1 air
652 4 -7.92 -650 651      imp:n=1 $ beam port 2 wall West
653 10 -1.205e-3 -651      imp:n=1 $ beam port 2 air
c -----

```

```

c =====
c Fission chamber support tube
c -----
670 6 -2.70 -615 616 u=25 imp:n=1 $
671 10 -1.205e-3 -616 u=25 imp:n=1 $
672 5 -1.0 615
u=25 imp:n=1 $
c -----
c
c Thermal column
c -----
c First part
700 6 -2.70 -700 (-701:702:-703:704:-705:706) imp:n=1
701 16 -1.60 701 -702 703 -704 705 -706 imp:n=1
c Second part
722 6 -2.70 -722 700 (-723:724:-725:726:-727:728)
imp:n=1
723 16 -1.60 723 -724 725 -726 727 -728 imp:n=1
c -----
c Third part
734 6 -2.70 733 -734 -110 -736 737 -738
(-743:744:746:-747:748) imp:n=1
735 11 -2.25 743 -744 -110 -746 747 -748 750 imp:n=1
750 10 -1.205e-3 -750 imp:n=1
c -----
c repeated structure tally
c -----
800 1 -5.95 -800 9 u=1 vol=80.424 imp:n=1 $
c Top of fuel tally
802 1 -5.95 -802 9 u=1 vol=1 imp:n=1 $
c Bottom of fuel tally
803 1 -5.95 -803 9 u=1 vol=1 imp:n=1 $
c -----
c Rabbit and cadmium covered cylinder
c -----
c Rabbit
830 9 -1.9769e-3 -830 831 u=18 imp:n=1 $ Polyethylene
831 9 -1.9769e-3 -831 832 u=18 imp:n=1 $ CO2
c Cadmium Cylinder
832 9 -1.9769e-3 -832 833 u=18 imp:n=1 $ Cadmium
833 9 -1.9769e-3 -833 u=18 imp:n=1 $ CO2
c -----
c =====
c Surface cards
c =====
c Fuel element
c -----
1 cz 1.740 $ fuel cylinder
2 cz 1.790 $ cladding cylinder
5 pz 0.001 $ bottom of lower graphite plug
6 pz 8.811 $ top of lower graphite plug
7 pz 46.911 $ top of UZrH active fuel
8 pz 55.671 $ top of upper graphite plug
9 cz 00.2285 $ Zr cylinder
10 cz 1.25 $ bottom fitting
11 pz -6.788 $ bottom surface for bottom fitting
c 14 cz 1.374 $ first top fitting's cylinder [dummy]
15 pz 59.221 $ top of 'first top fitting' cylinder
c -----
16 pz 57.221 $ top of cladd's top thickness
17 pz -1.55 $ bottom of cladd's bottom thickness
18 pz 8.891 $ Mo disk 0.08 cm thick below fuel
19 pz 46.831 $ Mo disk 0.08 cm thick above fuel
c -----
c Hexagonal first top fitting
c -----
20 p 1 1.73205 0 2.400
21 px 1.200
22 p -1 1.73205 0 -2.400
23 p 1 1.73205 0 -2.400

```

```

24 px -1.200
25 p -1 1.73205 0 2.400
c -----
c Control element
c -----
32 pz 2.102 $ top of bottom fitting for Shim
33 pz 4.642 $ guide tube bottom steel plug
34 pz 32.137 $ bottm poison plug Shim I, thick=1.59 cm
35 pz 32.099 $ bottm poison plug Shim II
36 pz 22.612 $ bottm poison plug Shim III
c -----
c Bottom adpater and grid plate lattice
c -----
50 c/z 1.9431 1.9431 2.86 $ 5.72 diameter hole
51 pz -24.416
52 pz -11.081 $ relates to sur 604--increaase/decrease
53 px 5.82939 $
54 px -1.94319
55 py 5.82939
56 py -1.94319
c -----
c Bottom adapter window
c -----
61 px 68.0100 $13.60196$ 5.82938 $
62 px -1.94318
63 py 44.6922
64 py -1.94318
c -----
c Lattice cell surfaces
c -----
70 px 1.9431 $
71 px -1.9431
72 py 1.9431
73 py -1.9431
c -----
c Cluster (Assembly) boundary surfaces
c -----
74 px 5.8292 $
75 px -1.9430
76 py 5.8292
77 py -1.9430
78 pz -6.7879 $ less than surf 11 by 0.0001
79 pz 59.220
c -----
c Core lattice
c -----
81 px 5.8294 $
82 px -1.9432
83 py 5.8294
84 py -1.9432
c -----
c Core window
c -----
91 pz -11.0809 $ -40.441 $ was bottom of pool
92 pz 100 $ 85.6721
93 px 68.0101 $ 5.829399
94 px -1.94311
95 py 36.91970 $
96 py -1.94311
c -----
c 99 rpp -1.9531 68.02 -1.9531 44.7 -41.441 86.6721
c -----
c Reactor Pool Tank: 3/8 in Al plate on side and 1/2 in on botton
c Diameter: 2.13 m (7 ft): 6.48 m High
c Al 6061 T6
c -----
100 c/z 37.0089 45.5379 106.5 $ tank actual radius is 106.5
101 c/z 37.0089 45.5379 107.45 $ tank wall radius is 107.45
102 pz 200.30 $ (was 602) top surface 6.48 m -45.70 cm
103 pz -45.70 $ bottom surface
c -----

```

```

c -----
c Bioshield (concrete)
c -----
c Lower part:      1.98 m (6.5 ft) thick and 3.35 m (11 ft) high
c First upper part:1.52 m (5 ft) thick and 0.61 m (2 ft)
c Second upper part:0.91 thick and 2.52 m
c Tank heigh is 6.48 m -(1.52 + 1.98 = 2.52
c -----
110 c/z 37.0089 45.5379 305.45    $ radius = 107.45 + 198
111 pz 140.3 $ = -45.7+335
c =====
c Shim I @ 5 Watt
c -----
c 100% removed is at pz=46.91 $ B4C
205 cz 1.52 $ B4c
206 cz 1.59 $ Al cladd
c Rod position at 65.4%--sur 475 pz =61.7621 (for top B4C)
207 pz 33.727 $ increase/decrease surf 34 also by 1.59 cm
c -----
c Shim II
c -----
c Poison and cladd are surfs 205 and 206 for Shim II, III
c Rod position at 65.3%
217 pz 33.689 $ increase/decrease surf 35 also by 1.59 cm
c -----
c Shim III at 70.1%
c -----
227 pz 24.202 $ increase/decrease surf 36 also by 1.59 cm
c -----
c Top handle holes for control element
c -----
231 cz 1.52 $ hole for element [0 0 0]
232 c/z 3.8862 0 1.52 $ hole for element [1 0 0]
233 c/z 0 3.8862 1.00 $ hole for element [0 1 0]
234 c/z 3.8862 3.8862 1.00 $ hole for element [1 1 0]
c -----
c Cladd of Shim in top handle
c -----
235 c/z 3.8862 0 1.59 $ cladd for element [1 0 0]
236 cz 1.59 $ cladd for element [0 0 0]
c -----
c Guide tube (top handle) Shim I
c -----
237 c/z 3.8862 0 1.740 $ cladd for element [1 0 0]$ guide
238 c/z 3.8862 0 1.790 $ cladd for element [1 0 0]$ guide
c -----
c Top handle side holes for control element
c -----
240 c/z 1.9431 -1.8000 0.8 $
241 c/z 1.9431 5.7000 0.8 $
242 c/z -1.8000 1.9431 0.8 $
243 c/z 5.7000 1.9431 0.8 $
c -----
245 c/z 1.9431 1.9431 0.50 $ top handle center hole for control
c -----
c Guide tube (top handle) Shim II
c -----
246 cz 1.740 $ hole for element [0 0 0]
247 cz 1.790 $ hole for element [0 0 0]
c -----
c Poison and cladd for Shim I very top section
c -----
272 rcc 3.8862 0 61.7621 0 0 10.065 1.52 $ [1 0 0] see sur 475
273 rcc 3.8862 0 61.7621 0 0 11.655 1.59 $ [1 0 0] see sur 475
c -----
c Guide tube (top section) Shim I
c -----
274 rcc 3.8862 0 61.7621 0 0 37.5336 1.740 $ [1 0 0] see sur 475
275 rcc 3.8862 0 61.7621 0 0 37.5337 1.790 $ [1 0 0] see sur 475
c -----

```

```

c      Poison and cladd for Shim II very top section
c      -----
331    rcc 0 0 61.7621 0 0 10.027 1.52 $ see surf 475
332    rcc 0 0 61.7621 0 0 11.617 1.59 $ see surf 475
c      -----
c      Guide tube (top section) Shim II
c      -----
334    rcc 0 0 61.7621 0 0 37.5334 1.740 $ see surf 475
335    rcc 0 0 61.7621 0 0 37.5335 1.790 $ see surf 475
c      -----
c      Poison and cladd for Shim III very top section
c      -----
381    rcc 0 0 61.7621 0 0 0.540 1.52 $ see surf 475
382    rcc 0 0 61.7621 0 0 2.130 1.59 $ see surf 475
c      -----
c      Guide tube (top section) Shim III
c      -----
384    rcc 0 0 61.7621 0 0 37.5338 1.740 $ see surf 475
385    rcc 0 0 61.7621 0 0 37.5339 1.790 $ see surf 475
c      -----
c      Top handle
c      -----
470    px 5.7785 $
471    px -1.8923
472    py 5.7785
473    py -1.8923
474    pz 59.2221
475    pz 61.7621
c      -----
c      Top handle arm support
476    px -1.3905
477    px 5.2767
478    pz 71.7865
480    p 0 1 -.14 -9.55
481    p 0 1 .14 13.436
c      -----
c      =====
c      Rabbit
c      -----
610    rpp -1.4503 5.3365 -1.4503 5.3365 7.182 69.7295 $ Graphite
611    rpp -1.6154 5.5016 -1.6154 5.5016 6.547 70.3645 $ Al wall
c      -----
c      Rabbit bottom fitting
c      -----
612    rcc 1.9431 1.9431 -6.788 0 0 6.35 0.9525 $ 3/4 in diameter
c      -----
c      Rabbit tube
c      -----
613    rcc 1.9431 1.9431 -0.438 0 0 80.0 1.905 $ 3/4 in diameter
614    rcc 1.9431 1.9431 -0.197 0 0 79.759 1.739 $ air
c      -----
c      Fission chamber support tube
c      -----
615    rcc 1.9431 1.9431 -6.788 0 0 70.8175 3.06 $ 3/4 in diameter
616    rcc 1.9431 1.9431 -6.788 0 0 70.8175 2.90 $ air
c      -----
c      Graphite reflectors
c      -----
620    rpp -1.4503 5.3365 -1.4503 5.3365 -0.915 61.6325
621    rpp -1.6154 5.5016 -1.6154 5.5016 -1.55 62.2675
c      -----
c      graphite reflectors bottom fitting
c      -----
622    rcc 1.9431 1.9431 -6.788 0 0 5.238 0.9525 $ 3/4 in diameter
c      -----
c      Graphite PuBe source holder
c      -----
625    rpp -1.4503 5.3365 -1.4503 5.3365 -6.788 57.0295
626    rpp -1.6154 5.5016 -1.6154 5.5016 -6.788 57.0295

```

```

627 rcc 1.9431 1.9431 -6.788 0 0 63.8175 1.905 $ 3/4 in diameter
628 rcc 1.9431 1.9431 -6.788 0 0 63.8175 1.739 $ air
c -----
c
c Through tube
c -----
630 c/x 45.5379 30.2630 7.62
631 c/x 45.5379 30.2630 6.82
632 px 348.0
633 px -274.0
c -----
c
c Through tube flux tally
634 rcc 18.03 45.5379 30.2630 15 0 0 6.8
c -----
c Beam ports
c -----
640 rcc 72.2 17.5279 30.2630 276.0 0 0 7.62 $ beam port 1 wall
641 rcc 73.0 17.5279 30.2630 275.2 0 0 6.82 $ beam port 1
650 rcc -17.2 17.5279 30.2630 -257.8 0 0 7.62 $ beam port 2 wall
651 rcc -18.0 17.5279 30.2630 -257.0 0 0 6.82 $ beam port 2
c =====
c Thermal column section
c -----
c Thermal column
c -----
c First part
700 rpp 5.4856 68.3516 -102.0460 -2.6670 -3.6230 59.2430 $
c -----
701 px 6.4386
702 px 67.3986
703 py -102.0460
704 py -3.6200
705 pz -2.6700
706 pz 58.2900
c -----
c Second part
722 rpp -4.6744 78.5116 -157.9261 -100.14 -13.7830 69.4030 $
c 723 rpp -3.8814 77.5586 -157.9261 -102.0460 -12.8300 68.4500 $
c -----
723 px -3.8814
724 px 77.5586
725 py -157.9261
726 py -102.0460
727 pz -12.8300
728 pz 68.4500
c -----
c Third part
c 734 rpp -14.6769 88.3541 -250.1617 -157.9261 -23.6255 79.2455 $
c -----
733 px -14.6769
734 px 88.3541
c 735 py -250.1617
736 py -157.9261
737 pz -23.6255
738 pz 79.2455
c -----
739 rpp -13.7239 87.4011 -249.2087 -159.8322 -22.6725 78.2925 $
743 px -13.7239
744 px 87.4011
c 745 py -249.2087
746 py -159.8322
747 pz -22.6725
748 pz 78.2925
c -----
c Front of access plug test zone
750 rpp 17.7239 57.4011 -162.8323 -159.8323 8.6725 48.2925 $
c -----
c repeated structure tally
c -----
800 rcc 0.0 0.0 22.86 0 0 10 1.6

```



```

mt1      zr/h.60t h/zr.60t
c      -----
c      Material #2: Zirconium
c      -----
m2      40000 -1.0 $
c      -----
c      Material #3:carbon
c      -----
m3      6000 -1.00 $
mt3     grph.60t
c      -----
c      Material #4: stailless steel 304 (Fe Cr Ni Mn) density 7.92
c      Los Alamos data.
c      -----
m4      26000 -0.695000 24000 -0.190000 28000 -0.095000 25055
        -0.020000 $
c      -----
c      Material #5: water
c      -----
m5      1001 2 8016 1$
mt5     lwtr.60t
c      -----
c      Material #6: Al 6061 T6--Aluminum Tank
m6      13027 -0.97511 29000 -0.00586 14000 -0.00622
        12000 -0.00897 24000 -0.00384
c      -----
c      Material #7: Boron Carbide
m7      5011 3.2 5010 .8 6000 1 $
c      -----
c      Material #8: Al 1100
c      m8      13027.66c -0.992120 29000 -0.004455 25055 -0.001013
c      30000 -0.002412$
c      -----
c      Material #9: Carbon Dioxide $ density=1.9769e-3 revise and cite
m9      6000 -0.272919 8016 -0.727081 $
c      -----
c      Material #10: Standard Air (Attix page 531)
m10     7014 -0.752308 7015 -0.002960 8016 -0.231687
        8017 -0.000094 6000 -0.000124 18000 -0.012827
c      -----
c      Material #11: Concrete (from Los Alamos Criticallity Primer)
m11     1001 -0.00453 8016 -0.5126 14000 -.36036
        13027 -0.03555 11023 -0.01527 20000 -0.05791
        26000 -0.01378
c      -----
c      Material #6: Al 6061 T6--Bottom adapter
m12     13027 -0.97511 29000 -0.00586 14000 -0.00622
        12000 -0.00897 24000 -0.00384
c      -----
c      Material #13: Molybdenum
m13     42000 -1.0 $
c      -----
c      Material #14: Cadmium
m14     48000 -1.0 $
c      -----
c      Material #14: Polyethylene
m15     1001 -0.143716 6012 -0.856284 $
c      -----
c      Material #16: Graphite
m16     6000 -1.0 $
mt16   grph.60t
c      -----
c      mplot tally=64 loglin xlims 1e-9 10
c      =====

```

A.3 MCNP Model of MUTR Pin Cell (Unit Cell)

```

MCNP      UMD Reactor Model (Pin Cell)
c      =====
c      =====
c
c      =====
c              Cell cards
c      =====
c      Fuel element
c      -----
1      3      -1.60      -1      5      -6      u=1 imp:n=1 $ lower graphite plug
2      1      -5.95      -1      9      18      -19      800      802      803      u=1 vol=1 imp:n=1
c              $ UZrH fuel
3      3      -1.60      -1      7      -8      u=1 imp:n=1 $ upper graphite plug
4      2      -6.50      -9      18      -19      u=1 imp:n=1 $ Zr rod in
5      4      -7.86      -10      -17      11      u=1 imp:n=1 $ bottom fitting
7      4      -7.86      (-21      24      -20      23      -25      22)      16      -15      u=1 imp:n=1
c              $ First hexagonal top fitting
8      13      -10.2      -1      -18      6      u=1 imp:n=1 $ Molybdenum disk
9      13      -10.2      -1      19      -7      u=1 imp:n=1 $ Molybdenum disk
c      -----
10     4      -7.92      -1      8      -16      u=1 imp:n=1 $plug above top grap plg
11     4      -7.92      -1      -5      17      u=1 imp:n=1 $ " below bttom grap plg
c      -----
c      Interior and exterior of element
c      -----
20     4      -7.86      -2      1      17      -16      u=1 imp:n=1 $ cladding
21     5      -1.0      2:(16      (21:-24:20:-23:25:-22)):(15):(-17      10):-11
c              u=1 imp:n=1 $ ouside element
c      -----
c
c      -----
c      Outside element
c      -----
99     5      -1.0      -70      71      -72      73      78      -79      imp:n=1      fill=1
c      -----
c
c      -----
c      Outside World
c      -----
199    0      (70:-71:72:-73:-78:79)      imp:n=0 $
c      -----
c      Top, Bottom, and Center of Fuel Tallies
800    1      -5.95      -800      9      u=1      vol=1      imp:n=1 $
c      Top of fuel tally
802    1      -5.95      -802      9      u=1      vol=1      imp:n=1 $
c      Bottom of fuel tally
803    1      -5.95      -803      9      u=1      vol=1      imp:n=1 $
c      -----
c
c      =====
c              Surface cards
c      =====
c      Fuel element
c      -----
1      cz      1.740      $ fuel cylinder
2      cz      1.790      $ cladding cylinder
5      pz      0.001      $ bottom of lower graphite plug
6      pz      8.811      $ top of lower graphite plug
7      pz      46.911     $ top of UZrH active fuel
8      pz      55.671     $ top of upper graphite plug
9      cz      00.2285    $ Zr cylinder
10     cz      1.25      $ bottom fitting
11     pz      -6.788     $ bottom surface for bottom fitting [dummy]
14     cz      1.40      $ first top fitting's cylinder [dummy]
15     pz      59.221     $ top of 'first top fitting' cylinder [dummy]

```

```

c -----
16 pz 57.221 $ top of cladd's top thickness
17 pz -1.55 $ bottom of cladd's bottom thickness
18 pz 8.891 $ Mo disk 0.08 cm thick below fuel
19 pz 46.831 $ Mo disk 0.08 cm thick above fuel
c -----
c Hexagonal first top fitting
c -----
20 p 1 1.73205 0 2.400
21 px 1.200
22 p -1 1.73205 0 -2.400
23 p 1 1.73205 0 -2.400
24 px -1.200
25 p -1 1.73205 0 2.400
c -----
c Lattice cell surfaces
c -----
*70 px 1.9431 $
*71 px -1.9431
*72 py 1.9431
*73 py -1.9431
c -----
78 pz -40.441$
79 pz 100.0
c -----
c Center of Fuel
c -----
800 rcc 0.0 0.0 22.86 0 0 10 1.6
c -----
c Top of fuel tally
802 rcc 0.0 0.0 46.731 0 0 -4.00 1.6
c Bottom of fuel tally
803 rcc 0.0 0.0 8.991 0 0 4.00 1.6
c -----

c =====
c Data cards
c =====
mode n p
kcode 5000 1.0 100 500
ksrc 0.7 0.0 30
c -----
c =====
c Tallies
c =====
c -----
fc74 Center of Fuel
f74:n 800
sd74 1
e74 1e-9 120ilog 20 $
c -----
c -----
fc84 Top of Fuel
f84:n 802
sd84 1
e84 1e-9 120ilog 20 $
c -----
c -----
fc94 Bottom of Fuel
f94:n 803
sd94 1
e94 1e-9 120ilog 20 $
c -----
c =====
c Materials
c =====
c Material #1: Uranium Zirconium Hydride--UZrH with H:Zr 1.65:1
c U is 8.5 w/o , with U235 enriched to < 20% =19.75% rest is ZrH
c S(alpha, beta) cross sections for both Hydrogen in ZrH and Zr
c in ZrH are used. The specification is in mt201 card.
c -----

```

```

m1      92238.66c -0.068385 92235.66c -0.016617 40000.42c -0.898617
        1001.66c -0.016383
mt1     h/zr.60t zr/h.60t
c      -----
c      Material #2: Zirconium
c      -----
m2      40000.42c 1 $
c      -----
c      Material #3:carbon
c      -----
m3      6000.66c 1 $
mt3     grph.60t
c      -----
c      Material #4: stailless steel 304 (Fe Cr Ni Mn) density 7.92
c      Los Alamos data.
c      -----
m4      26000.21c -0.695 24000.42c -0.190 28000.42c -0.095 25055.42c
        -0.020 $
c      -----
c      Material #5: water
c      -----
m5      1001.66c -0.11 8016.66c -0.89$
mt5     lwtr.60t
c      -----
c      Material #6: Al 6061 T6--Aluminum Tank
m6      13027.66c -0.97511 29000.50c -0.00586 14000.42c -0.00622
        12000.42c -0.00897 24000.42c -0.00384
c      -----
c      Material #7: Boron Carbide
m7      5010.42c -0.78260 6000.66c -0.21740 $
c      -----
c      Material #8: Pure Al
m8      13027.66c -1.0 $
c      -----
c      Material #13: Molybdenum
m13     42000 -1.0 $
c      -----
c      -----

```

Bibliography

-
- [1] DePriest, K. Russell, Cooper, Philip J. and Parma, Edward J., MCNP/MCNPX Model of the Annular Core Research Reactor, Sandia National Laboratories, Albuquerque, New Mexico, 2006.
- [2] Stamatelatos, I.E., Varvayanni, M., Tzika, F., Ale, A.B.F., Catsaros, N., Monte Carlo simulation of the Greek Research Reactor neutron irradiation facilities, Nuclear Instruments and Methods in Physics Research B 263 (2007) 136–139.
- [3] Aghara, Sukesh, Charlton, William, Characterization and quantification of an in-core neutron irradiation facility at a TRIGA II research reactor, Nuclear Instruments and Methods in Physics Research B 248 (2006) 181–190.
- [4] Huda, M. Q, Rahman, M, Sarker, M. M., Bhuiyan, S. I., Benchmark Analysis of TRIGA Mark II Research Reactor using Monte Carlo Techniques, Annals of Nuclear Energy, Volume 31, Issue 11, July 2004.
- [5] Kelly, John G., Griffin, Patrick J., and Fan, Wesley C., Benchmarking of the Sandia Pulsed Reactor III Cavity Neutron Spectrum for Electronic Parts Calibration and Testing, IEEE Transactions on Nuclear Science, Vol. 40, NO. 6, December 1993.
- [6] X-5 Monte Carlo Team, MCNP - A General Monte Carlo N-Particle Transport Code, Version 5, LA- UR-03-1987, Los Alamos National Laboratory, April 2003.
- [7] Persic, A., Ravnik, M., Zagar, T., Burn-up TRIGA MARK II Benchmark Experiment, Nuclear Energy in Central Europe 98', September, 1998.
- [8] Ravnik, M, Jeraj, R, Research Reactor Benchmarks, Nuclear Science and Engineering, Vol. 145, No. 1, Pages:145-152, 2003.
- [9] White, S. M., Held, K. D., Palmer, M. R. and Yanch, J. C. Biological Dosimetry for Epithermal Neutron Beams. Radiat. Res. 155, 776–782 (2001).
- [10] Rogus, R. D., Harling, O. K. and Yanch, J. C., Mixed field dosimetry of epithermal neutron beams for boron neutron capture therapy at the MITR-II research reactor. Med. Phys. 21, 1611–1625 (1994).
- [11] Lamarsh, John R., Introduction to Nuclear Reactor Theory, Addison-Wesley Publishing Company, Inc., 1966.
- [12] Case, Kenneth M., Zweifel, Paul F., Linear Transport Theory, Addison-Wesley Publishing Company, Inc., 1967.

-
- [13] Glasstone, Samuel and Alexander Sesonske, Nuclear Reactor Engineering: Reactor Design Basics, Chapman & Hall, Fourth Edition, Volume I, 1994.
- [14] Glasstone, Samuel and Edlund, Milton, The Elements of Nuclear Reactor Theory, D Van Nostrand Company, 1952.
- [15] Bell, George I and Samuel Glasstone, Nuclear Reactor Theory, Van Nostrand Reinhold Company, 1970.
- [16] Lewis, E. E and Miller, W. F., Jr., Computational Methods of Neutron Transport, John Wiley & Sons, 1984.
- [17] Duderstadt, James J., Hamilton, Louis j., Nuclear Reactor Analysis, John Wiley & Sons, Inc., New York, New York, 1976.
- [18] Clark, Jr., Melville, Hansen, Kent F., Numerical Methods of Reactor Analysis, Academic Press, 1964.
- [19] Alder, Berni, Methods in Computational Physics, Volume 1, Statistical Physics, Academic Press, 1963.
- [20] N. P. Buslenko, D. I. Golenko, Shreider, Yu A., The Monte Carlo Method: The Method of Statistical Trials, Pergamon Press Ltd., Headington Hill Hall, Oxford, London, 1966.
- [21] Dupree, Stephen A., Fraley, Stanley, A Monte Carlo Primer: A Practical Approach to Radiation Transport, Kluwer Academic/Plenum Publishers, New York, 2002.
- [22] Cashwell, E. D., and Everett, C. J., A Practical Manual on the Monte Carlo Method for Random Walk Problems, Pergamon Press, New York, New York, 1959.
- [23] Taylor, Theodore Brewster, Mc Reynolds, Dyson, Freeman John, Reactor with Prompt Negative Temperature Coefficient, and Fuel Element Therefor, US Patent 3,127,325, General Dynamics Corporation, New York, N.Y., March 31, 1964.
- [24] Fouquet, Douglas M., Razvi Junaid, Whittemore, William L., TRIGA Research Reactors: A Pathway to the Peaceful Applications of Nuclear Energy, Nuclear News, Vol. 46, No. 12, November 2003.
- [25] Wallace, Walter P., Encinitias; Simnad, Massoud T., Fuel Element, US Patent 3,119,747, General Dynamics Corporation, New York, N.Y., January 28, 1964.
- [26] Stone, Richard S., Sleeper Jr, H. P, Stahl, Ralph H., West, Gordon, Transient Behaviour of TRIGA, a Zirconium-Hydride, Water Moderated Reactor, Nuclear Science and Engineering: 6, 255-259 (1959).

-
- [27] UMCP, Safety Analysis Report, College Park, MD, University of Maryland, February 2000.
- [28] X-5 Monte Carlo Team, MCNP - A General Monte Carlo N-Particle Transport Code, Version 5, LA- UR-03-1987, Los Alamos National Laboratory, April 2003.
- [29] Harmon, Charles D., Busch Robert D., Briesmeister, Judith F., Forster, R. Arthur, Criticality Calculations with MCNP: A Primer, LA-12827-M, Los Alamos National Laboratory, Los Alamos, New Mexico, 1994.
- [30] Simnad, MT; Foushee, FC, West GB, Fuel Element for Pulsed TRIGA Research Reactors, Nuclear Technology, 28 (1): 31-56 1976.
- [31] Fuel Rod Assembly-4 Rod Fuel Cluster, Drawing # T4S210D105, UMTR, General Atomics, San Diego, CA.
- [32] Four Rod Fuel Cluster Lower Adapter, Drawing # T4M210D104, TRIGA Reactors, Gulf Energy Environmental Systems, General Atomics, San Diego, CA.
- [33] Four Rod Fuel Cluster Handle, Drawing # T4M210C101, UMTR, Gulf General Atomics Incorporated, San Diego, CA.
- [34] Guide Tube Control Rod, 3 Rod Fuel Cluster, Drawing # T4S210C105, UMTR, General Atomics, San Diego, CA.
- [35] William III, R. G., Gesh, C. J., Pagh, R. T., Compendium of Material Composition Data for Radiation Transport Modeling, Pacific Northwest National Laboratory, PNNL-15870, 2006.
- [36] Ball, D. R., Graphite for High Temperature Gas Cooled Nuclear Reactors, STP-NU-009, ASME Standards Technology, LLC, Three Park Avenue, New York, 2008.
- [37] The Aluminum Association Inc., "International Alloy Designations and Chemical Composition Limits for Wrought Aluminum and Wrought Aluminum Alloys," Arlington, Va, 2009.
- [38] Booth, Thomas E, A sample Problem for Variance Reduction in MCNP, Los Alamos Report LA-10363 UC-32, Los Alamos National Laboratory, Los Alamos, New Mexico, 1985.
- [39] Hendricks, John S., Culbertson, Christopher N., An Assessment of MCNP Weight Windows, PHYSOR 2000 ANS International Topical Meeting on "Advances in Reactor Physics and Mathematics and Computation into the Next Millennium," Pittsburgh, PA, May 7-11, 2000.

-
- [40] Lyon, William S., Guide to Activation Analysis, Robert E. Krieger Publishing Company, NY, 1972.
- [41] Burgett, Eric A., Novel Neutron Detectors, Ph.D. Thesis in Nuclear Engineering, Expected March, 2010, Georgia Institute of Technology, Atlanta, GA.
- [42] M. REGINATTO, The "Few-Channel" Unfolding Programs in the UMG Package: MXD_FC33, GRV_FC33 and IQU_FC33, UMG package, Version3.3, March 1, 2004.
- [43] M. REGINATTO, P. GOLDHAGEN, S. NEUMANN, "Spectrum Unfolding, Sensitivity Analysis and Propagation of Uncertainties with the Maximum Entropy Deconvolution Code MAXED", Nucl Inst. And Meth. A , 476, 242 (2002).
- [44] Lamarsh, R., Introduction to Nuclear Engineering, Third Edition, Prentice Hall, Inc., 2001.
- [45] Mc Reynolds, Andrew Wetherbee, Dijkstra, Lieuwe J., Fuel Element, US Patent 3,019,176, General Dynamics Corporation, New York, N.Y., January 30,1962.
- [46] Dee, John B., Simnad, Massoud T., Fuel Element, US Patent 3,352,757, General Dynamics Corporation, New York, N.Y., January 30,1967.
- [47] West, Gordon B, Peters, Ralph H., Nuclear Reactors, US Patent 4,186,050, General Atomic Company, San Diego, California, January 29,1980.
- [48] International Atomic Energy Agency, Nuclear Research Reactors in the World, An Online Database (<http://www.iaea.org/worldatom/rrdb/>), IAEA, Vienna, Austria.
- [49] Yi, Jason, Information in Regard to Standard TRIGA Fuel Element, General Atomics, TRIGA Division, (personal communication, December 1, 2009),
- [50] Cross Section Evaluation Working Group, The Evaluated Nuclear Data File ENDF/B-VI Summary Documentation, Report BNL-NCS-17541 (ENDF-201) (1991), edited by P.F. Rose, National Nuclear Data Center (NNDC), Brookhaven National Laboratory, Upton, NY, USA.
- [51] M.B. Chadwick, P. Oblozinsky, M. Herman et al., "ENDF/B-VII.0: Next Generation Evaluated Nuclear Data Library for Nuclear Science and Technology", Nuclear Data Sheets, vol. 107, pp. 2931-3060, 2006.
- [52] Data obtained from the Evaluated Nuclear Data File (ENDF/B-VII) using Sigma-3.0, the online ENDF retrieval and plotting system, February 2009.
- [53] Wilson, W. B., et. al., "Accelerator Transmutation Studies at Los Alamos with LAHET, MCNP, and CINDER90," Proceedings of the Workshop on Simulation of

Accelerator Radiation Environments, January 11-15, 1993, Santa Fe, New Mexico;
Los Alamos National Laboratory conference proceedings LA-12835-C pp.115-133
October 1994.

[54] Gavrillas, Mirela, The Gospel, MUTR Neutron Flux Measurement, University
of Maryland, College Park, Maryland, 1987.